POLITECNICO DI TORINO

Collegio di Ingegneria Biomedica

Master of Science in
Biomedical Engineering

Master of Science Thesis

Comparative Analysis of Lipoprotein Purification Techniques and Their Impact on Corona Formation

Supervisors:
Prof.ssa Laura Fabris - Politecnico di Torino
Prof. Francesco Stellacci - École Polytechnique Fédérale de Lausanne
Dr. Quy Ong Khac - École Polytechnique Fédérale de Lausanne
Ph.D. Ding Ren - École Polytechnique Fédérale de Lausanne

Candidate:
Laura Carbonara

Academic Year 2024-2025

“Ogni grande sogno
comincia con un sognatore.
Ricordati sempre, tu hai la forza,
la pazienza e la passione
per arrivare alle stelle
e cambiare il mondo”

Harriet Tubman

Abstract

The protein corona, caused by nanoparticle-protein interaction on the surface of nanoparticles, has long been studied due to its ability to modulate the particle's biological properties. It is a dynamic layer of proteins that adsorb onto nanoparticles, influencing their structural characteristics and functions. There are two types of protein corona: hard corona, composed of tightly bound and hardly dissociable proteins, and soft corona, composed of weakly bound proteins with more frequent exchange.

Lipoproteins, whose size ranges from 10 to 1000 nm, are an important family of nanoparticles; nevertheless, the study of the protein corona on lipoproteins remains largely unexplored. This thesis aims to investigate the protein corona composition of low-density lipoproteins (LDL) isolated through different extraction protocols and purification methods. Density gradient ultracentrifugation (DGUC), polyethylene glycol (PEG) precipitation, fast protein liquid chromatography (FPLC) and various combinations of them were applied.

The thesis focuses on evaluating how the isolation process influences the adsorption of serum proteins onto LDL, causing variations in the existence of hard corona and soft corona, which are reflected by their physical properties and protein composition.

Different isolation approaches result in LDL with different characteristics. Notably, DGUC has been observed to be particularly effective at removing the soft corona, where LDL extracted with DGUC are smaller. Indeed, these LDL also compose of much fewer numbers of proteins. This is likely due to the high centrifugal force and density separation that strip proteins from LDL surface during the isolation. In comparison, LDL extracted with merely FPLC (or PEG precipitation followed by FPLC) can keep more corona with them, resulting in larger size. More proteins were also detected from those LDL in the proteomics analysis.

These findings emphasize the importance of lipoprotein-protein interaction and corona on lipoproteins. By leveraging the nano-bio interaction through selecting suitable isolation protocols, the protein corona on lipoproteins can be regulated, paving the way for lipoprotein-based disease detection and therapy.

Table of Contents

Abstract ..... **i**

1. Introduction and Objectives **5**

1.1 The Protein Corona Theory 6

1.2 Introduction to Lipoproteins 9

1.3 Challenges in Protein Corona Characterization 12

1.4 Thesis Objectives 13

2. Materials **15**

3. Methods **17**

3.1 Extraction of LDL from Serum via DGUC 17

3.1.1 DGUC followed by FPLC 18

3.1.2 DGUC followed by PEG precipitation and FPLC 19

3.1.3 DGUC with Multiple Filtration Steps followed by FPLC 20

3.2 Extraction of LDL from Serum without DGUC 21

3.2.1 Extraction of LDL from Serum by FPLC 21

3.2.2 Extraction of LDL from Serum using PEG Precipitation followed by FPLC 22

3.3 Characterization Methods for Isolated LDL 23

3.3.1 FPLC Purification and Analysis of LDL 23

3.3.2 SDS-PAGE for LDL Protein Composition Analysis 24

3.3.3 DLS Analysis of LDL size 25

3.3.4 TEM Analysis of LDL structure 26

3.3.5 SV-AUC Analysis of LDL Physical Properties 26

3.3.6 MS-based Proteomics for Analyzing LDL Protein Composition 30

4. Results and Discussion 31

4.1 LDL Physical Properties 31

4.1.1 DLS Analysis of LDL Extracted from Serum via DGUC 31

4.1.2 DLS Analysis of LDL Extracted from Serum via FPLC and with PEG precipitation followed by FPLC 32

4.1.3 TEM Analysis of LDL Extracted from Serum via DGUC 33

4.1.4 TEM Analysis of LDL Extracted from Serum via FPLC and with PEG precipitation followed by FPLC 34

4.1.5 SV-AUC Analysis of LDL Extracted from Serum via DGUC 35

4.1.6 SV-AUC Analysis of LDL Extracted from Serum via FPLC and with PEG precipitation followed by FPLC 35

4.2 Discussion of the Physical Properties of LDL Isolated from Serum with and without DGUC 36

4.3 LDL Protein Composition 38

4.3.1 SDS-PAGE of LDL Extracted from Serum via DGUC 38

4.3.2 SDS-PAGE of LDL Extracted from Serum via FPLC and with PEG precipitation followed by FPLC 39

4.3.3 MS-Based Proteomics of LDL Extracted from Serum via DGUC 40

4.3.4 MS-Based Proteomics of LDL Extracted from Serum via FPLC and with PEG precipitation followed by FPLC 44

4.3.5 Discussion of the Protein Composition of LDL Isolated from Serum with and without DGUC 89

5. Conclusions and Future Work 91

6. List of Figures 93

7. List of Tables 95

References 97

Acknowledgements 103

1. Introduction and Objectives

Lipoproteins, naturally occurring nanoparticles in the human body, function as highly efficient carriers of lipids and cholesterol [1]. They are classified based on their size, density, cholesterol content, and the presence of specific apolipoproteins [1]. The main categories include chylomicrons (CM), very low-density lipoproteins (VLDL), low-density lipoproteins (LDL), intermediate-density lipoproteins (IDL), and high-density lipoproteins (HDL) [2].

Among them, LDL plays a key role in transporting cholesterol from the liver to peripheral tissues [3]. LDL is commonly labelled as "bad" cholesterol because it can accumulate in artery walls, contributing to blockages and elevating the risk of heart disease [4]. Conversely, HDL is considered "good" cholesterol, as it aids in removing excess cholesterol from the bloodstream, supporting cardiovascular health [4].

LDL particles range from 17 to 28 nm in diameter and are primarily composed of cholesterol, phospholipids, triglycerides, and proteins [2]. Their core is rich in cholesterol esters, while the outer layer consists of a phospholipid monolayer embedded with Apolipoprotein B-100, a ~550 kDa protein essential for maintaining structural integrity, regulating hepatic synthesis, and mediating interactions with the LDL receptor (LDL-r), thereby facilitating cellular uptake of LDL [3].

When LDL, like other nanoparticles, enter a biological environment, they interact with biomolecules present in the system [5]. Due to their high specific surface area and potential energy, nanoparticles rapidly adsorb proteins onto their surface [5]. This process leads to the formation of a protein corona, a stabilizing protein layer that reduces their energy state [5]. The protein corona alters the characteristics of LDL, influencing its biological behaviour including transportation and receptor-mediated endocytosis [6]. Additionally, the protein corona is classified into hard and soft coronas, depending on the binding strength between proteins and the nanoparticle surface [7].

Several isolation protocols are performed to analyse the composition of the protein corona surrounding LDL particles. Many of these protocols rely on a two-step process and the first one involves density gradient ultracentrifugation (DGUC) to remove triglyceride-rich particles and serum proteins based on density [8]. This is followed by fast protein liquid chromatography (FPLC) coupled with a size-exclusion column (SEC) to isolate lipoproteins by their size [8]. alternative approaches are also explored to optimize the isolation strategy and assess how different techniques might influence the characterization of the protein corona [9]. Polyethylene glycol (PEG) precipitation is one such alternative, offering a simple and efficient method to selectively aggregate and precipitate LDL while excluding smaller serum proteins [9].

In this thesis, we compare different combinations of these methods to explore the relationship between LDL isolation approaches and their corresponding protein corona [10]. Generally, LDL separated with or without DGUC are compared based on their physical properties and protein compositions. Different characterizations methods are employed including dynamic light scattering (DLS) and transmission electron microscopy (TEM) to assess the size distribution of LDL after extraction. Sedimentation velocity analytical ultracentrifugation (SV-

AUC) is applied to provide a detailed profile of LDL size distribution and corona composition without requiring labelling

To compare their protein compositions, we also performed sodium dodecyl sulphate-polyacrylamide gel electrophoresis (SDS-PAGE), which separates proteins by molecular weight, and allows the identification of major protein components and their variations across different isolation methods. Mass spectrometry-based (MS-based) label-free proteomics approaches are also applied to identify protein compositions of the corona.

By integrating these techniques, a comprehensive understanding of LDL-protein corona formation is achieved, providing a deeper insight into how different isolation methods influence the composition and the function of protein corona.

1.1 The Protein Corona Theory

Upon contact with plasma or other protein-containing biological fluids, the surface of nanoparticles is immediately decorated with proteins forming a biologically active protein layer that helps stabilize them in a low-energy state [11]. This phenomenon, known as “Protein Corona”, was first described by Kenneth A. Dawson et al. [12] in 2007 [13]. The interaction between biomolecules and nanoparticles results in the formation of two distinct types of protein corona: the hard corona and the soft corona [5].

The hard corona consists of proteins with a high binding affinity for the nanoparticle surface, forming a tightly bound inner layer that is often considered irreversible (Figure 1) [7].

In contrast, the soft corona forms the outer layer, consisting of proteins that are loosely attached through reversible interactions and weak protein-nanoparticle associations [6]. This layer remains in dynamic equilibrium with free proteins in biological fluids and readily responds to changes in protein composition [14]. When the concentration of free proteins declines, the soft corona rapidly dissociates [7]. Indeed, hard corona proteins remain bound to the nanoparticle surface for prolonged periods due to strong interactions, while soft corona proteins exhibit greater dynamism and can detach more easily under physiological conditions [14].

Notably, the most abundant proteins in plasma or other bodily fluids do not always dominate the hard corona, underscoring the intricate nature of protein-nanoparticle interactions in biological systems [15].

One widely accepted hypothesis suggests that hard corona proteins attach directly to the nanoparticle surface, while soft corona proteins associate indirectly by interacting with the hard corona layer [16]. However, Pareek and co-workers [6] suggest that both hard and soft corona proteins may bind directly to the nanoparticle surface, differing mainly in their binding affinities and interaction dynamics.

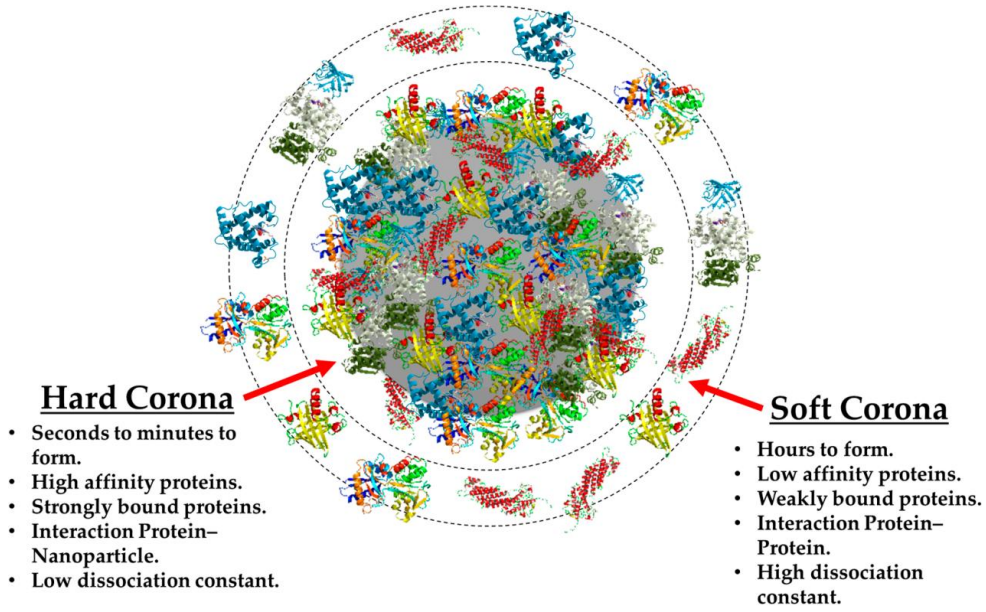

Figure 1 – Schematic comparison of the main differences between hard and soft coronas [7] .

When nanoparticles are introduced into a physiological environment, the first proteins to attach are typically those that are most abundant and mobile, such as serum albumin. Over time, these proteins with lower binding affinity are gradually displaced by less abundant proteins that exhibit a stronger attraction to the nanoparticle surface, including immunoglobulins, and complement factors [17], as illustrated in Figure 2. This dynamic exchange, known as the Vroman effect, is influenced by protein concentration and binding kinetics [18]. Over time, the nanoparticle-protein interaction reaches equilibrium, leading to the formation of two distinct layers [5]. The hard corona comprises tightly bound proteins that form a stable inner layer on the nanoparticle surface, while the soft corona consists of proteins with weaker interactions, creating a dynamic outer layer that can detach under physiological conditions [6].

This dynamic interaction can achieve equilibrium rapidly, often within about five minutes, although it may take several hours or even days based on exposure conditions. Once equilibrium is reached, the continuous turnover of proteins does not substantially change the overall makeup of the corona [18].

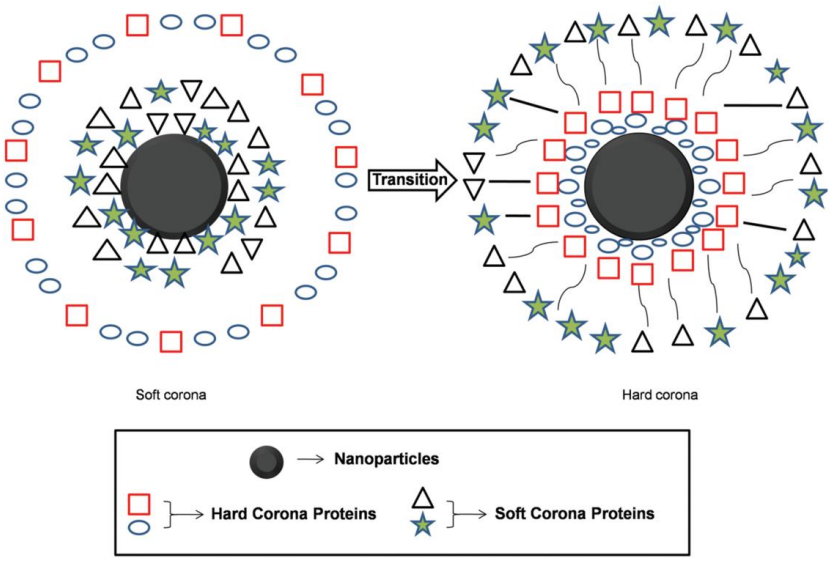

Figure 2 – Schematic illustration depicting the shift from a soft corona to a hard corona [5].

The adsorption–desorption process is dynamic and can be mathematically modelled to predict the interactions of nanoparticles with proteins [19]. Key parameters, such as the kinetic constants of these processes and the protein diffusion coefficient, provide insights into the interaction's reversibility and protein affinity for the nanoparticle surface [7]. The kinetics of protein adsorption can be described using the following equation:

$$P + S \underset{k_{des}}{\overset{k_{ads}}{\longleftrightarrow}} P_S \tag{1}$$

where P, S, and P_S refer to proteins, nano-surface and the complex formed upon their interaction, respectively. The kinetic constants k_{ads} and k_{des} define adsorption and desorption rates, respectively. The reversibility of the interaction is determined by these constants, with the process becoming irreversible when $k_{des} = 0$, which constrains the kinetic behaviour of the system [7].

To fully understand protein-nanoparticle interactions, it is essential to consider the different stages involved. Initially, when a nanoparticle is introduced into a biological fluid, both components are subjected to forces such as diffusion and convection, which facilitate their contact [19]. Additional factors, including diffusion coefficients, interfacial concentration, and protein concentration, also play a role in the process [18]. Once in proximity, proteins interact with the nanoparticle surface through various binding forces. These interactions ultimately lead to the attachment of proteins to specific regions of the nanoparticle [18].

The Langmuir model (Figure 3) is commonly utilized to analyze protein adsorption [20]. This model posits that the surfaces of nanomaterials have a finite number of adsorption sites, all possessing identical energy levels [21]. Adsorption is regarded as a reversible process that reaches equilibrium when the rates of adsorption and desorption are equal, leading to the formation of a monolayer [21]. However, this model has certain limitations in explaining the development of the protein corona. Some proteins can bind irreversibly to the surface of the nanomaterial, undergo conformational changes, and interact with other adsorbed proteins [7].

Additionally, the surfaces of nanomaterials are frequently heterogeneous, influencing the dynamics of binding [18]. Typically, the protein corona is composed of multiple layers, creating a highly dynamic structure where interactions between proteins and nanomaterials, as well as between proteins themselves, are critical [7].

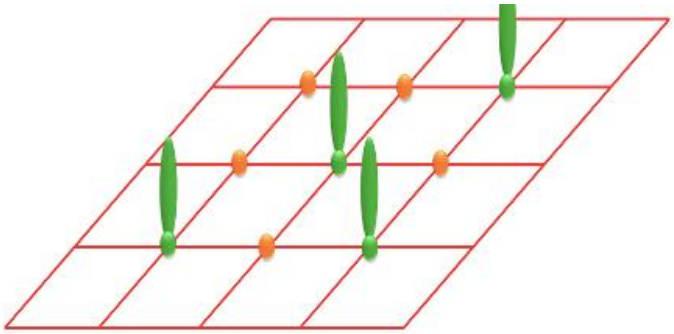

Figure 3 – Schematic representation of the equivalent free sites (orange) and occupied ones (green) on the surface of nanomaterial for the Langmuir model [7].

From a kinetic perspective, the interactions between proteins and nanoparticles in biological fluids are mainly influenced by non-covalent forces, such as electrostatic interactions, hydrophobic forces, and hydrogen bonds [6]. Although electrostatic interactions are frequently regarded as crucial in facilitating these interactions, they are not the only factors that contribute to the formation of the nanoparticle-protein corona [6]. Indeed, hydrophobic interactions and other non-specific forces also contribute considerably to the stabilization and overall composition of the protein corona [22]. These additional forces collaborate to influence the binding dynamics and stability of the corona, helping to maintain the integrity of the nanoparticle-protein complex under different physiological conditions [23]. Consequently, the formation of the corona is a complex process shaped by various forces, each of which is essential in determining the behaviour of the nanoparticle and its interactions within the biological environment [7].

1.2 Introduction to Lipoproteins

Lipoproteins are essential for lipid transport, as cholesterol and triglycerides are water-insoluble and must associate with proteins to circulate efficiently [24]. These macromolecular complexes facilitate the absorption and distribution of dietary lipids from the intestine, as well as the transport of lipids between the liver and peripheral tissues, including reverse cholesterol transport back to the liver [24]. Beyond their role in lipid metabolism, lipoproteins help eliminate hydrophobic and amphipathic toxic molecules, such as bacterial toxins, preventing their accumulation in areas of infection and inflammation [25].

Their structural composition allows them to perform these functions efficiently [26]. Lipoproteins have a hydrophobic core containing cholesterol esters and triglycerides, surrounded by a hydrophilic outer layer composed of phospholipids, free cholesterol, and apolipoproteins (Figure 4) [26].

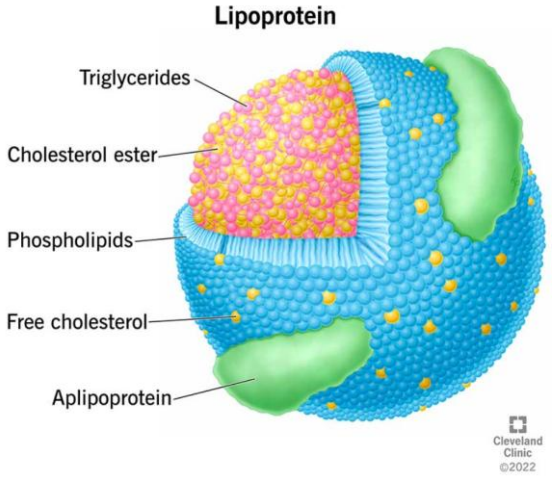

Figure 4 – Lipoprotein structural composition [26].

The composition of the outer layer plays a key role in determining how lipoproteins interact with cells and receptors, thereby influencing various metabolic pathways [27]. Plasma lipoproteins are categorized based on their size, lipid content, and apolipoprotein profile into seven distinct types: chylomicrons, chylomicron remnants, very low-density lipoproteins (VLDL), intermediate-density lipoproteins (IDL or VLDL remnants), low-density lipoproteins (LDL), high-density lipoproteins (HDL), and lipoprotein(a) (Lp(a)) [24]. Each of these classes serves specific metabolic roles and follows unique pathways in circulation (Table 1) [24].

Lipoprotein	Density (g/mL)	Size (nm)	Major Lipids	Major Apolipoproteins
Chylomicrons	<0.930	75-1200	Triglycerides	Apo B-48, Apo C, Apo E, Apo A-I, A-II, A-IV
Chylomicron Remnants	0.930 - 1.006	30-80	Triglycerides Cholesterol	Apo B-48, Apo E
VLDL	0.930 - 1.006	30-80	Triglycerides	Apo B-100, Apo E, Apo C
IDL	1.006 - 1.019	25-35	Triglycerides Cholesterol	Apo B-100, Apo E, Apo C
LDL	1.019 - 1.063	18-25	Cholesterol	Apo B-100
HDL	1.063 - 1.210	5-12	Cholesterol Phospholipids	Apo A-I, Apo A-II, Apo C, Apo E
Lp (a)	1.055 - 1.085	~30	Cholesterol	Apo B-100, Apo (a)

Table 1 – Overview of all the lipoprotein classes [24].

LDL particles, primarily derived from VLDL and IDL, serve as the main transporters of cholesterol in the bloodstream [28]. Each LDL particle contains a single Apo B-100 molecule, but variations in LDL size and density significantly influence its potential to contribute to atherosclerosis [28]. Conversely, HDL particles, often referred to as “good cholesterol”, play a

protective role by facilitating reverse cholesterol transport [28]. HDL removes excess cholesterol from peripheral tissues, including the arterial walls, and delivers it to the liver for recycling or excretion, thereby reducing the risk of atherosclerosis [4]. Maintaining a balance between LDL and HDL cholesterol is essential for cardiovascular health, as an excess of LDL contributes to plaque formation in arteries, while adequate HDL levels help mitigate this process [29].

At the molecular level, apolipoproteins are integral to lipoprotein metabolism, serving as structural components, receptor ligands, and enzyme regulators [30]. Apo B-100, produced in the liver, is a critical structural protein of VLDL, IDL, and LDL, playing a key role in LDL clearance by interacting with LDL receptors [30].

LDL receptors, predominantly found in the liver, recognize Apo B-100 and Apo E, mediating the uptake of LDL, IDL, and chylomicron remnants through endocytosis [24]. Once inside the cell, these lipoproteins undergo lysosomal degradation, releasing cholesterol [24]. This process regulates intracellular cholesterol homeostasis by inhibiting HMG-CoA reductase (a key enzyme in cholesterol synthesis), reducing LDL receptor expression, and thereby controlling cholesterol uptake [29]. The number of LDL receptors in liver cells plays a crucial role in determining plasma LDL levels [29]. Reduced receptor expression results in slower LDL clearance, leading to higher plasma LDL concentrations, while increased receptor expression enhances LDL uptake and lowers circulating LDL levels [29].

Due to their significant role in lipid metabolism and their implication in pathological conditions, extensive efforts have been made to establish reliable protocols for their isolation and purification [24][8].

Conventional LDL extraction methods have predominantly utilized density-based techniques, such as ultracentrifugation, which separates lipoproteins according to their buoyant density [31]. This method, often implemented alongside salt gradients, is widely recognized for its reliability and reproducibility [31]. To enhance separation, DGUC has been integrated with SEC, allowing for LDL isolation based not only on density but also on particle size (Figure 5) [8].

To assess how different techniques impact protein corona characterization, alternative methods have been investigated. One such approach is PEG precipitation, which efficiently aggregates and precipitates LDL while minimizing the presence of smaller plasma proteins [9].

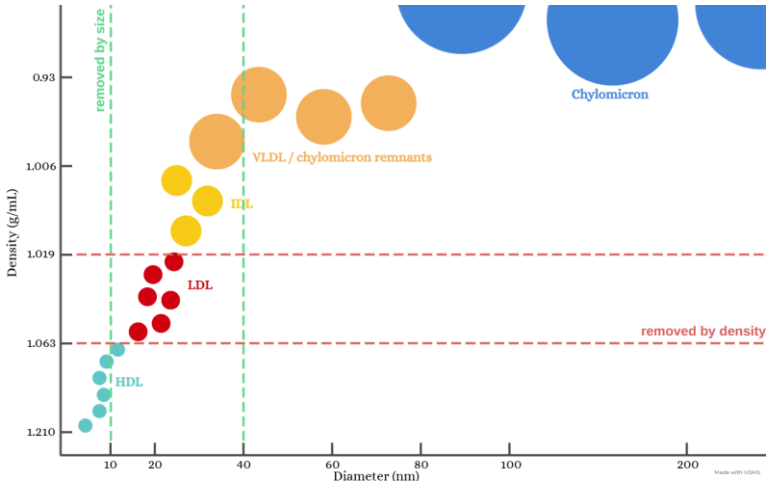

Figure 5 – Schematic overview of the size and density of various lipoproteins, including high-density lipoproteins (HDL), low-density lipoproteins (LDL), intermediate-density lipoproteins (IDL), very low-density lipoproteins (VLDL), and chylomicrons [made with VISME].

1.3 Challenges in Protein Corona Characterization

Despite significant advancements in the study of protein corona, accurately characterizing and isolating this dynamic nanoparticle-protein interface remains a considerable challenge. One of the fundamental obstacles lies in the highly dynamic nature of the protein corona itself [32]. Proteins continuously exchange between the nanoparticle surface and the surrounding biological environment, leading to constant rearrangements in corona composition [32]. This turnover makes it difficult to establish a clear distinction between the tightly bound hard corona and the more transient soft corona, as the boundaries between the two are not always well-defined [33]. The dynamic equilibrium between adsorption and desorption means that experimental conditions, such as temperature, pH, and ionic strength, can strongly influence corona stability, further complicating reproducibility [34].

Another significant challenge arises from the effects of various isolation and purification methods. Each technique employed to separate nanoparticles and their associated protein corona from biological fluids can introduce potential biases that may significantly alter the final composition of the corona. For example, high-speed ultracentrifugation can effectively isolate LDL particles and remove contaminants but may also eliminate loosely bound proteins. In contrast, milder techniques like SEC or precipitation-based methods might retain more proteins but risk co-isolating non-specifically bound biomolecules, which can result in misinterpretation of the findings. Thus, the selection of isolation methods directly impacts the observed properties of the corona.

In addition to challenges related to isolation, the analytical techniques used for characterizing the protein corona have their own limitations. Methods such as MS and SDS-PAGE provide valuable insights into protein composition but differ in sensitivity, specificity, and their ability to detect low-abundance proteins. While MS is highly sensitive, it may still overlook proteins present in trace amounts that are critical for the functionality of the corona. The complexity of biological fluids, which contain thousands of proteins at varying concentrations, adds another layer of difficulty in identifying and quantifying proteins associated with the corona.

1.4 Thesis Objectives

The primary objective of this thesis is to investigate the composition and characteristics of the protein corona associated with LDL particles and how different isolation and purification methods influence the purity and homogeneity of the LDL population. By systematically comparing various extraction techniques, including DGUC, PEG precipitation, and FPLC, this research aims to determine how each method affects the retention or removal of both the hard and soft coronas. Particular attention is given to the effects of these methods on the physical properties of LDL and protein composition, to better understand how methodological variations shape experimental outcomes. Proteomic analysis is employed to refine protein corona characterization, offering deeper insights into the interaction between LDL and corona proteins. Ultimately, by harnessing the unique protein-nanoparticle interactions that occur between lipoproteins and surrounding biomolecules, through the careful selection and optimization of appropriate isolation protocols, it becomes possible to manipulate and control the formation of the protein corona on lipoproteins. This ability to regulate the protein composition surrounding lipoproteins opens exciting possibilities for advancing lipoprotein-based approaches in disease detection and therapeutic applications, offering a promising pathway for more targeted and effective strategies in both diagnostics and treatment.

2. Materials

1X phosphate buffer saline (pH = 7.4, without calcium, magnesium), sodium chloride (NaCl), ethylenediaminetetraacetic acid disodium (EDTA), sodium bromide (NaBr), sudan red 7B, polyethylene glycol (PEG) 10000, healthy human serum H5667 were purchased from Sigma-Aldrich. This serum was from USA males with AB type blood and was heat-inactivated serum extracted from clotted whole blood.
Sodium hydroxide (NaOH), acetone, Qubit Protein Assay Kit (100 assays), NuPAGE™ 4 to 12% Bis-Tris Gel, NuPAGE™ LDS Sample Buffer (4×), Invitrogen™ NuPAGE™ Sample Reducing Agent (10×), NuPAGE™ MES SDS Running Buffer (20×), Invitrogen™ NuPAGE™ Tricine SDS Sample Buffer (2×), PageRuler Unstained Broad Range Protein Ladder, uranyl acetate, low-density lipoprotein from human plasma (LDL) were purchased from ThermoFisher Scientific.
Potassium bromide (KBr) was purchased from Millipore.
Ultra-Clear centrifuge tubes were purchased from Beckman Coulter.
Chromafil Xtra PES-45/25 syringe filters were purchased from Macherey-Nagel Gmbh & Co.
InstantBlue® Coomassie Protein Stain was purchased from Abcam.
Carbon Film 400 Mesh Copper Grid was purchased from Electron Microscopy Sciences.
Polystyrene (PS) cuvettes were purchased from Sarstedt.

3. Methods

3.1 Extraction of LDL from Serum via DGUC

The protocol established by Redgrave et al. [35] is employed with modifications. Specifically, 11.4 g NaCl, 0.1 g EDTA and 1 mL 1M NaOH are dissolved in 1000 mL Milli-Q water to achieve a density of 1.006 g/mL. The solution is marked as A. 100 mL A is mixed with 1.017 g NaBr to achieve a solution with density at 1.019 g/mL, marked as B. 100 mL A is mixed with 7.83 g NaBr to achieve a solution with density at 1.063 g/mL, marked as C.
To achieve a discontinuous density gradient in a 38.5 mL Ultra-Clear centrifuge tube (25×89 mm), 4 mL A is added first, followed by 9 mL B and 9 mL C. B and C are layered carefully at the bottom of the previous layers. 9 mL H5667 and 2.925 g KBr are mixed to adjust serum's density to 1.21 g/mL, which is layered at last.
The prepared tubes are placed into the rotor of the Optima XPN-80 Ultracentrifuge (Beckman Coulter) equipped with a swinging-bucket rotor SW32 (Beckman Coulter) and centrifuged at 31500 rpm and 8 °C for 48 hours, as shown in Figure 6.

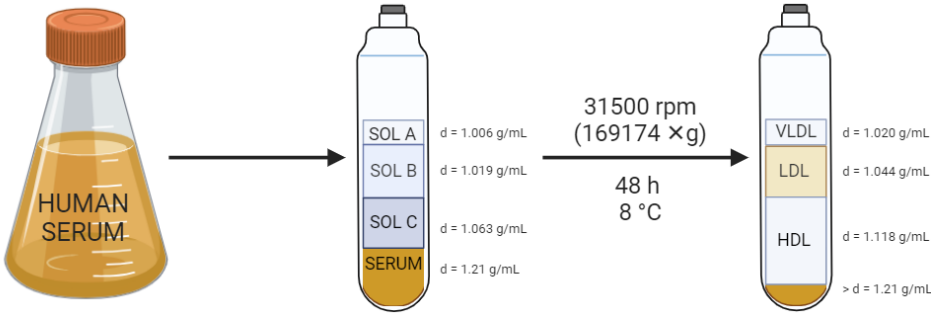

Figure 6 – Schematic representation of the outlined protocol for LDL extraction.

Following ultracentrifugation, the upper 5 mL of the gradient, corresponding to the VLDL fraction, is carefully removed and discarded using a pipette with a cut tip. The visible 8 mL of yellow band (Figure 7), representing the LDL fraction, is then collected, while the remaining 18 mL are discarded.

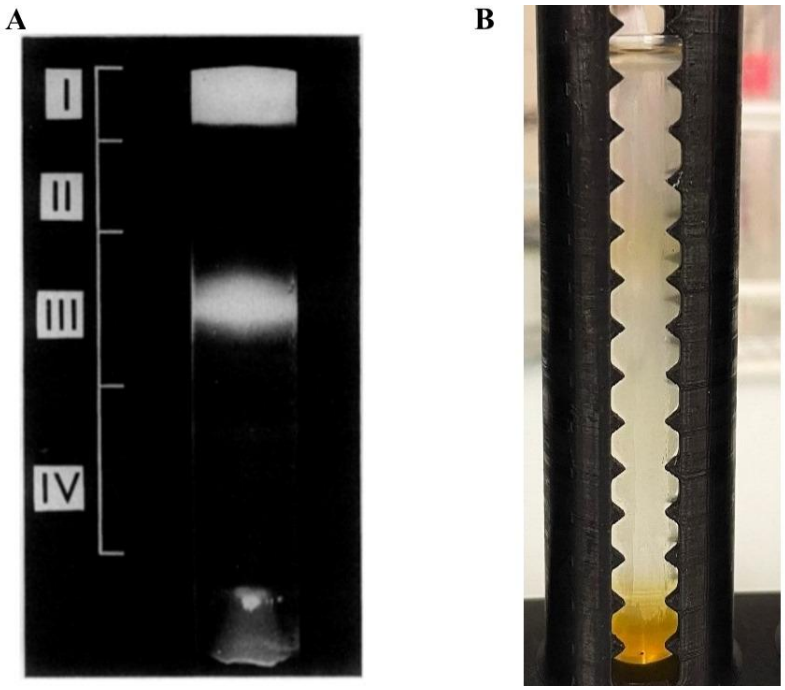

Figure 7 – Photographs of the gradient in the centrifuge tube following lipoproteins separation. (A) In band III, LDL is clearly visible as a distinct orange-yellow band [35]. (B) Consistently with findings from [35], the formation of band III, corresponding to LDL fraction, is also observed in this experiment.

3.1.1 DGUC followed by FPLC

The band collected in 3.1 is concentrated using a Amicon® Ultra-15 Centrifugal Filters Ultracel-100K (20 min, 5000 rpm, 10 °C), before purification using SEC. The FPLC workstation consists of an automatic ÄKTA go™ system Cytiva, and a Superdex 200 Increase 10/300 GL agarose-crosslinked column (Cytiva, Sweden AB). 1X PBS is used as the elution and equilibration buffer.

One injection is performed into the column using a 500 µL capillary loop and a flow rate of 0.75 mL/min. The sample absorption at 280 nm is automatically recorded and applied to group different fractions based on absorption peaks. For collection, the fraction size is kept at 0.5 mL. Liquids from the same peak are collected. Specifically, the only peak obtained includes fractions 5, 6 and 7 and it corresponds to 8-9 mL of the elution volume (Figure 8).

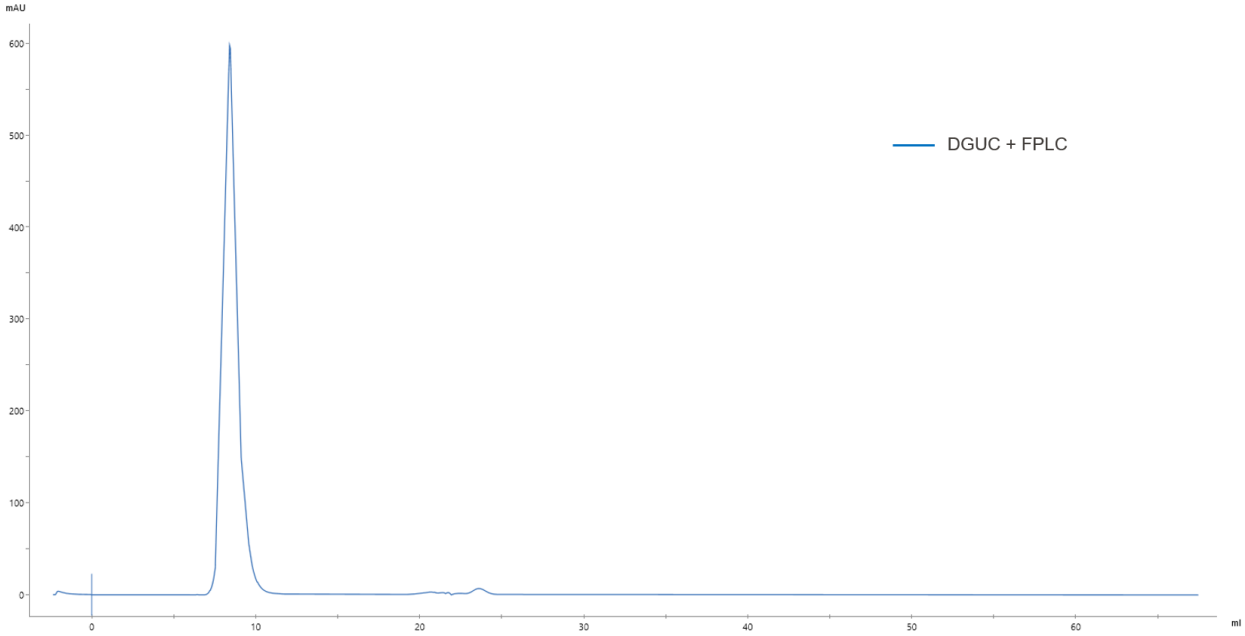

Figure 8 – Chromatogram obtained through FPLC according to the outlined protocol.

3.1.2 DGUC followed by PEG precipitation and FPLC

5 mL of the LDL band collected after DGUC is concentrated using Amicon® Ultra-15 Centrifugal Filters Ultracel-100K under 5500 rpm, 4 °C until the total volume is 0.6 mL.
The concentrated sample is then diluted to a final volume of 6.0 mL with 1X PBS and centrifuged at 17000 × g for 30 minutes at 4 °C using the Sorvall Legend X1R Centrifuge (ThermoFisher Scientific).
The sample is filtered through a 0.45 µm PES membrane. 1.2 mL of a 50% (w/v) PEG 10K solution is added to the supernatant. After thorough vortexing, the sample is incubated at 4 °C for 1 hour and then centrifuged at 1800 × g for 15 minutes at 4 °C using the same centrifuge. The supernatant is carefully discarded, and the sedimented lipoproteins are resuspended in 0.7 mL of 1X PBS. Complete dissolution of the pellet is achieved through vortexing and sonication using an ultrasonic bath (Ultrasonic Bath Sonicator).
LDL is purified after PEG precipitation using SEC. It is performed one injection into the column using a 500 µL capillary loop and a flow rate of 0.75 mL/min. The outlined procedure is shown in Figure 9.

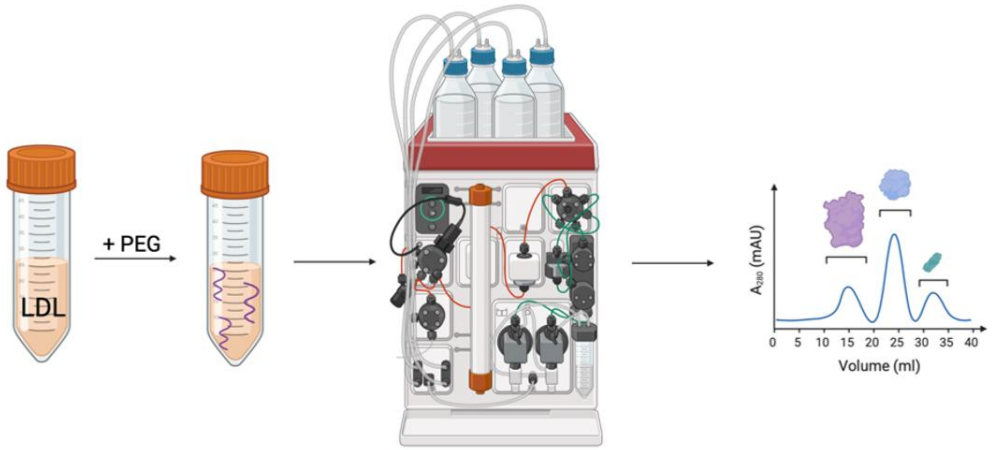

Figure 9 – Schematic representation of the procedure outlined above.

A distinct peak, corresponding to 8-9 mL of the elution volume, is observed (Figure 10), and the respective fractions are collected.

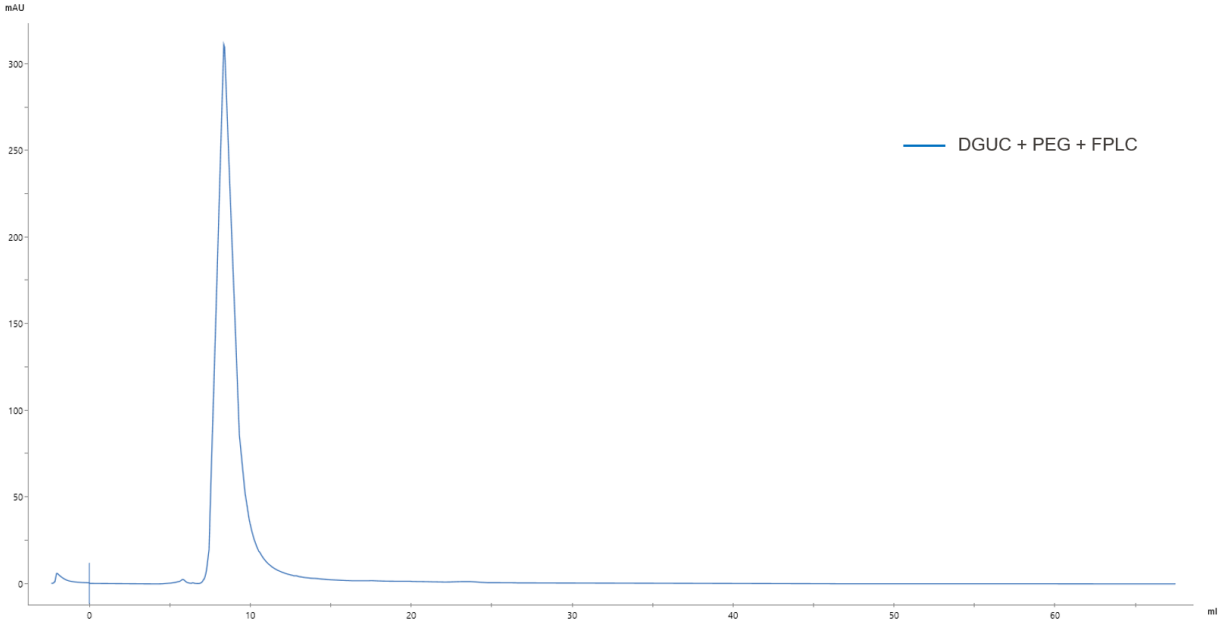

Figure 10 – Chromatogram obtained through FPLC according to the outlined method.

3.1.3 DGUC with Multiple Filtration Steps followed by FPLC

After collecting the LDL band following DGUC, 5 mL is subjected to multiple filtrations using a Amicon® Ultra-15 Centrifugal Filters Ultracel-100K under 5500 rpm, 4 °C until the total volume is 0.6 mL. Subsequently, FPLC is performed. The outlined procedure is shown in Figure 11. One injection is made into the column using a 500 µL capillary loop and a flow rate of 0.75 mL/min. The only peak present, corresponding to 8-9 mL of the elution volume, is collected (Figure 12).

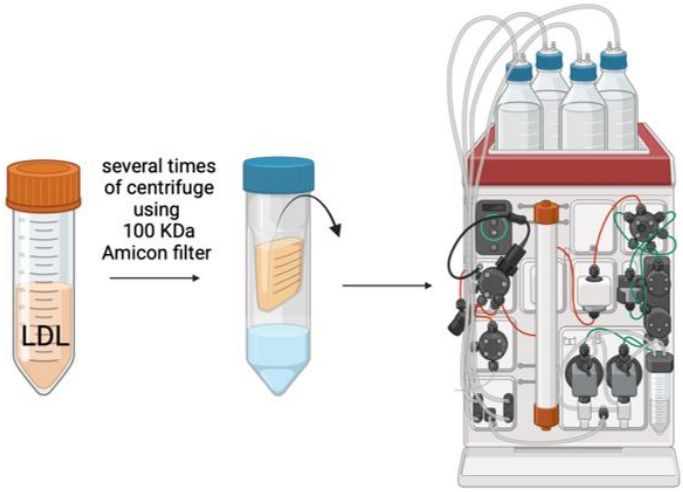

Figure 11 – Schematic representation of the procedure outlined above.

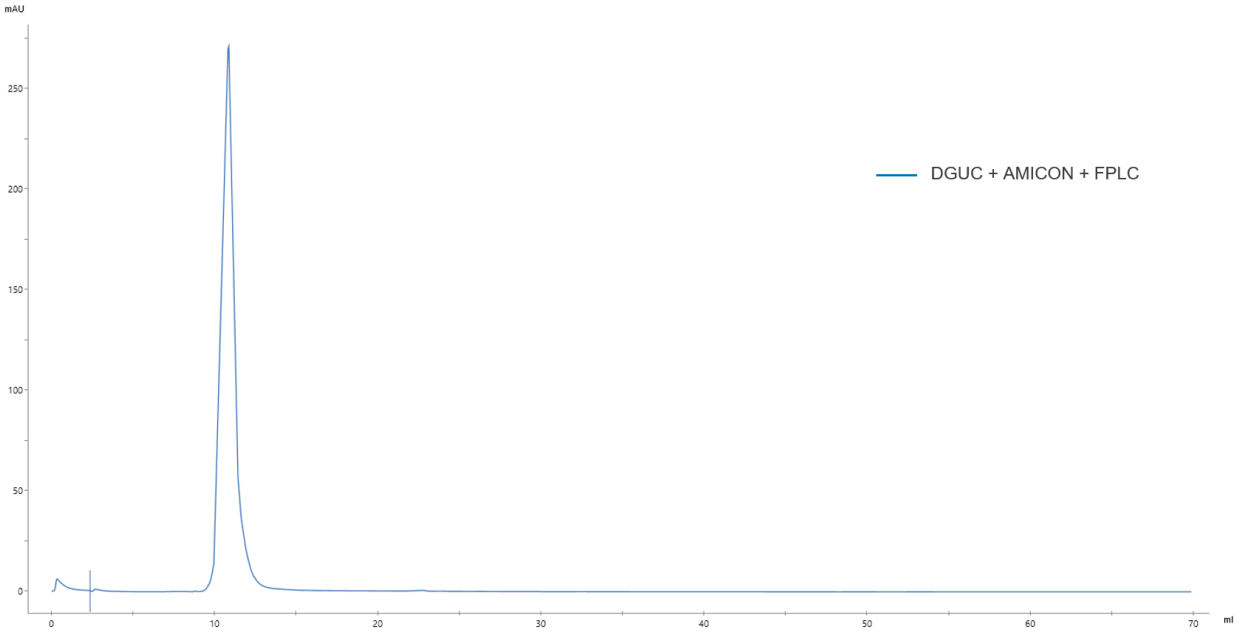

Figure 12 – Chromatogram obtained through FPLC according to the outlined method.

3.2 Extraction of LDL from Serum without DGUC

This analysis starts with Human Serum H5667 as the initial sample, which is diluted 40 times with PBS to reach a final volume of 1 mL, marked as “serum”.

3.2.1 Extraction of LDL from Serum by FPLC

The second sample is obtained by performing FPLC on Human Serum H5667. The first peak shown in Figure 13, corresponding to 8-9 mL of the elution volume, is collected and marked as “serum-FPLC”.

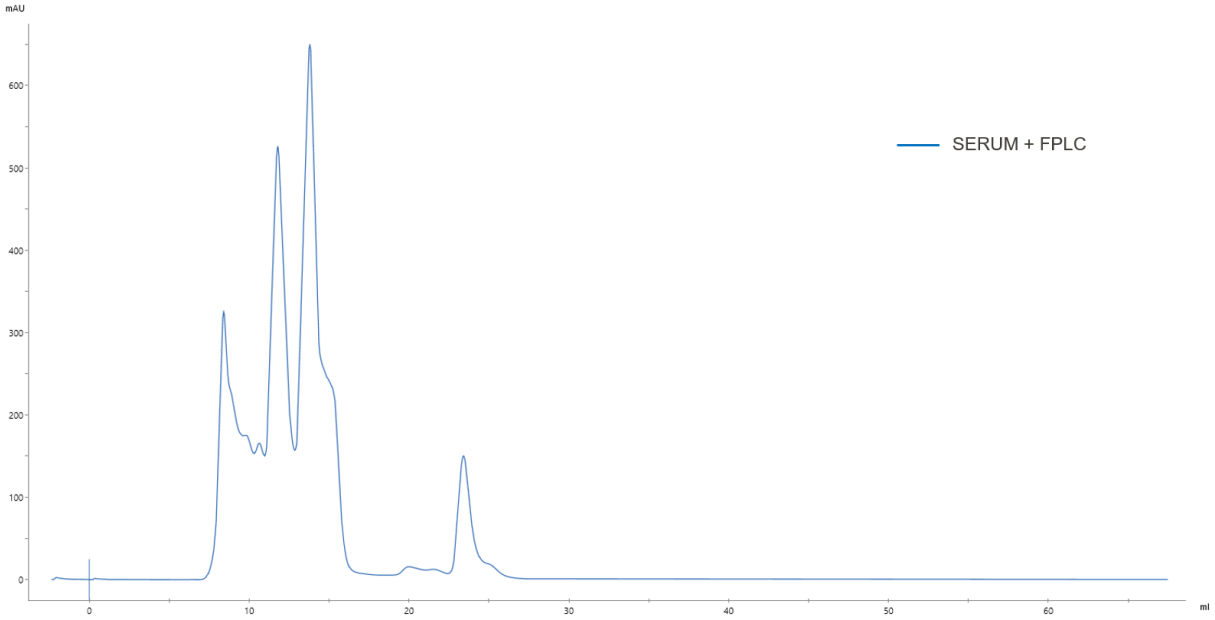

Figure 13 – Chromatogram acquired via FPLC from H5667 Human Serum.

3.2.2 Extraction of LDL from Serum using PEG Precipitation followed by FPLC

0.6 mL of Human Serum H5667 is diluted to a final volume of 6.0 mL with 1X PBS and centrifuged at 17000 × g for 30 minutes at 4 °C using the Sorvall Legend X1R Centrifuge.
The sample is filtered through a 0.45 µm PES membrane. 1.2 mL of a 50% (w/v) PEG 10K solution is added to the supernatant. After thorough vortexing, the sample is incubated at 4 °C for 1 hour and then centrifuged at 1800 × g for 15 minutes at 4 °C using the same centrifuge. The supernatant is carefully discarded, and the sedimented lipoproteins are resuspended in 1 mL of 1X PBS. The complete dissolution of the pellet is ensured through vortexing and sonication.
Another round of precipitation is performed by adding 0.2 mL of PEG 10K (50% w/v solution) to the resuspended sample. The mixture is vortexed, incubated at 4 °C for 30 minutes and centrifuged again under the same conditions (1800 × g, 4 °C, for 15 minutes) using the Centrifuge 5424 R (Eppendorf). After centrifugation, the supernatant is discarded, and the pellet is resuspended in 0.7 mL of 1X PBS. The complete dissolution of the pellet is ensured through vortexing and sonication.
After PEG precipitation the sample is purified using SEC. It is performed one injection into the column using a 500 µL capillary loop and a flow rate of 0.75 mL/min. The outlined procedure is shown in Figure 14.

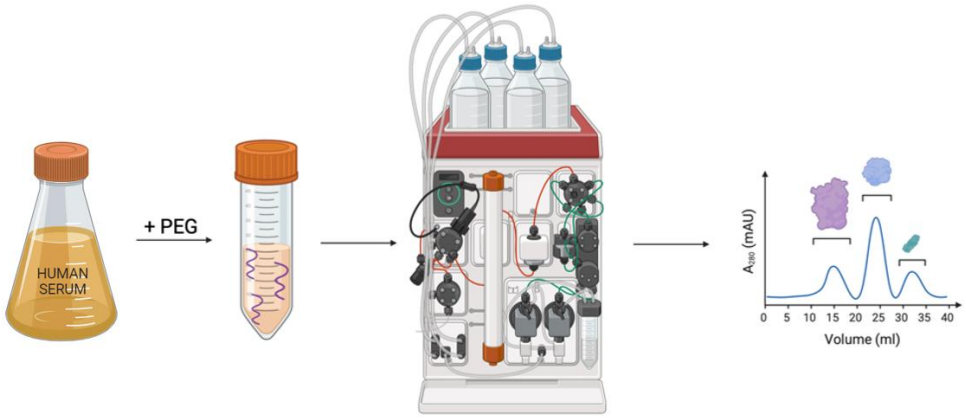

Figure 14 – Schematic representation of the procedure outlined above.

The first peak shown in Figure 15, corresponding to 8-9 mL of the elution volume, is collected and marked as "serum-PEG-FPLC".

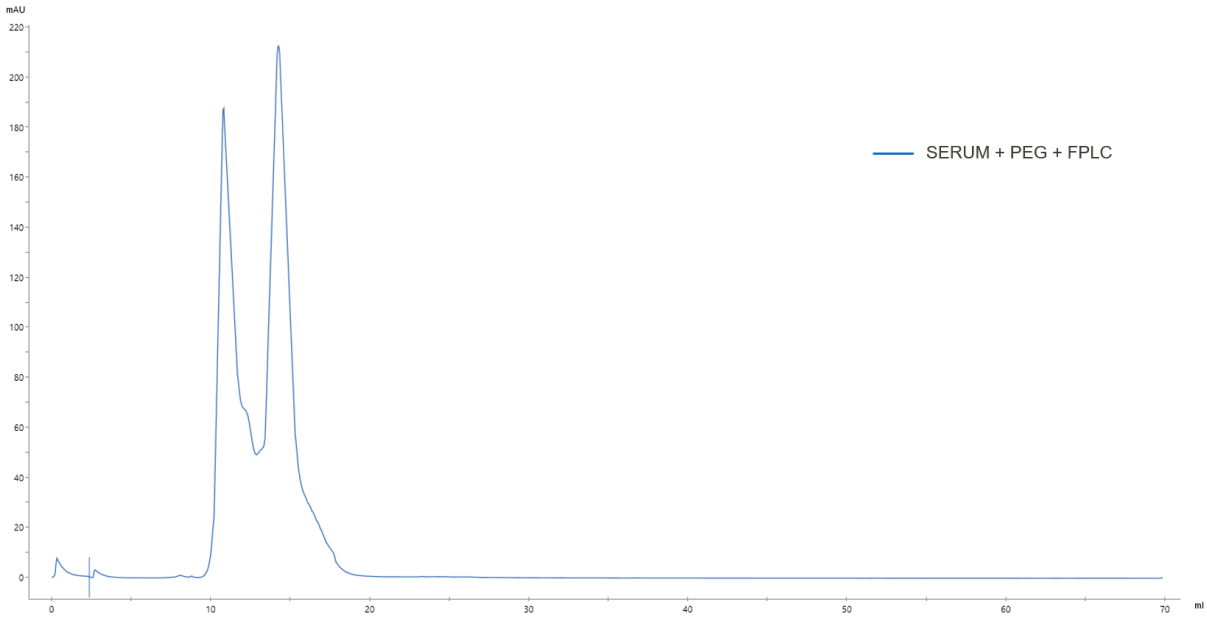

Figure 15 – Chromatogram acquired via FPLC following PEG precipitation of H5667 Human Serum.

3.3 Characterization Methods for Isolated LDL

3.3.1 FPLC Purification and Analysis of LDL

FPLC is a medium-pressure technique used for protein purification. It utilizes a peristaltic pump to ensure a stable flow rate, while injection valves regulate the eluent composition [36]. The system is automated, integrating sample injectors, gradient controllers, and detectors to monitor separation efficiency [36].

For these experiments, the Superdex 200 Increase 10/300 GL column is used with an ÄKTA go™ system (Figure 16). This SEC column, composed of a cross-linked agarose and dextran matrix, enables the separation of proteins ranging from 10 to 600 kDa [37]. It has a total volume of 24 mL, operates at flow rates between 0.5 and 1.5 mL/min, and can withstand

pressures up to 5 MPa [37].
Proper column maintenance and sample preparation are essential. The process begins with selecting an appropriate buffer, typically 1X PBS. Before sample injection, the column must be equilibrated with at least two column volumes of PBS. After use, thorough washing with a PBS volume four times greater than the loop volume is required.
Sample volume and concentration are also critical factors. The Superdex 200 Increase 10/300 GL column is designed for protein concentrations between 1–5 mg/mL [37]. In this thesis, a 500 µL injection loop is used, determining the injection volume.

Figure 16 – ÄKTA go™ protein purification system from Cytiva.

3.3.2 SDS-PAGE for LDL Protein Composition Analysis

SDS-PAGE is a technique used to separate proteins primarily by their molecular weight. In this method, proteins are treated with SDS, which imparts a uniform negative charge to them [38].
To perform SDS-PAGE, a NuPAGE™ 4-12% Bis-Tris Gel (1.0 mm×12 well) is used in combination with NuPAGE™ MES SDS Running Buffer (20×). The running buffer is diluted at a 1:20 ratio by mixing 50 mL of the stock solution with 1 L of Milli-Q water. Once prepared, the gel cassette is carefully opened to create the wells for sample loading. The gel is then placed into the electrophoresis chamber, and the running buffer is poured into the chamber to cover the gel.
For sample preparation, 5 µg of protein is taken from each sample, with the corresponding volume calculated based on the protein concentration measured using the Qubit Protein Assay

Kit and the Qubit 4 Fluorometer (Thermo Fisher Scientific).
If reducing agent is required, 5 µL of Bolt LDS Sample Buffer (4×) and 5 µL of NuPAGE™ Sample Reducing Agent (10×) are added to each tube. For non-reducing SDS-PAGE, 10 µL of Tricine SDS Sample Buffer (2×) is used instead. A total volume of 20 µL from each prepared sample is then loaded into the wells of the gel. For molecular weight reference, 5 µL of PageRuler Unstained Broad Range Protein Ladder is loaded into one well.
Electrophoresis is carried out at 150 V, 120 mA, and 150 W for a total duration of 45 minutes, during which proteins migrate through a polyacrylamide gel matrix. Once the electrophoresis is complete, the gel is carefully removed from the apparatus and placed into a container with InstantBlue® Coomassie Protein Stain. The protein bands are visualized and imaged using the GelDoc Go Gel Imaging System (Bio Rad).
Under reducing conditions, the bands correspond to the molecular weight of individual polypeptide subunits, while in the absence of reducing agents, the bands reflect the molecular weight of the intact protein [38]. By comparing migration patterns under both conditions, the total protein size and the size of its subunits can be determined [39].

3.3.3 DLS Analysis of LDL size

DLS is a technique used to analyze the size distribution of particles, typically in the nanometer to the submicron range, by measuring the scattering of laser light caused by particles in suspension [40]. The scattered light intensity fluctuates due to the random motion of particles driven by Brownian motion [41]. These fluctuations provide insights into the hydrodynamic size and movement of the particles, with smaller particles moving more rapidly than larger ones [41]. However, DLS has limited resolution, which can complicate the accurate characterization of polydisperse samples that contain a wide range of particle sizes.
This technique operates by directing a monochromatic laser at particles suspended in a liquid [42]. As the laser interacts with the particles, it scatters in different directions, creating an interference pattern that fluctuates due to particle motion. These fluctuations are captured by a detector positioned at a fixed angle, typically 90° or 173°, and analyzed for Doppler broadening [42]. The intensity fluctuations are processed by a digital autocorrelator, which generates a correlation function that provides information about the particles' diffusion coefficients. Using the Stokes-Einstein equation, the hydrodynamic radius of the particles can be determined, reflecting their apparent size, including the hydration shell and solvation layers surrounding them [40].
In this thesis, the Litesizer 500 (Anton Paar) is used to determine the hydrodynamic size and distribution of LDL particles (Figure 17). Specifically, the size distribution chart is generated through the one-page workflow of the Litesizer 100/500 software.
For DLS analysis, samples are prepared in disposable polystyrene cuvettes (10×10×45 mm). The system temperature is kept constant at 20 °C, and up to 60 scans are performed, each lasting 10 seconds. Measurements are conducted in a backscatter configuration, with a 10 mM NaCl solution used as the solvent to minimize electrostatic interactions between particles.

Figure 17 – Anton Paar Litesizer 500 Particle Analyzer.

3.3.4 TEM Analysis of LDL structure

TEM is a method used for visualizing structures at the atomic level. To produce an image in TEM, a high-energy electron beam is transmitted through an ultra-thin sample, typically less than 100 nm thick, which is transparent to electrons [43]. The microscope consists of a series of electromagnetic lenses and apertures that focus the electron beam onto the sample and magnify the resultant image [44]. This image is then projected onto a phosphor screen or captured by a specialized camera [44].

For negative-stained TEM characterization, sample preparation begins with 400 Mesh Copper Grids coated with a carbon film. Since these grids are hydrophobic, they are treated using the ELMO Glow Discharge System. This treatment exposes the grids to a glow discharge at 30 mA for 30 seconds.

Subsequently, 4 µL of the sample are applied to the carbon-coated side of the grid. The sample is allowed to sediment for 1 minute, then excess liquid is blotted off with filter paper. The grid is then washed with a drop of water for 30 seconds, blotted again, and stained with 5 µL of 1% (v/v) uranyl acetate for 1 minute. Finally, the grid is blotted once more and allowed to air-dry at room temperature for 1 minute before being ready for TEM analysis.

The images are recorded and acquired using a Talos L120C (120 kV) microscope equipped with a Ceta S 16M CMOS camera (4k×4k).

3.3.5 SV-AUC Analysis of LDL Physical Properties

AUC is a technique used to study particles' sedimentation behaviour and provide insights into their size and molar mass. Developed by Svedberg in the 1920s [45], AUC analyzes nanoparticles ranging from 1 nm to 5000 nm by separating them based on density and molecular weight. It operates through two main approaches: SV and SE.

In SV experiments, high-speed centrifugation forces particles to sediment, allowing for the

determination of particle size and shape based on the sedimentation coefficient s and diffusion coefficient D [45]. This approach enables the analysis of particle motion under high centrifugal forces [45]. Conversely, SE experiments, conducted at lower speeds, establish an equilibrium between sedimentation and back-diffusion of particles in solution [46]. They are primarily used to determine molar mass, stoichiometry, and equilibrium constants in protein interactions [47][48].
The experiments are conducted using the Beckman Coulter XL-I ultracentrifuge (Figure 18).

Figure 18 – Beckman Coulter XL-I.

For velocity runs, sector-shaped sample compartments are employed to minimize convection disturbances [49]. These compartments are essential as they allow the particles to move along radial paths, preventing interference from wall collisions [49]. Double-sector cells are used to measure absorbance differences between the sample and solvent sectors, helping to account for solvent redistribution and absorption effects under high centrifugal forces (Figure 19) [49].

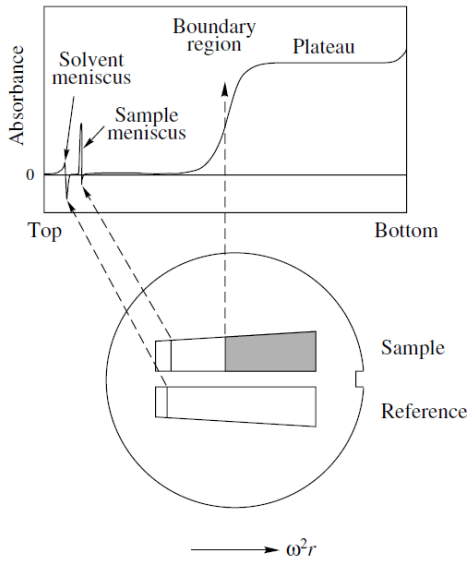

Figure 19 – In a double-sector centerpiece, the sample moves towards the bottom of the sector-shaped container to minimize convection. The reference sector is typically filled just slightly more than the sample sector to ensure that the solvent meniscus does not overlap with the sample profile [50].

With the 8-hole Beckman rotors, up to seven samples can be analyzed simultaneously, with one position reserved for a radial calibration cell.

The absorbance detection system operates similarly to a double-beam spectrophotometer and follows the Beer-Lambert law [50]. It uses monochromatic light across a broad wavelength range, allowing the identification of different species with non-overlapping absorption spectra [49]. Specifically, the system includes several key components: a Xenon flash lamp for light generation, a monochromator to select the desired wavelength, a sample cell to hold the sample, a slit assembly to track radial absorbance changes, and a photomultiplier tube (PMT) to convert light signals into digital data (Figure 20) [51].

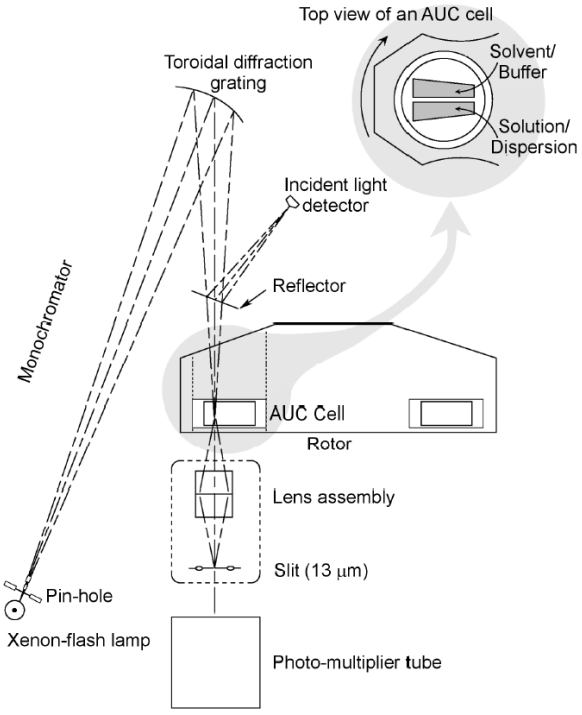

Figure 20 – The light path in an absorbance optical system (Beckman Coulter Optima XL-A/XL-I AUC) [50].

This setup ensures high precision, with a typical accuracy of ± 0.01 optical density (OD) [49].
The SV experiments are conducted using absorbance optics. For this reason, it is essential to keep the absorbance within the linear range of Beer's Law (0.2–1.0 OD). The sample cells are assembled with standard double-sector centerpieces featuring quartz windows. The reference sector is filled with 430 µl of buffer, while the sample sector holds 420 µl of the sample solution.
Once the cells are assembled, they are loaded into the rotor along with a properly balanced counterweight. The rotor is then inserted into the centrifuge, the monochromator is positioned, and the vacuum system is activated (Figure 21).

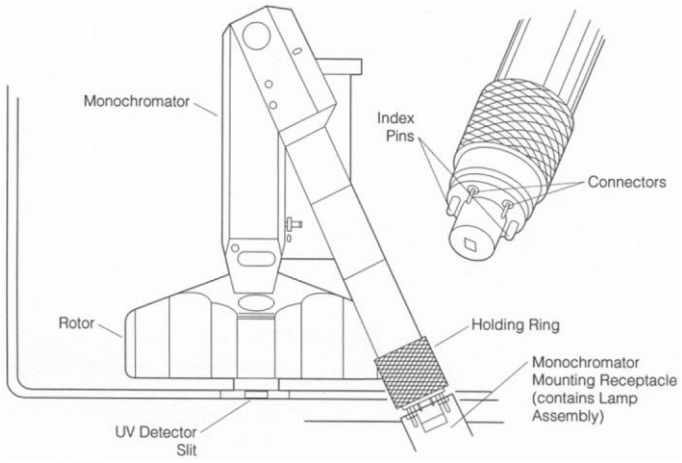

Figure 21 – Mounting the monochromator [51].

Initially, the speed is set to zero while the rotor remains stationary, allowing the diffusion pump to activate and reduce the vacuum to below 100 µm. This step ensures that the temperature measurement accurately reflects the rotor's temperature. Once the desired temperature is reached, the system is allowed to equilibrate for at least two hours before acceleration, minimizing convection effects caused by temperature gradients and stabilizing the samples.
Key operating parameters in SV experiments include temperature, rotor speed, scan timing, and the number of scans. To maximize the number of data sets for analysis, the scan delay and scan interval should be set to zero in the Beckman Coulter ProteomeLab software.
The resolution of solution components is proportional to ω^2, meaning higher rotor speeds improve the differentiation of components. Additionally, to ensure consistent hydrodynamic measurements, sedimentation and diffusion coefficients are typically standardized to 20 °C.
All these parameters are controlled through the instrument's hard-key console, with real-time values displayed alongside preset conditions for continuous monitoring (Figure 22).

Figure 22 – Console of Beckman Coulter XL-I.

3.3.6 MS-based Proteomics for Analyzing LDL Protein Composition

Proteomics is the study of proteins in a biological model, focusing on their identification, quantification, characterization, and functional understanding under various conditions [52].
The set of proteins expressed at any given time in a cell, tissue, or organism is referred to as the proteome [52]. MS-based proteomics is a technique used for identifying and characterizing proteins [53]. This method involves enzymatically digesting proteins and analyzing the resulting peptides using liquid chromatography coupled with tandem mass spectrometry (LC-MS/MS) [52]. The peptides are identified by comparing their MS/MS spectra to theoretical spectra from protein databases, with statistical algorithms ensuring accurate identification [52][54].
At the Proteomics Core Facility (PCF) at EPFL [52], high-resolution MS is used to measure the mass-to-charge ratio (m/z) of peptide ions and fragments for detailed analysis. The workflow begins with the lysis of biological samples to extract proteins, which are then denatured, reduced, and alkylated before being enzymatically digested into smaller peptides suitable for analysis [54]. The peptides are introduced into an LC system where they are separated before being ionized by electrospray ionization (ESI), which converts them into charged particles [54]. Once ionized, the peptides are filtered in the mass spectrometer using a quadrupole mass filter, based on their m/z ratio [54]. They are then fragmented in a collision cell to produce product ions, which are isolated and detected by a second quadrupole [54]. The resulting mass spectra are compared to theoretical spectra from protein databases [52][54].
Quantification is performed using label-free methods, such as peak intensity-based quantification and spectral counting, to measure protein abundance across different conditions [55].
For the proteomic analysis, each sample is prepared in technical triplicate. Protein concentration is measured using the Qubit Protein Assay Kit in combination with the Qubit 4 Fluorometer. Based on the measured concentration, the appropriate sample volume is calculated to adjust the total protein amount to 100 µg.
Subsequently, the samples are submitted to the PCF for processing and performing the MS analysis to investigate the protein composition of the lipoprotein corona.

4. Results and Discussion

4.1 LDL Physical Properties

4.1.1 DLS Analysis of LDL Extracted from Serum via DGUC

The results in this subsection are based on samples processed with DGUC for LDL isolation. This method allows for the separation of lipoprotein classes according to their density. To enhance the isolation process, various techniques are applied post-DGUC. One approach involves further separating the LDL fraction using FPLC to account for both size and density, referred to as the DGUC-FPLC sample. Another method involves PEG precipitation prior to FPLC, labelled as the DGUC-PEG-FPLC sample, while the third approach includes multiple filtration steps between DGUC and FPLC purification, marked as the DGUC-filtrations-FPLC sample.

The DLS analysis presented in Figure 23 provides an evaluation of the size distribution of LDL particles isolated using the different purification methods described above. The number-weighted distribution curves show a dominant peak around 20 nm for all conditions, indicating that the main LDL population remains similar across the different purification strategies. Specifically, the number-weight DLS curves highlight the number of particles within each size range, normalizing based on the total number of particles.

This approach reflects the relative frequency of each size, with a greater emphasis on the more abundant particles. However, slight variations in peak height and width suggest differences in particle size distribution and potential aggregation among the samples.

Notably, the LDL fractions obtained via DGUC-filtrations-FPLC, as well as DGUC-FPLC, display a slightly more pronounced peak, suggesting a tendency toward a more uniform particle population. In contrast, the method DGUC-PEG-FPLC exhibits a broader distribution, which may suggest a higher presence of polydisperse species, although the distinction is not strongly marked.

To ensure the reliability of the results and account for potential variability, three separate DLS measurements are performed for each sample. The peak mean values and standard deviations are reported in Table 2 for clarity and comparison. The peak of the LDL fraction obtained through DGUC-PEG-FPLC is at a smaller mean diameter compared to the other fractions, but the standard deviation, on the other hand, increases. These findings support the previous hypotheses, which were based on a visual inspection of the graph.

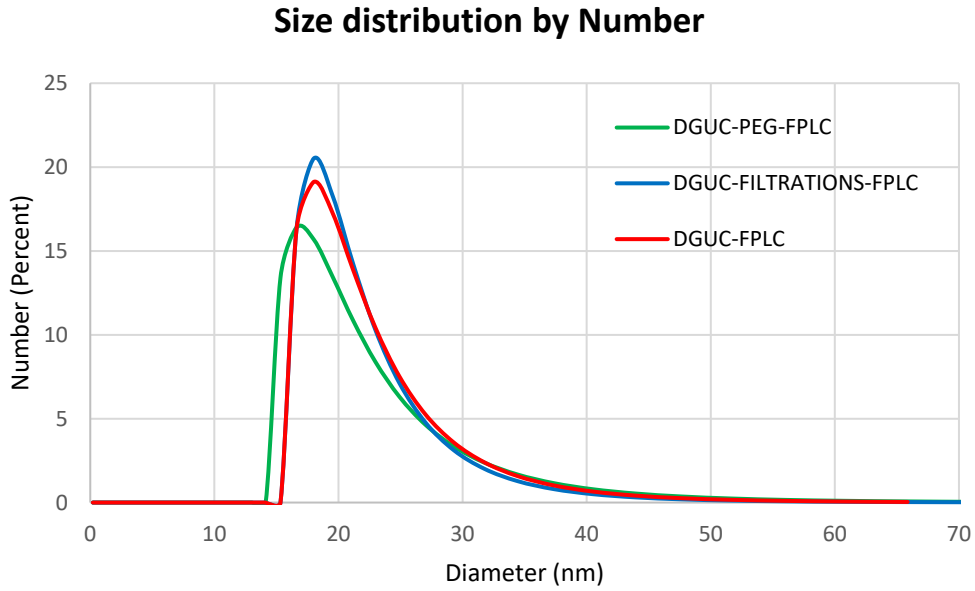

Figure 23 – Number-weighted DLS distribution of LDL particles isolated from different DGUC purification methods.

Samples	Peaks Mean (nm)	Dv. Standard (nm)
DGUC-FPLC	21.692	3.946
DGUC-PEG-FPLC	20.873	4.025
DGUC-filtrations-FPLC	21.487	3.816

Table 2 – Mean and standard deviation values from three measurements for each analyzed sample.

4.1.2 DLS Analysis of LDL Extracted from Serum via FPLC and with PEG precipitation followed by FPLC

The results in this subsection are based on samples processed directly from Human Serum H5667 for LDL isolation using different strategies. These methods comprise the direct analysis of serum as a control, FPLC purification (serum-FPLC sample), and an additional PEG precipitation step prior to FPLC (serum-PEG-FPLC sample).

The DLS analysis illustrated in Figure 24 evaluates the size distribution of LDL particles obtained from these approaches. The number-weighted distribution curve for the serum sample exhibits a sharp peak around 10 nm, confirming the presence of various serum components, such as albumin and other small lipoproteins. In contrast, the serum-FPLC sample exhibits a dominant peak between 20-25 nm, corresponding to the peak collected from the SEC-based purification at an elution time of 8-9 mL, which aligns with the LDL size range. This indicates that FPLC effectively isolates LDL based on size. Finally, the serum-PEG-FPLC sample also

shows a peak in the LDL size range but with a broader distribution, which points to a more polydisperse distribution.
To ensure the reliability of these results, three independent DLS measurements are performed for each sample, with the mean values and standard deviations reported in Table 3 for clarity and comparison. These results confirm that FPLC purification enhances LDL isolation, with some variations in polydispersity when PEG precipitation is applied. As expected, the serum sample shows a mean particle size of 12.01 nm, reflecting smaller serum components.

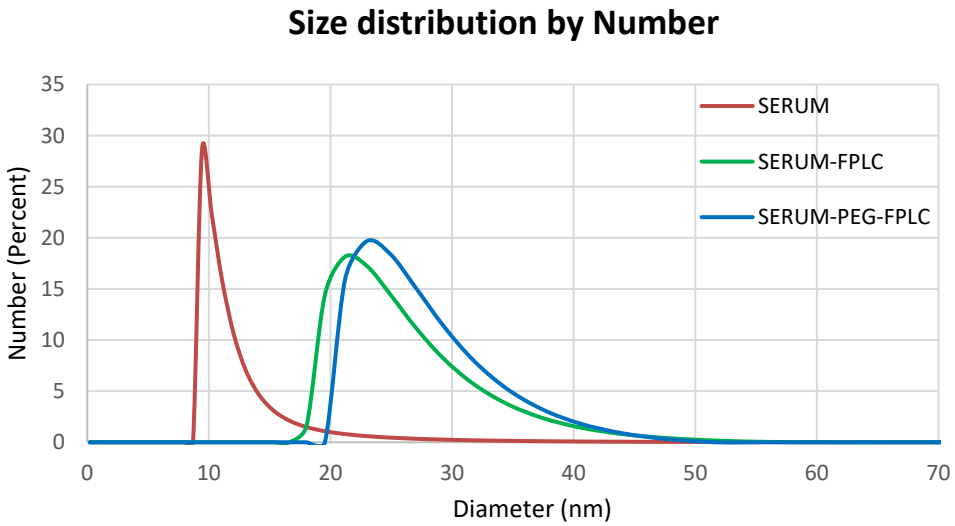

Figure 24 – Number-weighted DLS distribution of LDL particles isolated directly from serum without DGUC.

Samples	Peaks Mean (nm)	Dv. Standard (nm)
Serum	12.00995	2.22108
Serum-FPLC	22.33432	3.83515
Serum-PEG-FPLC	23.18824	3.84929

Table 3 – Mean and standard deviation values from three measurements for each analyzed sample.

4.1.3 TEM Analysis of LDL Extracted from Serum via DGUC

A negative-stained TEM characterization is conducted on LDL particles extracted from serum using the DGUC-FPLC method. The result, presented in Figure 25, demonstrates that the isolated lipoproteins are highly homogeneous, with significantly reduced contamination.
The sample exhibits a consistent size distribution, predominantly ranging from 20 to 30 nm in diameter. This indicates that the DGUC-FPLC method effectively isolates LDL particles with a uniform structure, providing a reliable approach for studies on lipoprotein properties and behaviour.

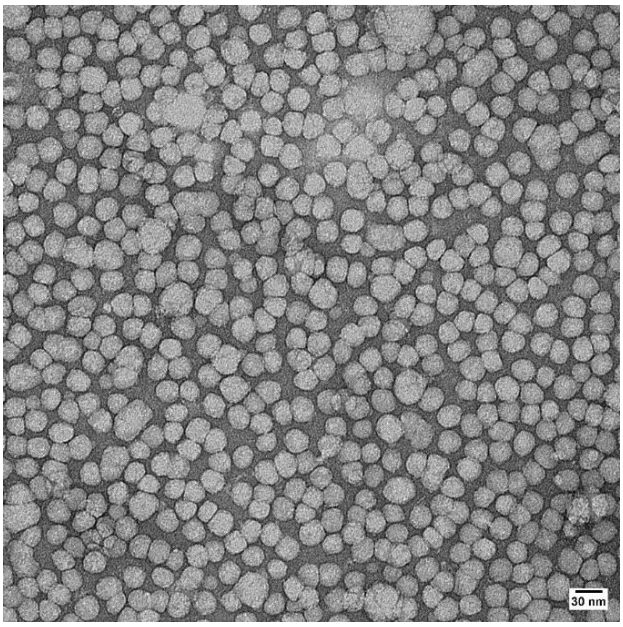

Figure 25 – Negative-stained TEM image of LDL particles extracted via the DGUC-FPLC method.

4.1.4 TEM Analysis of LDL Extracted from Serum via FPLC and with PEG precipitation followed by FPLC

A negative-stained TEM analysis is performed on LDL particles extracted using the serum-FPLC method. The result, shown in Figure 26, reveals a noticeable presence of impurities and a less homogeneous and uniform distribution of particles. The isolated lipoproteins exhibit a broader size range, suggesting that the serum-FPLC method does not isolate LDL with the same level of purity and uniformity. These findings underscore the challenges in achieving high-quality LDL isolation directly from serum, indicating the need for further refinement of the extraction process to enhance particle homogeneity and purity.

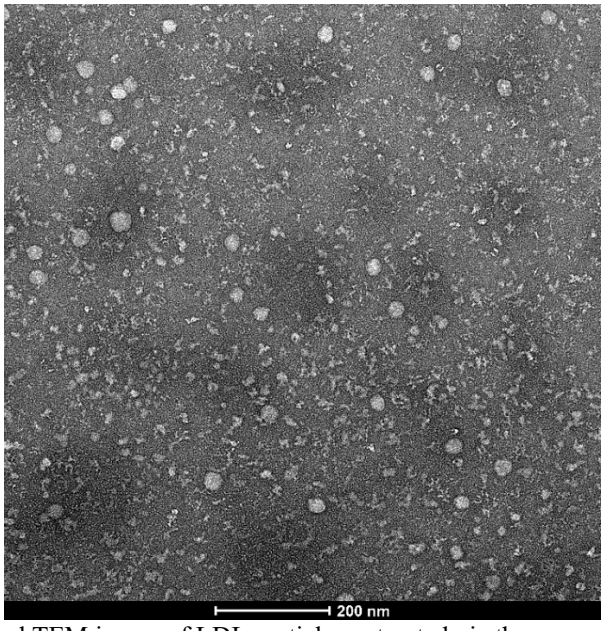

Figure 26 – Negative-stained TEM image of LDL particles extracted via the serum-FPLC method [Ekaterina Poliukhina].

4.1.5 SV-AUC Analysis of LDL Extracted from Serum via DGUC

The SV-AUC analysis presented in Figure 27 provides insights into the sedimentation behaviour of LDL fractions isolated from serum using DGUC. The graph illustrates the distributions of the normalized sedimentation coefficient by area, allowing for a comparative assessment of the impact of additional purification steps on LDL particles. The x-axis indicates the sedimentation coefficient, which correlates with the size and shape of particles in solution, while the y-axis represents the normalized concentration distribution $c(s)$, providing information on the relative abundance of species at different sedimentation rates.
The main peak around ~7 S suggests that the predominant particle population remains similar across all purification methods, with the overlap of curves indicating no substantial changes in average particle size between conditions.

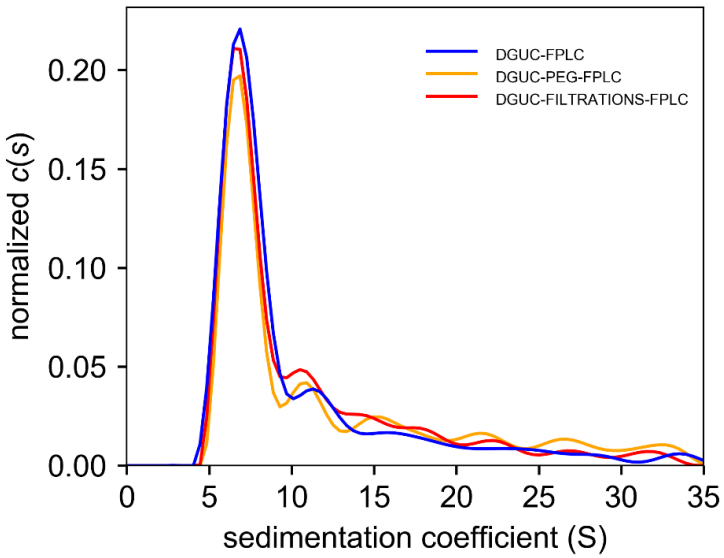

Figure 27 – Normalized sedimentation coefficient distributions of LDL particles obtained through different purification methods using DGUC.

4.1.6 SV-AUC Analysis of LDL Extracted from Serum via FPLC and with PEG precipitation followed by FPLC

Figure 28 illustrates the normalized sedimentation coefficient distribution for serum, serum-FPLC, and serum-PEG-FPLC fractions. The normalization to the maximum value ensures that differences in total protein concentration do not bias the comparison, allowing for a clearer assessment of how different purification steps affect the relative distribution of LDL and other macromolecular components across the fractions.
The serum sample displays a prominent peak at around 4-5 S, consistent with the presence of albumin and other similarly sized macromolecular species, alongside a secondary peak at approximately 7 S, which indicates the LDL species. Additional small peaks at higher S-values suggest the presence of larger protein aggregates.
The serum-FPLC fraction shows a broader distribution with a large peak beyond 10 S, indicating the presence of complexes or aggregates. Finally, the serum-PEG-FPLC sample

shows a major peak overlapping with that of serum and serum-FPLC at approximately 7 S, confirming the presence of LDL. However, compared to the other samples, its profile indicates a reduction in the relative abundance of higher S-value components. This supports the role of PEG precipitation in selectively depleting large, high-molecular-weight protein complexes [56] while preserving specific protein and lipoprotein populations. Overall, this analysis highlights the distinct sedimentation behaviours among the three samples, reflecting differences in protein-lipoprotein interactions.

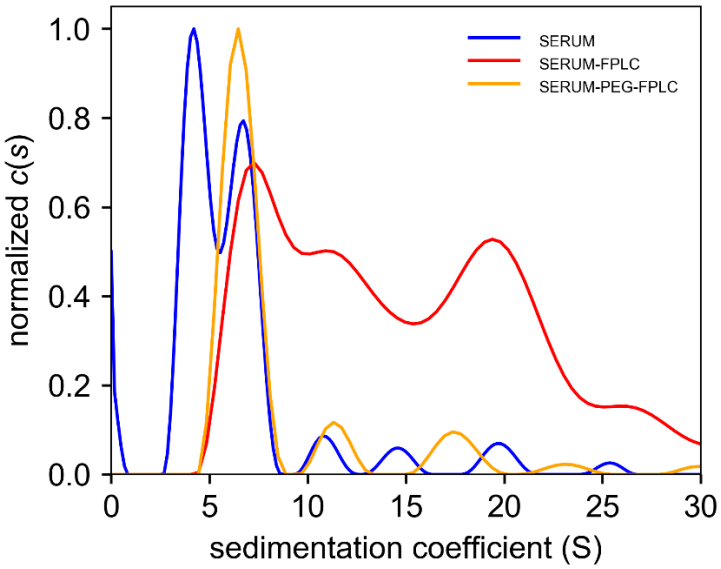

Figure 28 – Normalized sedimentation coefficient distributions of LDL particles purified directly from serum using different methods [the serum-PEG-FPLC SV-AUC analysis was performed by Ekaterina Poliukhina].

4.2 Discussion of the Physical Properties of LDL Isolated from Serum with and without DGUC

When comparing the samples obtained from serum with and without DGUC, several key differences in particle size distribution and polydispersity emerge. The LDL populations obtained through DGUC-based methods consistently show a dominant peak around 20 nm, suggesting a more uniform LDL distribution across the different DGUC purification strategies. Among these, DGUC-FPLC and DGUC-filtrations-FPLC samples exhibit more defined peaks, indicating a more uniform particle population. On the other hand, the DGUC-PEG-FPLC fraction shows a broader distribution, like the serum-PEG-FPLC result, suggesting a higher degree of polydispersity and a more heterogeneous particle population.

Samples derived from PEG precipitation (both serum-PEG-FPLC and DGUC-PEG-FPLC) demonstrate greater variability, showing wider distributions and increased polydispersity. The broader size distributions observed in both methods suggest the presence of polydisperse species, with this variability being more pronounced in samples starting directly from serum.

Overall, the DGUC-derived samples exhibit a more consistent particle size distribution, resulting in a more purified and size-uniform LDL population (Figure 29).

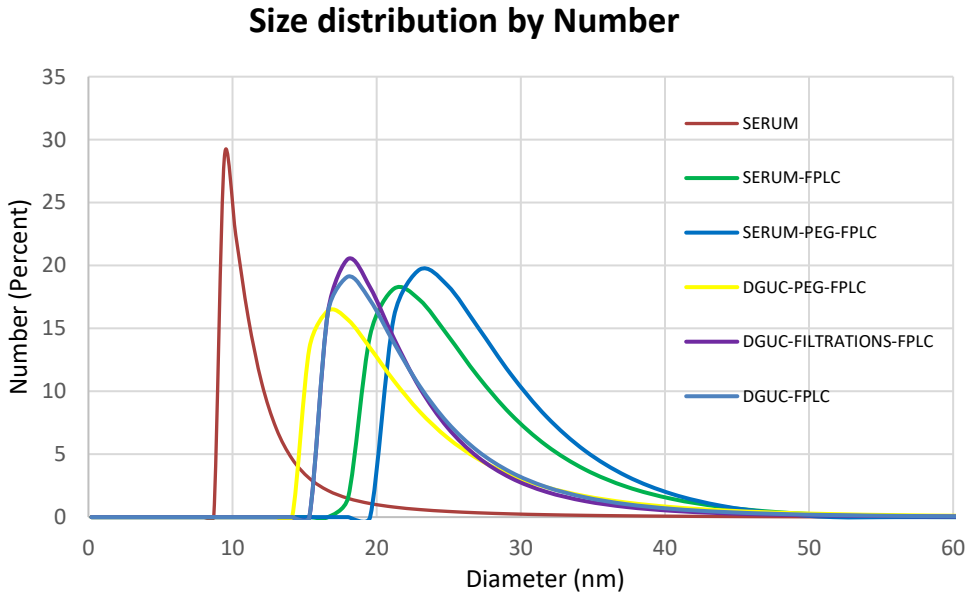

Figure 29 – Number-weighted DLS distribution of LDL particles isolated from all different purification methods.

A comparison of LDL particle homogeneity and purity is conducted using negative-stained TEM characterization for samples extracted via the DGUC-FPLC and serum-FPLC methods. The TEM image of the DGUC-FPLC method (Figure 25) show that the isolated LDL particles are highly uniform and homogeneous, with significantly reduced contamination. The particles exhibit a consistent size range, mainly between 20 to 30 nm in diameter, suggesting that the DGUC-FPLC method effectively isolates LDL with a well-defined structure and high purity, making it a reliable approach for lipoprotein studies. In contrast, the TEM image of LDL particles isolated using the serum-FPLC method (Figure 26) reveals noticeable impurities and a less homogeneous particle distribution. The isolated lipoproteins have a broader size range, suggesting that the serum-FPLC method does not achieve the same level of purity and uniformity as the DGUC-FPLC method. This comparison highlights the superiority of the latter for achieving more consistent and pure LDL isolation.

Furthermore, a comparison of the sedimentation behaviour of LDL fractions isolated from all six purification methods is shown in Figure 30. This analysis provides a comprehensive view of how various purification strategies influence LDL particle distribution and sedimentation characteristics. The sedimentation coefficient distributions reveal distinct differences between the samples. The LDL fractions isolated using the DGUC-based methods exhibit a sharp, well-defined peak around 7 S, indicating a more consistent and uniform LDL population. In contrast, the serum-FPLC fraction presents a broad distribution, with several additional and huge peaks extending beyond 10 S. This indicates the presence of high-molecular-weight protein aggregates or complexes, highlighting the presence of contaminants in the serum-FPLC fraction. This wider distribution indicates that the serum-FPLC method leads to a less purified LDL fraction than the DGUC-based method, which is consistent with the TEM findings.

Overall, this comparison emphasizes the superior effectiveness of DGUC in isolating a more uniform and refined LDL population, which exhibit significantly less variability, confirming its reliability for achieving high-purity LDL isolation.

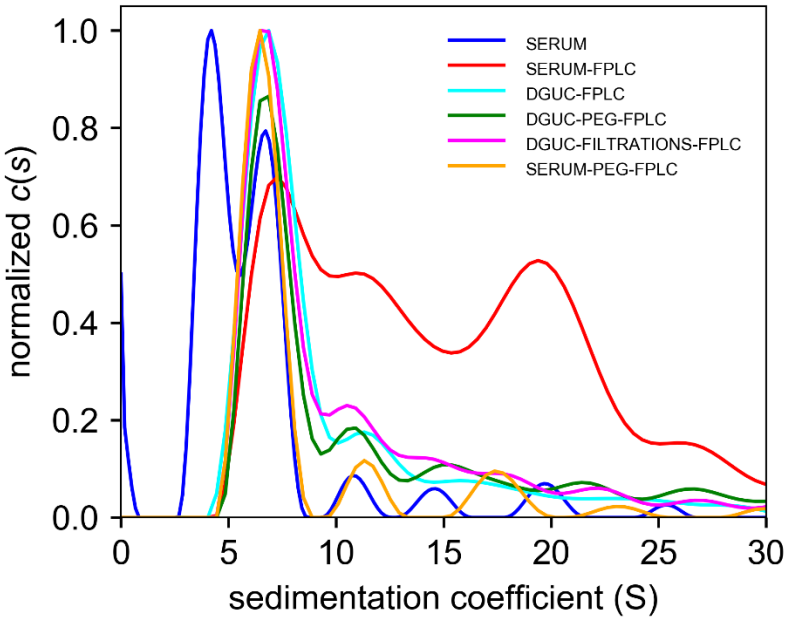

Figure 30 – Normalized sedimentation coefficient distributions based on the maximum value of all six analyzed conditions [the serum-PEG-FPLC SV-AUC analysis was performed by Ekaterina Poliukhina].

4.3 LDL Protein Composition

4.3.1 SDS-PAGE of LDL Extracted from Serum via DGUC

The analysis begins with SDS-PAGE, a technique that separates proteins based on molecular weight, offering key insights into the protein composition of LDL fraction obtained after DGUC, as shown in Figure 31.

The molecular weight marker on the left provides a reference for estimating the sizes of the separated proteins. Notably, all the samples further processed by FPLC, PEG precipitation, or filtrations, exhibit faint bands around 30 kDa and between 150 and 250 kDa under reducing conditions, along with a prominent band above 250 kDa (Figure 31B). These bands are likely attributed to apolipoproteins such as Apo B, a major structural protein of LDL. The faint intensity of the lower bands may suggest low abundance during the isolation process, as Apo B exists in different forms, with Apo B-100 being the predominant form in LDL. The presence of Apo B-100 over 250 kDa is consistent with its known molecular weight (~550 kDa) and confirms its identity as a key component of the LDL fraction.

In the DGUC-FPLC sample, a specific band around 15 kDa is observed under non-reducing conditions, which likely corresponds to a smaller fragment of Apo B (Figure 31A).

The absence of distinct banding patterns across the lanes for the various purification methods implies that these techniques do not significantly alter the protein composition of the samples. This finding suggests that the primary proteins associated with LDL are effectively retained across the different processing techniques, underscoring the effectiveness of the initial DGUC isolation.

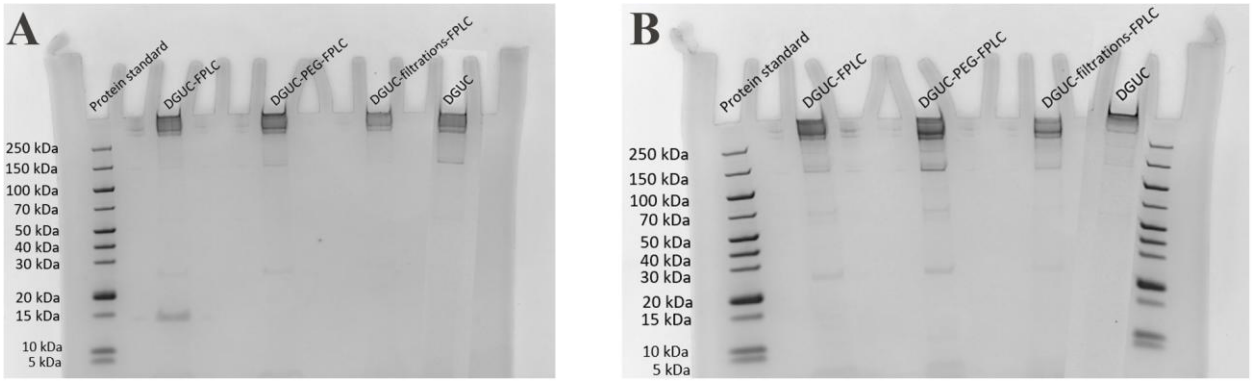

Figure 31 – (A) SDS-PAGE without reducing agent. (B) SDS-PAGE with reducing agent.

4.3.2 SDS-PAGE of LDL Extracted from Serum via FPLC and with PEG precipitation followed by FPLC

SDS-PAGE is used to analyze the protein composition of the lipoprotein fraction extracted directly from serum, without prior isolation via DGUC, providing insights into the effects of different purification steps.

Key differences emerge between non-reducing (Figure 32A) and reducing (Figure 32B) conditions, highlighting the role of disulfide bonds in stabilizing protein complexes. Without a reducing agent, high molecular weight bands appear more pronounced in the serum-FPLC and serum-PEG-FPLC lanes. In contrast, the serum lane of the non-reducing gel shows a strong band between 50 and 70 kDa, corresponding to albumin, the most abundant protein in human serum, which has a molecular weight of approximately 66 kDa. Other faint bands appear between 50 and 100 kDa, possibly representing transferrin (~76 kDa), and around 150 kDa, corresponding to immunoglobulin G (IgG) in its native form.

Under reducing conditions, the serum protein profile changes significantly. IgG separates into its heavy and light chains, with bands appearing at approximately 50 kDa and 25 kDa, respectively. Moreover, the lower molecular weight band between 20 and 30 kDa becomes more evident, likely corresponding to additional subunits of proteins that were part of disulfide-stabilized complexes.

The serum-FPLC and serum-PEG-FPLC lanes exhibit a protein composition distinct from untreated serum, confirming that purification steps modify the protein profile.

Indeed, following FPLC purification, the protein profile becomes more defined, with a noticeable reduction in non-LDL-associated proteins, suggesting that this step effectively eliminates a portion of the serum contaminants. On the other hand, the additional PEG precipitation step before FPLC does not appear to significantly alter the banding pattern.

In the non-reducing gel, both serum-FPLC and serum-PEG-FPLC show a pronounced high molecular weight band corresponding to Apo B-100. Faint bands around 150 kDa suggest that IgG is still present.

Under reducing conditions, the disappearance of high molecular weight bands and the sharpening of distinct protein bands further confirm that some of the observed protein complexes are stabilized by disulfide bonds. Finally, IgG heavy and light chains remain visible at 50 kDa and 25 kDa, respectively, confirming the persistence of immunoglobulins.

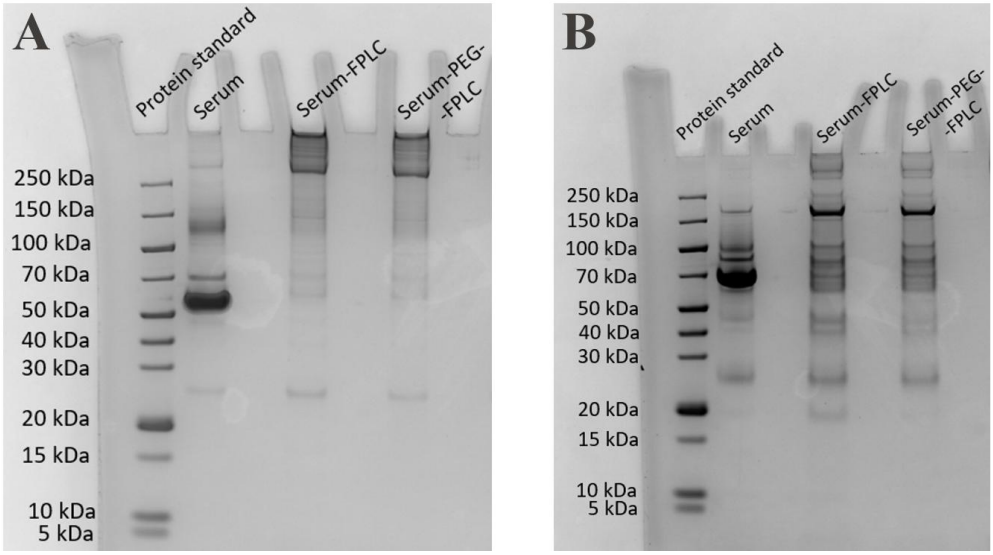

Figure 32 – (A) SDS-PAGE without reducing agent. (B) SDS-PAGE with reducing agent.

The SDS-PAGE performed to examine the protein composition of all the six samples discussed in this thesis, provides insight into the effects of each processing technique. Comparing Figure 31 and Figure 32, it is evident that the DGUC-based methods yield the cleanest protein profile, retaining only the primary LDL-associated proteins such as Apo B-100, with fewer contaminants. In contrast, the serum sample displays a complex mixture of proteins, reflecting the inherent variability and the presence of various macromolecular components that contribute to its heterogeneous profile. Although serum-FPLC and serum-PEG-FPLC enhance the protein profile, they do not fully remove all contaminants. The additional step of PEG precipitation before FPLC provides some purification but does not significantly alter the overall protein composition compared to FPLC alone.

4.3.3 MS-Based Proteomics of LDL Extracted from Serum via DGUC

In this subsection, we present the results of the MS-based proteomics analysis of DGUC-FPLC, DGUC-PEG-FPLC, and DGUC-filtrations-FPLC samples. The primary objective is to investigate potential differences in the protein corona surrounding LDL particles extracted using these different methods.

Table 4, Table 5 and Table 6 display the top 20 proteins with the highest spectrum counts in DGUC-FPLC, DGUC-PEG-FPLC, and DGUC-filtrations-FPLC, respectively.

The spectrum count refers to the number of times a specific peptide or protein is detected, essentially reflecting the frequency with which a particular peptide is observed during the measurement. Although the spectrum count is often used as a proxy for protein abundance, it is important to note that these results are very poorly quantitative. The spectrum count can correlate to the actual protein abundance to some extent, but it does not provide precise quantitative data. Thus, while the data is useful for identifying trends and providing qualitative insights into the protein composition of the LDL particles across different samples, it does not offer definitive quantitative conclusions.

In all three samples, there is a clear abundance of Apo B, the main structural protein of LDL. This is evident from the consistently high spectrum count observed across all conditions. This result was expected, as the primary goal of these experiments was to isolate LDL from plasma. Given that Apo B is primarily associated with LDL, its dominance confirms the successful enrichment of these particles in all three sample preparations.

After Apo B, the most abundant proteins are complement C3, apolipoprotein A-I, alpha-1-antitrypsin, alpha-2-macroglobulin, and Lp(a). Their consistent presence across all conditions suggests that these proteins are either strongly associated with LDL particles or tend to co-purify with them during the extraction process.

Complement C3 is known to interact with lipoproteins and plays a role in immune response and lipid metabolism. Its presence in all samples indicates that a fraction of LDL particles may carry C3-bound complexes, possibly linked to inflammation or immune-modulatory functions of lipoproteins.

Apolipoprotein A-I is the major protein of HDL but can also be found in LDL fractions due to lipoprotein remodelling or minor HDL contamination. Its co-purification with LDL suggests some overlap between lipoprotein subfractions, as LDL and HDL share dynamic lipid-exchange processes.

The persistent detection of alpha-1-antitrypsin and alpha-2-macroglobulin in all three conditions suggests that these proteins might have an affinity for LDL or are carried along due to their interactions with lipoprotein-bound proteases or inflammatory components. Both proteins are implicated in lipid metabolism, which could explain their association with LDL particles.

The consistent enrichment of these proteins across all conditions highlights the complexity of LDL-associated proteins, reinforcing the idea that LDL particles carry more than just cholesterol. They also serve as carriers of biologically active proteins that may contribute to both normal physiology and disease processes.

Isoform 1 of immunoglobulin heavy constant mu is detected with the highest spectrum counts in the DGUC-FPLC sample, but not in DGUC-PEG-FPLC or DGUC-filtrations-FPLC. This suggests that the initial ultracentrifugation and FPLC purification retains a fraction of immune-related proteins, whereas the additional steps in the other two methods remove or significantly reduced them, along with loosely bound proteins, including immunoglobulins. PEG precipitation enriches lipoproteins while reducing free plasma proteins, while additional filtration steps likely eliminate immune complexes or proteins that are not strongly associated with LDL.

The presence of beta-2-glycoprotein 1 in the DGUC-PEG-FPLC sample suggests that PEG precipitation may favour the retention of LDL-associated proteins involved in lipid transport and immune interactions.

Full Name	Gene Name	MW (Da)	Spectrum Count
Apolipoprotein B-100	APOB	515540	6217
Complement C3	C3	150850	324
Apolipoprotein A-I	APOA1	30777	254
Alpha-1-antitrypsin	SERPINA1	46989	189
Alpha-2-macroglobulin	A2M	163290	171
Apolipoprotein(a)	LPA	226.54	131
Apolipoprotein A-IV	APOA4	45371	122
Complement C5	C5	188300	112
Serotransferrin	TF	77049	106
Complement C4	C4A	192780	104
Complement factor B	CFB	140940	103
			89
C4b-binding protein alpha chain	C4BPA	67033	82
Prothrombin	F2	70036	81
Ceruloplasmin (Fragment)	CP	20761	74
Inter-alpha-trypsin inhibitor heavy chain H2	ITIH2	106460	71
Apolipoprotein D (Fragment)	APOD	24158	68
Alpha-1-antichymotrypsin	SERPINA3	47650	68
Haptoglobin-related protein	HPR	39029	65
Immunoglobulin heavy constant gamma 1	IGHG1	43911	63
Isoform 1 of Immunoglobulin heavy constant mu	IGHM	49439	60

Table 4 – Full names, gene names, molecular weights, and spectrum counts of the top 20 proteins with the highest spectrum counts in DGUC-FPLC sample.

Full Name	Gene Name	MW (Da)	Spectrum Count
Apolipoprotein B-100	APOB	515540	5835
Complement C3	C3	150850	297
Apolipoprotein A-I	APOA1	30777	241
Alpha-1-antitrypsin	SERPINA1	46989	172
Alpha-2-macroglobulin	A2M	163290	166
Apolipoprotein(a)	LPA	226540	125
Apolipoprotein A-IV	APOA4	45371	111
Complement C5	C5	188300	103
Serotransferrin	TF	77049	102
Complement C4-A	C4A	192780	101
Complement factor B	CFB	140940	99
			97
			95
Ceruloplasmin (Fragment)	CP	20761	75
C4b-binding protein alpha chain	C4BPA	67033	71
Prothrombin	F2	70036	71

Inter-alpha-trypsin inhibitor heavy chain H2	ITIH2	106460	68
Alpha-1-antichymotrypsin	SERPINA3	47650	67
Haptoglobin-related protein	HPR	39029	65
Apolipoprotein D (Fragment)	APOD	24158	65
Keratin, type II cytoskeletal 1	KRT1	66038	62
Beta-2-glycoprotein 1	APOH	38298	60
Immunoglobulin heavy constant gamma 1	IGHG1	43911	60

Table 5 – Full names, gene names, molecular weights, and spectrum counts of the top 20 proteins with the highest spectrum counts in DGUC-PEG-FPLC sample.

Full Name	Gene Name	MW (Da)	Spectrum Count
Apolipoprotein B-100	APOB	515540	4678
Complement C3	C3	150850	268
Apolipoprotein A-I	APOA1	30777	183
Alpha-1-antitrypsin	SERPINA1	46989	146
Alpha-2-macroglobulin	A2M	163290	143
Apolipoprotein(a)	LPA	226540	108
Keratin, type I cytoskeletal 14	KRT14	51621	108
Serotransferrin	TF	77049	96
Complement C4-A	C4A	192780	93
			92
Apolipoprotein A-IV	APOA4	45371	92
Complement C5	C5	188300	86
Keratin, type II cytoskeletal 1	KRT1	66038	85
Complement C2	CFB	140940	79
Keratin, type II cytoskeletal 6B	KRT6B	60066	71
Ceruloplasmin (Fragment)	CP	20761	70
Keratin, type I cytoskeletal 9	KRT9	62064	69
Prothrombin	F2	70036	63
Alpha-1-antichymotrypsin	SERPINA3	47650	59
C4b-binding protein alpha chain	C4BPA	67033	58
Haptoglobin-related protein	HPR	39029	58
Apolipoprotein D (Fragment)	APOD	24158	58
Inter-alpha-trypsin inhibitor heavy chain H2	ITIH2	106460	57
Keratin, type I cytoskeletal 10	KRT10	63345	57
Immunoglobulin heavy constant gamma 1	IGHG1	43911	56

Table 6 – Full names, gene names, molecular weights, and spectrum counts of the top 20 proteins with the highest spectrum counts in DGUC-filtrations-FPLC sample.

4.3.4 MS-Based Proteomics of LDL Extracted from Serum via FPLC and with PEG precipitation followed by FPLC

In this subsection, the results of the MS-based proteomics analysis of serum, serum-FPLC and serum-PEG-FPLC samples, are presented. The primary objective of this analysis is to investigate potential differences in the protein corona surrounding these particles and to evaluate the efficiency of selective precipitation by PEG.
Table 7, Table 8 and Table 9 display the top 20 proteins with the highest spectrum counts in serum, serum-FPLC, and serum-PEG-FPLC, respectively.

Full Name	Gene Name	MW (Da)	Spectrum Count
Isoform 1 of Serum albumin precursor	ALB	69366.9	1896
Serotransferrin	TF	77050.2	381
Complement C3	C3	187149.1	285
Isoform 1 of Immunoglobulin heavy constant gamma 1	IGHG1	36105	258
Alpha-2-macroglobulin	A2M	163289.9	219
Haptoglobin	HP	49105.5	163
Apolipoprotein A-I	APOA1	30778.5	136
Alpha-1-antitrypsin	SERPINA1	100996.6	124
Complement C4-A	C4A	192876.9	115
Sushi domain-containing protein		169887.5	113
Apolipoprotein B-100	APOB	515554.7	111
Immunoglobulin kappa constant	IGKC	11764.8	91
Ceruloplasmin	CP	122221.9	85
Isoform 1 of Immunoglobulin heavy constant alpha 1	IGHA1	37653.8	77
Hemopexin	HPX	51676.5	76
Isoform 3 of Vitamin D-binding protein	GC	55077.9	66
Complement C2	C2	140943.5	63
Isoform 1 of Immunoglobulin heavy constant mu	IGHM	49438.8	62
Isoform 1 of Immunoglobulin heavy constant gamma 3	IGHG3	41285.9	59
Isoform 1 of Fibronectin	FN1	256494.2	57

Table 7 – Full names, gene names, molecular weights, and spectrum counts of the top 20 proteins with the highest spectrum counts in serum.

Full Name	Gene Name	MW (Da)	Spectrum Count
Alpha-2-macroglobulin	A2M	163289.9	771
Complement C3	C3	187149.1	429
Apolipoprotein B-100	APOB	515554.7	356
Haptoglobin	HP	49105.5	259
Isoform 1 of Immunoglobulin heavy constant mu	IGHM	49438.8	227
Isoform 1 of Serum albumin precursor	ALB	69366.9	205
Alpha-1-antitrypsin	SERPINA1	100996.6	188
Isoform 1 of Fibronectin	FN1	256494.2	158
Inter-alpha-trypsin inhibitor heavy chain H2	ITIH2	106465.5	145
Complement C2	C2	140943.5	138
Inter-alpha-trypsin inhibitor heavy chain H1	ITIH1	101389.8	123
Complement C5	C5	188623.3	115
Isoform 1 of Immunoglobulin heavy constant alpha 1	IGHA1	37653.8	109
Prothrombin	F2	70036.8	102
Immunoglobulin kappa constant	IGKC	11764.8	101
Complement C4-A	C4A	192876.9	100
Apolipoprotein A-I	APOA1	30778.5	100
C4b-binding protein alpha chain	C4BPA	67033	97
Isoform 1 of Immunoglobulin heavy constant gamma 1	IGHG1	36105	91
Sushi domain-containing protein		169887.5	89
Gelsolin	GSN	85697.8	85

Table 8 – Full names, gene names, molecular weights, and spectrum counts of the top 20 proteins with the highest spectrum counts in serum-FPLC.

Full Name	Gene Name	MW (Da)	Spectrum Count
Alpha-2-macroglobulin	A2M	163289.9	558
Complement C3	C3	187149.1	263
Apolipoprotein B-100	APOB	515554.7	242
Isoform 1 of Immunoglobulin heavy constant mu	IGHM	49438.8	135
Isoform 1 of Serum albumin precursor	ALB	69366.9	120
Alpha-1-antitrypsin	SERPINA1	100996.6	109
Isoform 1 of Fibronectin	FN1	256494.2	108

Complement C2	C2	140943.5	99
Inter-alpha-trypsin inhibitor heavy chain H1	ITIH1	101389.8	88
Inter-alpha-trypsin inhibitor heavy chain H2	ITIH2	106465.5	87
Haptoglobin	HP	49105.5	86
Immunoglobulin kappa constant	IGKC	11764.8	81
C4b-binding protein alpha chain	C4BPA	67033	80
Complement C5	C5	188623.3	72
Complement C4-A	C4A	192876.9	70
Isoform 1 of Immunoglobulin heavy constant alpha 1	IGHA1	37653.8	66
Gelsolin	GSN	85697.8	66
Isoform 1 of Immunoglobulin heavy constant gamma 1	IGHG1	36105	64
Sushi domain-containing protein		169887.5	62
Plasminogen	PLG	92487.6	60
Prothrombin	F2	70036.8	60
Apolipoprotein A-I	APOA1	30778.5	59

Table 9 – Full names, gene names, molecular weights, and spectrum counts of the top 20 proteins with the highest spectrum counts in serum-PEG-FPLC.

An analysis on the probability count has been performed to assess the likelihood that the protein has been correctly identified. The probability count refers to the confidence score associated with the identification of a peptide or a protein. A higher probability count suggests a greater confidence in the accuracy of the identification.

Table 10, Table 11 and Table 12 present the proteins with a probability count higher than 95% for serum, serum-FPLC, and serum-PEG-FPLC, respectively. These proteins are considered present in the samples because only those with a probability count above this threshold are considered reliable and counted as identified.

Full names of the proteins identified with a probability count above 95% in serum	**Gene names of the proteins identified with a probability count above 95% in serum**	**MW (Da)**
Alpha-1-antitrypsin	SERPINA1	100996.6
Immunoglobulin kappa variable 2-40	IGKV2-40	13310.6
SAA2-SAA4 readthrough	SAA2-SAA4	23354.3
Coagulation factor V	F5	251710.5
Immunoglobulin heavy variable 3-49	IGHV3-49	13056
Complement C1q B chain (Fragment)	C1QB	26722.8

Titin	TTN	3994242.8
Immunoglobulin heavy variable 6-1	IGHV6-1	13481.4
Immunoglobulin heavy variable 3-15	IGHV3-15	12926
Immunoglobulin heavy variable 1-18	IGHV1-18	12820.3
Immunoglobulin heavy variable 1-24	IGHV1-24	12824.2
Immunoglobulin heavy variable 5-51	IGHV5-51	12674.9
Complement C4-A	C4A	192876.9
Ig-like domain-containing protein (Fragment)	LOC102724971	12964.8
Keratin, type I cytoskeletal 10	KRT10	63347.8
Vitamin K-dependent protein S	PROS1	73758.4
Immunoglobulin heavy variable 3-72	IGHV3-72	11167.5
Immunoglobulin lambda constant 7 (Fragment)	IGLC7	11253.1
Angiotensinogen	AGT	52070.5
C-X-C motif chemokine		21143
Sushi domain-containing protein		169887.5
Complement C5	C5	188623.3
Complement C8 alpha chain	C8A	62616.1
Coagulation factor XII	F12	67790.6
Complement component C8 beta chain	C8B	66947.8
Inter-alpha-trypsin inhibitor heavy chain H3	ITIH3	103776.2
Plasminogen	PLG	92487.6
Apolipoprotein L1	APOL1	47383.3
Complement subcomponent C1r	C1R	81890.5
Complement C2	C2	140943.5
Immunoglobulin lambda-like polypeptide 5	IGLL5	23062.9
Apolipoprotein D (Fragment)	APOD	24158.6
HGF activator	HGFAC	71482.3
Protein Z-dependent protease inhibitor	SERPINA10	55115.6
Macrophage stimulating 1	MST1	80317.8
Complement factor I	CFI	65749.8
Cartilage oligomeric matrix protein	COMP	227277.3
Haptoglobin	HP	49105.5

Uncharacterized protein (Fragment)		76884.5
Apolipoprotein C-II	APOC4-APOC2	20049.7
Sulfhydryl oxidase 1	QSOX1	82578.7
CD5 antigen-like	CD5L	38085.9
Ficolin-3	FCN3	32903.3
Attractin	ATRN	158536.3
Apolipoprotein M	APOM	21253.9
Ceruloplasmin	CP	122221.9
Prothrombin	F2	70036.8
Isoform 2 of Haptoglobin	HP	38451.4
Haptoglobin-related protein	HPR	39029.5
Coagulation factor IX	F9	51777.6
Coagulation factor X	F10	54732.1
Antithrombin-III	SERPINC1	52604.1
Alpha-1-antitrypsin	SERPINA1	46737.9
Alpha-1-antichymotrypsin	SERPINA3	47653
Alpha-2-macroglobulin	A2M	163289.9
Complement C3	C3	187149.1
Isoform LMW of Kininogen-1	KNG1	47883.6
Immunoglobulin J chain	JCHAIN	18098.5
Immunoglobulin kappa variable 3-20	IGKV3-20	12557.7
Immunoglobulin heavy variable 3-7	IGHV3-7	12942.7
Immunoglobulin heavy variable 3-9	IGHV3-9	12945.1
Polymeric immunoglobulin receptor	PIGR	83283.4
Immunoglobulin kappa constant	IGKC	11764.8
Isoform 1 of Immunoglobulin heavy constant gamma 1	IGHG1	36105
Isoform 1 of Immunoglobulin heavy constant gamma 2	IGHG2	35899.2
Isoform 1 of Immunoglobulin heavy constant gamma 3	IGHG3	41285.9
Immunoglobulin heavy constant gamma 4	IGHG4	43830.8
Isoform 1 of Immunoglobulin heavy constant mu	IGHM	49438.8
Isoform 1 of Immunoglobulin heavy constant alpha 1	IGHA1	37653.8
Isoform 1 of Immunoglobulin heavy constant alpha 2	IGHA2	36590.5
Isoform 1 of Immunoglobulin heavy constant delta	IGHD	42352.2

Hemoglobin subunit delta	HBD	16055.2
Keratin, type I cytoskeletal 14	KRT14	254176.8
Apolipoprotein A-I	APOA1	30778.5
Apolipoprotein E	APOE	36153.5
Apolipoprotein C-I	APOC1	9332.4
Apolipoprotein C-III	APOC3	10852.3
Fibrinogen alpha chain	FGA	94973.4
Fibrinogen beta chain	FGB	55928.6
Fibrinogen gamma chain	FGG	51513.3
C-reactive protein	CRP	25039
Serum amyloid P-component	APCS	25387.7
Complement C1q subcomponent subunit A	C1QA	26016.6
Complement C1q subcomponent subunit C	C1QC	25774
Complement component C9	C9	63174.9
Beta-2-glycoprotein 1	APOH	38298.5
Leucine-rich alpha-2-glycoprotein	LRG1	38179.7
Isoform 1 of Fibronectin	FN1	256494.2
Protein AMBP	AMBP	38999.6
Alpha-1-acid glycoprotein 1	ORM1	23540.2
Alpha-2-HS-glycoprotein	AHSG	39339.5
Transthyretin	TTR	15886.9
Isoform 3 of Vitamin D-binding protein	GC	55077.9
Serotransferrin	TF	77050.2
Hemopexin	HPX	51676.5
Coagulation factor XI	F11	70109.2
C4b-binding protein alpha chain	C4BPA	67033
Vitronectin	VTN	54306.1
Vitamin K-dependent protein C	PROC	52071.2
Apolipoprotein B-100	APOB	515554.7
Histidine-rich glycoprotein	HRG	59576.6
Alpha-1B-glycoprotein	A1BG	54253.3
Keratin, type II cytoskeletal 1	KRT1	66040.3
von Willebrand factor	VWF	309251.2
Sex hormone-binding globulin	SHBG	43780.6
Immunoglobulin kappa variable 3-11	IGKV3-11	12575.7

Isoform 3 of Plasma protease C1 inhibitor	SERPING1	351432.7
Coagulation factor XIII B chain	F13B	75511.7
Tetranectin	CLEC3B	22537
Thyroxine-binding globulin	SERPINA7	46325.6
Heparin cofactor 2	SERPIND1	57072.9
Cholinesterase	BCHE	68420.1
Immunoglobulin kappa variable 4-1	IGKV4-1	51048.5
Gelsolin	GSN	85697.8
Complement C2	C2	83268.8
Apolipoprotein A-IV	APOA4	45372.3
Complement component C8 gamma chain	C8G	22277.3
Corticosteroid-binding globulin	SERPINA6	45142.1
Apolipoprotein(a)	LPA	282914
Monocyte differentiation antigen CD14	CD14	40076.6
Complement factor H	CFH	139096.2
Alpha-2-antiplasmin	SERPINF2	54566.6
Keratin, type I cytoskeletal 16	KRT16	51269
Complement C1s subcomponent	C1S	76684.2
Immunoglobulin lambda constant 3	IGLC3	11265.2
Immunoglobulin heavy variable 4-38-2	IGHV4-38-2	13016.1
Complement component C7	C7	93516.6
Isoform 4 of Clusterin	CLU	48803.6
Complement component C6	C6	104786.2
L-selectin	SELL	42187.8
Carboxypeptidase N catalytic chain	CPN1	52286.4
Insulin-like growth factor-binding protein 3	IGFBP3	31674.1
Lipopolysaccharide-binding protein	LBP	53386
Alpha-1-acid glycoprotein 2	ORM2	23603.3
Inter-alpha-trypsin inhibitor heavy chain H2	ITIH2	106465.5
Inter-alpha-trypsin inhibitor heavy chain H1	ITIH1	101389.8
Pregnancy zone protein	PZP	163862
C4b-binding protein beta chain	C4BPB	28357.2
Glutathione peroxidase 3	GPX3	25553.2

Carboxypeptidase N subunit 2	CPN2	60558.7
Isoform 2 of Vitamin K-dependent protein Z	PROZ	47052.1
Fibulin-1	FBLN1	77211.6
Zinc-alpha-2-glycoprotein	AZGP1	34258.6
Serum paraoxonase/arylesterase 1	PON1	39732.4
Properdin	CFP	51274.1
Kallistatin	SERPINA4	48544
Cadherin-5	CDH5	87529.5
Keratin, type I cytoskeletal 9	KRT9	62065.9
Isoform 2 of Insulin-like growth factor-binding protein complex acid labile subunit	IGFALS	70239.5
Pigment epithelium-derived factor	SERPINF1	46314.3
Isoform Short of Complement factor H-related protein 2	CFHR2	27896.3
Biotinidase	BTD	61133.4
Afamin	AFM	69070.1
Isoform 2 of Mannan-binding lectin serine protease 1	MASP1	81859.6
Selenoprotein P	SELENOP	43173.7
Lumican	LUM	38431.5
Phospholipid transfer protein	PLTP	54741.2
Lysozyme C	LYZ	68363.7
Hemoglobin subunit beta	HBB	15998
Hemoglobin subunit alpha	HBA1	15257.6
Phosphatidylinositol-glycan-specific phospholipase D	GPLD1	92338.9
Complement factor H-related protein 1	CFHR1	37650.4
Galectin-3-binding protein	LGALS3BP	65332.1
Apolipoprotein F	APOF	35400.3
Hyaluronan-binding protein 2	HABP2	62671.4
Inter-alpha-trypsin inhibitor heavy chain H4	ITIH4	103358.4
Serum paraoxonase/lactonase 3	PON3	39608.1
Transforming growth factor-beta-induced protein ig-h3	TGFBI	74682.9
Isoform 4 of Extracellular matrix protein 1	ECM1	63562.7
Retinol-binding protein	RBP4	22974
Peptidase inhibitor 16	PI16	49471
Isoform C of Proteoglycan 4	PRG4	141093.1

Carboxypeptidase B2	CPB2	48424.7
Beta-Ala-His dipeptidase	CNDP1	56693.1
Isoform 2 of N-acetylmuramoyl-L-alanine amidase	PGLYRP2	68001
Complement factor H-related protein 5	CFHR5	64418.3
Interleukin-1 receptor accessory protein	IL1RAP	65419.4
Cartilage acidic protein 1	CRTAC1	71421.1
Complement C1r subcomponent-like protein	C1RL	53497.5
Fetuin-B	FETUB	91235.5
IgGFc-binding protein	FCGBP	571982.8
Keratin, type II cytoskeletal 6A	KRT6A	195111
Alpha-S1-casein	CSN1S1	22975.2
Isoform 1 of Serum albumin precursor	ALB	69366.9
Protease I precursor Lysyl endopeptidase Achromobacter lyticus		68125.5
Apolipoprotein A-II	APOA2	14914.4
Bos Taurus 121 kDa Protein		121458.7
Keratin, type II cytoskeletal 2 epidermal	KRT2	201453.3

Table 10 – Full names, gene names, molecular weights, and probability counts of the proteins with a probability count above 95% in serum.

Full names of the proteins identified with a probability count above 95% in serum-FPLC	**Genes names of the proteins identified with a probability count above 95% in serum-FPLC**	**MW (Da)**
Alpha-1-antitrypsin	SERPINA1	100996.6
Immunoglobulin lambda variable 4-69	IGLV4-69	12773.7
Immunoglobulin lambda variable 3-10	IGLV3-10	12441
Immunoglobulin heavy variable 1/OR15-1 (non-functional) (Fragment)	IGHV1OR15-1	13011.6
Immunoglobulin kappa variable 2-40	IGKV2-40	13310.6
Cell adhesion molecule L1 like	CHL1	130796.9
SAA2-SAA4 readthrough	SAA2-SAA4	23354.3
Coagulation factor V	F5	251710.5
Immunoglobulin heavy variable 3-49	IGHV3-49	13056
Complement C1q B chain (Fragment)	C1QB	26722.8

Titin	TTN	3994242.8
Immunoglobulin heavy variable 6-1	IGHV6-1	13481.4
Immunoglobulin heavy variable 3-15	IGHV3-15	12926
Immunoglobulin heavy variable 1-18	IGHV1-18	12820.3
Immunoglobulin heavy variable 5-51	IGHV5-51	12674.9
Complement C4-A	C4A	192876.9
Ig-like domain-containing protein (Fragment)	LOC102724971	12964.8
Tenascin-X	TNXB	456176.8
Keratin, type I cytoskeletal 10	KRT10	63347.8
Vitamin K-dependent protein S	PROS1	73758.4
Immunoglobulin heavy variable 3-72	IGHV3-72	11167.5
Immunoglobulin lambda constant 7 (Fragment)	IGLC7	11253.1
Integrin beta	ITGB1	87925.5
Angiotensinogen	AGT	52070.5
Pyruvate kinase	PKM	65930.9
C-X-C motif chemokine		21143
Sushi domain-containing protein		169887.5
Complement C5	C5	188623.3
Complement C8 alpha chain	C8A	62616.1
Coagulation factor XII	F12	67790.6
Complement component C8 beta chain	C8B	66947.8
MBL associated serine protease 2	MASP2	74726.5
Inter-alpha-trypsin inhibitor heavy chain H3	ITIH3	103776.2
Proprotein convertase subtilisin/kexin type 9	PCSK9	87202.5
Soluble scavenger receptor cysteine-rich domain-containing protein SSC5D	SSC5D	165740.6
Plasminogen	PLG	92487.6
Apolipoprotein L1	APOL1	47383.3
complement subcomponent C1r	C1R	81890.5
Complement C2	C2	140943.5
Immunoglobulin lambda-like polypeptide 5	IGLL5	23062.9
Apolipoprotein D (Fragment)	APOD	24158.6
HGF activator	HGFAC	71482.3

Neuropilin 1	NRP1	72095.8
Protein Z-dependent protease inhibitor	SERPINA10	55115.6
Macrophage stimulating 1	MST1	80317.8
Complement factor I	CFI	65749.8
Cartilage oligomeric matrix protein	COMP	227277.3
Haptoglobin	HP	49105.5
Uncharacterized protein (Fragment)		76884.5
Actin gamma 1	ACTG1	80113.5
Cathelicidin antimicrobial peptide	CAMP	19591.6
Apolipoprotein C-II	APOC4-APOC2	20049.7
Sulfhydryl oxidase 1	QSOX1	82578.7
CD5 antigen-like	CD5L	38085.9
Ficolin-3	FCN3	32903.3
Attractin	ATRN	158536.3
Apolipoprotein M	APOM	21253.9
Ceruloplasmin	CP	122221.9
Coagulation factor XIII A chain	F13A1	83268.3
Prothrombin	F2	70036.8
Isoform 2 of Haptoglobin	HP	38451.4
Haptoglobin-related protein	HPR	39029.5
Coagulation factor IX	F9	51777.6
Coagulation factor X	F10	54732.1
Complement factor D	CFD	27032.4
Carbonic anhydrase 1	CA1	28870.4
Antithrombin-III	SERPINC1	52604.1
Alpha-1-antitrypsin	SERPINA1	46737.9
Alpha-1-antichymotrypsin	SERPINA3	47653
Alpha-2-macroglobulin	A2M	163289.9
Complement C3	C3	187149.1
Isoform LMW of Kininogen-1	KNG1	47883.6
Immunoglobulin J chain	JCHAIN	18098.5
Immunoglobulin kappa variable 3-20	IGKV3-20	12557.7
Immunoglobulin heavy variable 3-7	IGHV3-7	12942.7
Immunoglobulin heavy variable 3-9	IGHV3-9	12945.1
Polymeric immunoglobulin	PIGR	83283.4

receptor		
Immunoglobulin kappa constant	IGKC	11764.8
Isoform 1 of Immunoglobulin heavy constant gamma 1	IGHG1	36105
Isoform 1 of Immunoglobulin heavy constant gamma 2	IGHG2	35899.2
Isoform 1 of Immunoglobulin heavy constant gamma 3	IGHG3	41285.9
Immunoglobulin heavy constant gamma 4	IGHG4	43830.8
Isoform 1 of Immunoglobulin heavy constant mu	IGHM	49438.8
Isoform 1 of Immunoglobulin heavy constant alpha 1	IGHA1	37653.8
Isoform 1 of Immunoglobulin heavy constant alpha 2	IGHA2	36590.5
Isoform 1 of Immunoglobulin heavy constant delta	IGHD	42352.2
Hemoglobin subunit delta	HBD	16055.2
Keratin, type I cytoskeletal 14	KRT14	254176.8
Apolipoprotein A-I	APOA1	30778.5
Apolipoprotein E	APOE	36153.5
Apolipoprotein C-I	APOC1	9332.4
Fibrinogen alpha chain	FGA	94973.4
Fibrinogen beta chain	FGB	55928.6
Fibrinogen gamma chain	FGG	51513.3
Serum amyloid P-component	APCS	25387.7
Complement C1q subcomponent subunit A	C1QA	26016.6
Complement C1q subcomponent subunit C	C1QC	25774
Complement component C9	C9	63174.9
Beta-2-glycoprotein 1	APOH	38298.5
Leucine-rich alpha-2-glycoprotein	LRG1	38179.7
Isoform 1 of Fibronectin	FN1	256494.2
Protein AMBP	AMBP	38999.6
Alpha-1-acid glycoprotein 1	ORM1	23540.2
Alpha-2-HS-glycoprotein	AHSG	39339.5
Transthyretin	TTR	15886.9
Isoform 3 of Vitamin D-binding protein	GC	55077.9
Serotransferrin	TF	77050.2
Hemopexin	HPX	51676.5
Coagulation factor XI	F11	70109.2

C4b-binding protein alpha chain	C4BPA	67033
Vitronectin	VTN	54306.1
Vitamin K-dependent protein C	PROC	52071.2
Fructose-bisphosphate aldolase A	ALDOA	39420.6
Apolipoprotein B-100	APOB	515554.7
Phosphatidylcholine-sterol acyltransferase	LCAT	140132.7
Histidine-rich glycoprotein	HRG	59576.6
Alpha-1B-glycoprotein	A1BG	54253.3
Keratin, type II cytoskeletal 1	KRT1	66040.3
von Willebrand factor	VWF	309251.2
Sex hormone-binding globulin	SHBG	43780.6
Glyceraldehyde-3-phosphate dehydrogenase	GAPDH	36053.4
Immunoglobulin kappa variable 3-11	IGKV3-11	12575.7
Fructose-bisphosphate aldolase B	ALDOB	39473.3
Isoform 3 of Plasma protease C1 inhibitor	SERPING1	351432.7
Coagulation factor XIII B chain	F13B	75511.7
Tetranectin	CLEC3B	22537
Thyroxine-binding globulin	SERPINA7	46325.6
Heparin cofactor 2	SERPIND1	57072.9
Cholinesterase	BCHE	68420.1
Immunoglobulin kappa variable 4-1	IGKV4-1	51048.5
Gelsolin	GSN	85697.8
Complement C2	C2	83268.8
Apolipoprotein A-IV	APOA4	45372.3
Platelet glycoprotein Ib alpha chain	GP1BA	71542.6
Complement component C8 gamma chain	C8G	22277.3
Profilin-1	PFN1	15054.3
Thrombospondin-1	THBS1	129381.7
Corticosteroid-binding globulin	SERPINA6	45142.1
Apolipoprotein(a)	LPA	282914
Monocyte differentiation antigen CD14	CD14	40076.6
Complement factor H	CFH	139096.2
Alpha-2-antiplasmin	SERPINF2	54566.6
Coagulation factor VII	F7	161349.3

Keratin, type I cytoskeletal 16	KRT16	51269
Complement C1s subcomponent	C1S	76684.2
Complement C4-B	C4B	192752.8
Immunoglobulin lambda constant 3	IGLC3	11265.2
Immunoglobulin heavy variable 4-38-2	IGHV4-38-2	13016.1
Complement component C7	C7	93516.6
Isoform 4 of Clusterin	CLU	48803.6
Endoplasmic reticulum chaperone BiP	HSPA5	72334.7
Mannose-binding protein C	MBL2	26144.1
Keratin, type II cytoskeletal 5	KRT5	62379.6
Complement component C6	C6	104786.2
Carboxypeptidase N catalytic chain	CPN1	52286.4
Desmoplakin	DSP	331781.4
Lipopolysaccharide-binding protein	LBP	53386
Alpha-1-acid glycoprotein 2	ORM2	23603.3
Inter-alpha-trypsin inhibitor heavy chain H2	ITIH2	106465.5
Inter-alpha-trypsin inhibitor heavy chain H1	ITIH1	101389.8
Pregnancy zone protein	PZP	163862
C4b-binding protein beta chain	C4BPB	28357.2
Glutathione peroxidase 3	GPX3	25553.2
Carboxypeptidase N subunit 2	CPN2	60558.7
Isoform 2 of Vitamin K-dependent protein Z	PROZ	47052.1
Fibulin-1	FBLN1	77211.6
Isoform 4 of Tenascin	TNC	230863.6
Serum paraoxonase/arylesterase 1	PON1	39732.4
Properdin	CFP	51274.1
Kallistatin	SERPINA4	48544
Mannosyl-oligosaccharide 1,2-alpha-mannosidase IA	MAN1A1	72971.7
Thrombospondin-4	THBS4	105869.2
Keratin, type I cytoskeletal 9	KRT9	62065.9
Isoform 2 of Insulin-like growth factor-binding protein complex acid labile subunit	IGFALS	70239.5
Pigment epithelium-derived factor	SERPINF1	46314.3

Isoform Short of Complement factor H-related protein 2	CFHR2	27896.3
Biotinidase	BTD	61133.4
Afamin	AFM	69070.1
Mannan-binding lectin serine protease 1	MASP1	79247.4
Isoform 2 of Mannan-binding lectin serine protease 1	MASP1	81859.6
Selenoprotein P	SELENOP	43173.7
Lumican	LUM	38431.5
Phospholipid transfer protein	PLTP	54741.2
Hemoglobin subunit beta	HBB	15998
Hemoglobin subunit alpha	HBA1	15257.6
Phosphatidylinositol-glycan-specific phospholipase D	GPLD1	92338.9
Dermcidin	DCD	11284.1
Complement factor H-related protein 1	CFHR1	37650.4
Prolow-density lipoprotein receptor-related protein 1	LRP1	504591.8
Galectin-3-binding protein	LGALS3BP	65332.1
EGF-containing fibulin-like extracellular matrix protein 1	EFEMP1	54639.1
Contactin-1	CNTN1	113322.8
Hyaluronan-binding protein 2	HABP2	62671.4
Inter-alpha-trypsin inhibitor heavy chain H4	ITIH4	103358.4
Procollagen C-endopeptidase enhancer 1	PCOLCE	47972.5
Serum paraoxonase/lactonase 3	PON3	39608.1
Ficolin-2	FCN2	34001.6
Adiponectin	ADIPOQ	26414.2
Isoform 4 of Extracellular matrix protein 1	ECM1	63562.7
Vasorin	VASN	236295.2
Plexin domain-containing protein 2	PLXDC2	59583
Peptidase inhibitor 16	PI16	49471
Hornerin	HRNR	282372.7
Isoform C of Proteoglycan 4	PRG4	141093.1
Carboxypeptidase B2	CPB2	48424.7
Beta-Ala-His dipeptidase	CNDP1	56693.1
Isoform 2 of N-acetylmuramoyl-L-alanine amidase	PGLYRP2	68001
Isoform 9 of Collectin-11	COLEC11	29005.9

Complement factor H-related protein 5	CFHR5	64418.3
Adipocyte plasma membrane-associated protein	APMAP	46481.5
Interleukin-1 receptor accessory protein	IL1RAP	65419.4
Cartilage acidic protein 1	CRTAC1	71421.1
Complement C1r subcomponent-like protein	C1RL	53497.5
Fetuin-B	FETUB	91235.5
Prenylcysteine oxidase 1	PCYOX1	56642.2
Neurogenic locus notch homolog protein 3	NOTCH3	243622
IgGFc-binding protein	FCGBP	571982.8
Keratin, type II cytoskeletal 6A	KRT6A	195111
Isoform 1 of Serum albumin precursor	ALB	69366.9
Isoform 1 of Keratin, type I cytoskeletal 13	KRT13	104945.1
Protease I precursor Lysyl endopeptidase Achromobacter lyticus		68125.5
Keratin 4	KRT4	63912.2
Apolipoprotein A-II	APOA2	14914.4
Bos Taurus 121 kDa Protein		121458.7
Keratin, type II cytoskeletal 2 epidermal	KRT2	201453.3

Table 11 – Full names, gene names, molecular weights, and probability counts of the proteins with a probability count above 95% in serum-FPLC.

Full names of the proteins identified with a probability count above 95% in serum-PEG-FPLC	**Gene names of the proteins identified with a probability count above 95% in serum-PEG-FPLC**	**MW (Da)**
Alpha-1-antitrypsin	SERPINA1	100996.6
Immunoglobulin lambda variable 4-69	IGLV4-69	12773.7
Immunoglobulin heavy variable 1/OR15-1 (non-functional) (Fragment)	IGHV1OR15-1	13011.6
Immunoglobulin kappa variable 2-40	IGKV2-40	13310.6
Cell adhesion molecule L1 like	CHL1	130796.9
SAA2-SAA4 readthrough	SAA2-SAA4	23354.3
Coagulation factor V	F5	251710.5
Immunoglobulin heavy variable 3-49	IGHV3-49	13056
Complement C1q B chain (Fragment)	C1QB	26722.8

Titin	TTN	3994242.8
Immunoglobulin heavy variable 3-15	IGHV3-15	12926
Immunoglobulin heavy variable 1-18	IGHV1-18	12820.3
Immunoglobulin heavy variable 5-51	IGHV5-51	12674.9
Complement C4-A	C4A	192876.9
Immunoglobulin lambda variable 5-45 (Fragment)	IGLV5-45	13215.4
Ig-like domain-containing protein (Fragment)	LOC102724971	12964.8
Tenascin-X	TNXB	456176.8
Keratin, type I cytoskeletal 10	KRT10	63347.8
Vitamin K-dependent protein S	PROS1	73758.4
Immunoglobulin heavy variable 3-72	IGHV3-72	11167.5
Immunoglobulin lambda constant 7 (Fragment)	IGLC7	11253.1
Angiotensinogen	AGT	52070.5
Sushi domain-containing protein		169887.5
Complement C5	C5	188623.3
Complement C8 alpha chain	C8A	62616.1
Coagulation factor XII	F12	67790.6
Complement component C8 beta chain	C8B	66947.8
MBL associated serine protease 2	MASP2	74726.5
Inter-alpha-trypsin inhibitor heavy chain H3	ITIH3	103776.2
Proprotein convertase subtilisin/kexin type 9	PCSK9	87202.5
Plasminogen	PLG	92487.6
Apolipoprotein L1	APOL1	47383.3
complement subcomponent C1r	C1R	81890.5
Complement C2	C2	140943.5
Immunoglobulin lambda-like polypeptide 5	IGLL5	23062.9
Apolipoprotein D (Fragment)	APOD	24158.6
HGF activator	HGFAC	71482.3
Neuropilin 1	NRP1	72095.8
Protein Z-dependent protease inhibitor	SERPINA10	55115.6
Macrophage stimulating 1	MST1	80317.8
Complement factor I	CFI	65749.8

Cartilage oligomeric matrix protein	COMP	227277.3
Haptoglobin	HP	49105.5
Uncharacterized protein (Fragment)		76884.5
Actin gamma 1	ACTG1	80113.5
Cathelicidin antimicrobial peptide	CAMP	19591.6
Apolipoprotein C-II	APOC4-APOC2	20049.7
CD5 antigen-like	CD5L	38085.9
Ficolin-3	FCN3	32903.3
Attractin	ATRN	158536.3
Apolipoprotein M	APOM	21253.9
Ceruloplasmin	CP	122221.9
Coagulation factor XIII A chain	F13A1	83268.3
Prothrombin	F2	70036.8
Isoform 2 of Haptoglobin	HP	38451.4
Haptoglobin-related protein	HPR	39029.5
Coagulation factor IX	F9	51777.6
Coagulation factor X	F10	54732.1
Complement factor D	CFD	27032.4
Antithrombin-III	SERPINC1	52604.1
Alpha-1-antitrypsin	SERPINA1	46737.9
Alpha-1-antichymotrypsin	SERPINA3	47653
Alpha-2-macroglobulin	A2M	163289.9
Complement C3	C3	187149.1
Isoform LMW of Kininogen-1	KNG1	47883.6
Immunoglobulin J chain	JCHAIN	18098.5
Immunoglobulin kappa variable 1-17	IGKV1-17	12779
Immunoglobulin kappa variable 3-20	IGKV3-20	12557.7
Immunoglobulin heavy variable 3-7	IGHV3-7	12942.7
Immunoglobulin heavy variable 3-9	IGHV3-9	12945.1
Polymeric immunoglobulin receptor	PIGR	83283.4
Immunoglobulin kappa constant	IGKC	11764.8
Isoform 1 of Immunoglobulin heavy constant gamma 1	IGHG1	36105
Isoform 1 of Immunoglobulin heavy constant gamma 2	IGHG2	35899.2

Isoform 1 of Immunoglobulin heavy constant gamma 3	IGHG3	41285.9
Immunoglobulin heavy constant gamma 4	IGHG4	43830.8
Isoform 1 of Immunoglobulin heavy constant mu	IGHM	49438.8
Isoform 1 of Immunoglobulin heavy constant alpha 1	IGHA1	37653.8
Isoform 1 of Immunoglobulin heavy constant alpha 2	IGHA2	36590.5
Isoform 1 of Immunoglobulin heavy constant delta	IGHD	42352.2
Hemoglobin subunit delta	HBD	16055.2
Apolipoprotein A-I	APOA1	30778.5
Apolipoprotein E	APOE	36153.5
Apolipoprotein C-I	APOC1	9332.4
Fibrinogen alpha chain	FGA	94973.4
Fibrinogen beta chain	FGB	55928.6
Fibrinogen gamma chain	FGG	51513.3
Serum amyloid P-component	APCS	25387.7
Complement C1q subcomponent subunit A	C1QA	26016.6
Complement C1q subcomponent subunit C	C1QC	25774
Complement component C9	C9	63174.9
Beta-2-glycoprotein 1	APOH	38298.5
Leucine-rich alpha-2-glycoprotein	LRG1	38179.7
Isoform 1 of Fibronectin	FN1	256494.2
Protein AMBP	AMBP	38999.6
Alpha-1-acid glycoprotein 1	ORM1	23540.2
Alpha-2-HS-glycoprotein	AHSG	39339.5
Transthyretin	TTR	15886.9
Isoform 3 of Vitamin D-binding protein	GC	55077.9
Serotransferrin	TF	77050.2
Hemopexin	HPX	51676.5
Coagulation factor XI	F11	70109.2
C4b-binding protein alpha chain	C4BPA	67033
Vitronectin	VTN	54306.1
Vitamin K-dependent protein C	PROC	52071.2
Apolipoprotein B-100	APOB	515554.7
Phosphatidylcholine-sterol acyltransferase	LCAT	140132.7

Histidine-rich glycoprotein	HRG	59576.6
Alpha-1B-glycoprotein	A1BG	54253.3
Keratin, type II cytoskeletal 1	KRT1	66040.3
von Willebrand factor	VWF	309251.2
Sex hormone-binding globulin	SHBG	43780.6
Immunoglobulin kappa variable 3-11	IGKV3-11	12575.7
Isoform 3 of Plasma protease C1 inhibitor	SERPING1	351432.7
Coagulation factor XIII B chain	F13B	75511.7
Tetranectin	CLEC3B	22537
Thyroxine-binding globulin	SERPINA7	46325.6
Heparin cofactor 2	SERPIND1	57072.9
Cholinesterase	BCHE	68420.1
Immunoglobulin kappa variable 4-1	IGKV4-1	51048.5
Gelsolin	GSN	85697.8
Complement C2	C2	83268.8
Apolipoprotein A-IV	APOA4	45372.3
Platelet glycoprotein Ib alpha chain	GP1BA	71542.6
Complement component C8 gamma chain	C8G	22277.3
Profilin-1	PFN1	15054.3
Thrombospondin-1	THBS1	129381.7
Corticosteroid-binding globulin	SERPINA6	45142.1
Apolipoprotein(a)	LPA	282914
Monocyte differentiation antigen CD14	CD14	40076.6
Complement factor H	CFH	139096.2
Alpha-2-antiplasmin	SERPINF2	54566.6
Coagulation factor VII	F7	161349.3
Complement C1s subcomponent	C1S	76684.2
Complement C4-B	C4B	192752.8
Immunoglobulin lambda constant 3	IGLC3	11265.2
Immunoglobulin heavy variable 4-38-2	IGHV4-38-2	13016.1
Complement component C7	C7	93516.6
Isoform 4 of Clusterin	CLU	48803.6
Endoplasmic reticulum chaperone BiP	HSPA5	72334.7
Mannose-binding protein C	MBL2	26144.1

Complement component C6	C6	104786.2
Carboxypeptidase N catalytic chain	CPN1	52286.4
Lipopolysaccharide-binding protein	LBP	53386
Alpha-1-acid glycoprotein 2	ORM2	23603.3
Inter-alpha-trypsin inhibitor heavy chain H2	ITIH2	106465.5
Inter-alpha-trypsin inhibitor heavy chain H1	ITIH1	101389.8
Pregnancy zone protein	PZP	163862
C4b-binding protein beta chain	C4BPB	28357.2
Glutathione peroxidase 3	GPX3	25553.2
Carboxypeptidase N subunit 2	CPN2	60558.7
Isoform 2 of Vitamin K-dependent protein Z	PROZ	47052.1
Fibulin-1	FBLN1	77211.6
Serum paraoxonase/arylesterase 1	PON1	39732.4
Properdin	CFP	51274.1
Kallistatin	SERPINA4	48544
Thrombospondin-4	THBS4	105869.2
Keratin, type I cytoskeletal 9	KRT9	62065.9
Isoform 2 of Insulin-like growth factor-binding protein complex acid labile subunit	IGFALS	70239.5
Pigment epithelium-derived factor	SERPINF1	46314.3
Biotinidase	BTD	61133.4
Afamin	AFM	69070.1
Mannan-binding lectin serine protease 1	MASP1	79247.4
Isoform 2 of Mannan-binding lectin serine protease 1	MASP1	81859.6
Lumican	LUM	38431.5
Phospholipid transfer protein	PLTP	54741.2
Hemoglobin subunit beta	HBB	15998
Hemoglobin subunit alpha	HBA1	15257.6
Phosphatidylinositol-glycan-specific phospholipase D	GPLD1	92338.9
Complement factor H-related protein 1	CFHR1	37650.4
Prolow-density lipoprotein receptor-related protein 1	LRP1	504591.8
Galectin-3-binding protein	LGALS3BP	65332.1
Platelet-activating factor acetylhydrolase	PLA2G7	50079.6

Hyaluronan-binding protein 2	HABP2	62671.4
Inter-alpha-trypsin inhibitor heavy chain H4	ITIH4	103358.4
Procollagen C-endopeptidase enhancer 1	PCOLCE	47972.5
Serum paraoxonase/lactonase 3	PON3	39608.1
Transforming growth factor-beta-induced protein ig-h3	TGFBI	74682.9
Adiponectin	ADIPOQ	26414.2
Isoform 4 of Extracellular matrix protein 1	ECM1	63562.7
Vasorin	VASN	236295.2
Plexin domain-containing protein 2	PLXDC2	59583
Isoform C of Proteoglycan 4	PRG4	141093.1
Carboxypeptidase B2	CPB2	48424.7
Beta-Ala-His dipeptidase	CNDP1	56693.1
Isoform 2 of N-acetylmuramoyl-L-alanine amidase	PGLYRP2	68001
Isoform 9 of Collectin-11	COLEC11	29005.9
Complement factor H-related protein 5	CFHR5	64418.3
Adipocyte plasma membrane-associated protein	APMAP	46481.5
Cartilage acidic protein 1	CRTAC1	71421.1
Complement C1r subcomponent-like protein	C1RL	53497.5
Fetuin-B	FETUB	91235.5
Prenylcysteine oxidase 1	PCYOX1	56642.2
Neurogenic locus notch homolog protein 3	NOTCH3	243622
IgGFc-binding protein	FCGBP	571982.8
Isoform 1 of Serum albumin precursor	ALB	69366.9
Protease I precursor Lysyl endopeptidase Achromobacter lyticus		68125.5
Cytochrome c - Bos taurus (Bovine)	CYCS	11704.1
Apolipoprotein A-II	APOA2	14914.4
Bos Taurus 121 kDa protein		121458.7
Keratin, type II cytoskeletal 2 epidermal	KRT2	201453.3

Table 12 – Full names, gene names, molecular weights, and probability counts of the proteins with a probability count above 95% in serum-PEG-FPLC.

The proteins common to all three samples, as well as the proteins identified between pairs of samples, have been determined. Table 13, Table 14, Table 15 and Table 16 present the full list of proteins identified with a probability count above 95% in both serum and serum-FPLC, serum and serum-PEG-FPLC, and serum, serum-FPLC, and serum-PEG-FPLC, respectively.

Full names of the proteins identified with a probability count above 95% in both serum and serum-FPLC	**Gene names of the proteins identified with a probability count above 95% in both serum and serum-FPLC**	**MW (Da)**
Alpha-1-antitrypsin	SERPINA1	100996.6
Immunoglobulin kappa variable 2-40	IGKV2-40	13310.6
SAA2-SAA4 readthrough	SAA2-SAA4	23354.3
Coagulation factor V	F5	251710.5
Immunoglobulin heavy variable 3-49	IGHV3-49	13056
Complement C1q B chain (Fragment)	C1QB	26722.8
Titin	TTN	3994242.8
Immunoglobulin heavy variable 6-1	IGHV6-1	13481.4
Immunoglobulin heavy variable 3-15	IGHV3-15	12926
Immunoglobulin heavy variable 1-18	IGHV1-18	12820.3
Immunoglobulin heavy variable 5-51	IGHV5-51	12674.9
Complement C4-A	C4A	192876.9
Ig-like domain-containing protein (Fragment)	LOC102724971	12964.8
Keratin, type I cytoskeletal 10	KRT10	63347.8
Vitamin K-dependent protein S	PROS1	73758.4
Immunoglobulin heavy variable 3-72	IGHV3-72	11167.5
Immunoglobulin lambda constant 7 (Fragment)	IGLC7	11253.1
Angiotensinogen	AGT	52070.5
C-X-C motif chemokine		21143
Sushi domain-containing protein		169887.5
Complement C5	C5	188623.3
Complement C8 alpha chain	C8A	62616.1
Coagulation factor XII	F12	67790.6
Complement component C8 beta chain	C8B	66947.8
Inter-alpha-trypsin inhibitor heavy chain H3	ITIH3	103776.2
Plasminogen	PLG	92487.6
Apolipoprotein L1	APOL1	47383.3
complement subcomponent C1r	C1R	81890.5
Complement C2	C2	140943.5
Immunoglobulin lambda-like polypeptide 5	IGLL5	23062.9

Apolipoprotein D (Fragment)	APOD	24158.6
HGF activator	HGFAC	71482.3
Protein Z-dependent protease inhibitor	SERPINA10	55115.6
Macrophage stimulating 1	MST1	80317.8
Complement factor I	CFI	65749.8
Cartilage oligomeric matrix protein	COMP	227277.3
Haptoglobin	HP	49105.5
Uncharacterized protein (Fragment)		76884.5
Apolipoprotein C-II	APOC4-APOC2	20049.7
Sulfhydryl oxidase 1	QSOX1	82578.7
CD5 antigen-like	CD5L	38085.9
Ficolin-3	FCN3	32903.3
Attractin	ATRN	158536.3
Apolipoprotein M	APOM	21253.9
Ceruloplasmin	CP	122221.9
Prothrombin	F2	70036.8
Isoform 2 of Haptoglobin	HP	38451.4
Haptoglobin-related protein	HPR	39029.5
Coagulation factor IX	F9	51777.6
Coagulation factor X	F10	54732.1
Antithrombin-III	SERPINC1	52604.1
Alpha-1-antitrypsin	SERPINA1	46737.9
Alpha-1-antichymotrypsin	SERPINA3	47653
Alpha-2-macroglobulin	A2M	163289.9
Complement C3	C3	187149.1
Isoform LMW of Kininogen-1	KNG1	47883.6
Immunoglobulin J chain	JCHAIN	18098.5
Immunoglobulin kappa variable 3-20	IGKV3-20	12557.7
Immunoglobulin heavy variable 3-7	IGHV3-7	12942.7
Immunoglobulin heavy variable 3-9	IGHV3-9	12945.1
Polymeric immunoglobulin receptor	PIGR	83283.4
Immunoglobulin kappa constant	IGKC	11764.8
Isoform 1 of Immunoglobulin heavy constant gamma 1	IGHG1	36105
Isoform 1 of Immunoglobulin heavy constant gamma 2	IGHG2	35899.2
Isoform 1 of Immunoglobulin heavy constant gamma 3	IGHG3	41285.9
Immunoglobulin heavy constant	IGHG4	43830.8

gamma 4		
Isoform 1 of Immunoglobulin heavy constant mu	IGHM	49438.8
Isoform 1 of Immunoglobulin heavy constant alpha 1	IGHA1	37653.8
Isoform 1 of Immunoglobulin heavy constant alpha 2	IGHA2	36590.5
Isoform 1 of Immunoglobulin heavy constant delta	IGHD	42352.2
Hemoglobin subunit delta	HBD	16055.2
Keratin, type I cytoskeletal 14	KRT14	254176.8
Apolipoprotein A-I	APOA1	30778.5
Apolipoprotein E	APOE	36153.5
Apolipoprotein C-I	APOC1	9332.4
Fibrinogen alpha chain	FGA	94973.4
Fibrinogen beta chain	FGB	55928.6
Fibrinogen gamma chain	FGG	51513.3
Serum amyloid P-component	APCS	25387.7
Complement C1q subcomponent subunit A	C1QA	26016.6
Complement C1q subcomponent subunit C	C1QC	25774
Complement component C9	C9	63174.9
Beta-2-glycoprotein 1	APOH	38298.5
Leucine-rich alpha-2-glycoprotein	LRG1	38179.7
Isoform 1 of Fibronectin	FN1	256494.2
Protein AMBP	AMBP	38999.6
Alpha-1-acid glycoprotein 1	ORM1	23540.2
Alpha-2-HS-glycoprotein	AHSG	39339.5
Transthyretin	TTR	15886.9
Isoform 3 of Vitamin D-binding protein	GC	55077.9
Serotransferrin	TF	77050.2
Hemopexin	HPX	51676.5
Coagulation factor XI	F11	70109.2
C4b-binding protein alpha chain	C4BPA	67033
Vitronectin	VTN	54306.1
Vitamin K-dependent protein C	PROC	52071.2
Apolipoprotein B-100	APOB	515554.7
Histidine-rich glycoprotein	HRG	59576.6
Alpha-1B-glycoprotein	A1BG	54253.3
Keratin, type II cytoskeletal 1	KRT1	66040.3

von Willebrand factor	VWF	309251.2
Sex hormone-binding globulin	SHBG	43780.6
Immunoglobulin kappa variable 3-11	IGKV3-11	12575.7
Isoform 3 of Plasma protease C1 inhibitor	SERPING1	351432.7
Coagulation factor XIII B chain	F13B	75511.7
Tetranectin	CLEC3B	22537
Thyroxine-binding globulin	SERPINA7	46325.6
Heparin cofactor 2	SERPIND1	57072.9
Cholinesterase	BCHE	68420.1
Immunoglobulin kappa variable 4-1	IGKV4-1	51048.5
Gelsolin	GSN	85697.8
Complement C2	C2	83268.8
Apolipoprotein A-IV	APOA4	45372.3
Complement component C8 gamma chain	C8G	22277.3
Corticosteroid-binding globulin	SERPINA6	45142.1
Apolipoprotein(a)	LPA	282914
Monocyte differentiation antigen CD14	CD14	40076.6
Complement factor H	CFH	139096.2
Alpha-2-antiplasmin	SERPINF2	54566.6
Keratin, type I cytoskeletal 16	KRT16	51269
Complement C1s subcomponent	C1S	76684.2
Immunoglobulin lambda constant 3	IGLC3	11265.2
Immunoglobulin heavy variable 4-38-2	IGHV4-38-2	13016.1
Complement component C7	C7	93516.6
Isoform 4 of Clusterin	CLU	48803.6
Complement component C6	C6	104786.2
Carboxypeptidase N catalytic chain	CPN1	52286.4
Lipopolysaccharide-binding protein	LBP	53386
Alpha-1-acid glycoprotein 2	ORM2	23603.3
Inter-alpha-trypsin inhibitor heavy chain H2	ITIH2	106465.5
Inter-alpha-trypsin inhibitor heavy chain H1	ITIH1	101389.8
Pregnancy zone protein	PZP	163862
C4b-binding protein beta chain	C4BPB	28357.2
Glutathione peroxidase 3	GPX3	25553.2
Carboxypeptidase N subunit 2	CPN2	60558.7

Isoform 2 of Vitamin K-dependent protein Z	PROZ	47052.1
Fibulin-1	FBLN1	77211.6
Serum paraoxonase/arylesterase 1	PON1	39732.4
Properdin	CFP	51274.1
Kallistatin	SERPINA4	48544
Keratin, type I cytoskeletal 9	KRT9	62065.9
Isoform 2 of Insulin-like growth factor-binding protein complex acid labile subunit	IGFALS	70239.5
Pigment epithelium-derived factor	SERPINF1	46314.3
Isoform Short of Complement factor H-related protein 2	CFHR2	27896.3
Biotinidase	BTD	61133.4
Afamin	AFM	69070.1
Isoform 2 of Mannan-binding lectin serine protease 1	MASP1	81859.6
Selenoprotein P	SELENOP	43173.7
Lumican	LUM	38431.5
Phospholipid transfer protein	PLTP	54741.2
Hemoglobin subunit beta	HBB	15998
Hemoglobin subunit alpha	HBA1	15257.6
Phosphatidylinositol-glycan-specific phospholipase D	GPLD1	92338.9
Complement factor H-related protein 1	CFHR1	37650.4
Galectin-3-binding protein	LGALS3BP	65332.1
Hyaluronan-binding protein 2	HABP2	62671.4
Inter-alpha-trypsin inhibitor heavy chain H4	ITIH4	103358.4
Serum paraoxonase/lactonase 3	PON3	39608.1
Isoform 4 of Extracellular matrix protein 1	ECM1	63562.7
Peptidase inhibitor 16	PI16	49471
Isoform C of Proteoglycan 4	PRG4	141093.1
Carboxypeptidase B2	CPB2	48424.7
Beta-Ala-His dipeptidase	CNDP1	56693.1
Isoform 2 of N-acetylmuramoyl-L-alanine amidase	PGLYRP2	68001
Complement factor H-related protein 5	CFHR5	64418.3
Interleukin-1 receptor accessory protein	IL1RAP	65419.4
Cartilage acidic protein 1	CRTAC1	71421.1
Complement C1r subcomponent-like protein	C1RL	53497.5

Fetuin-B	FETUB	91235.5
IgGFc-binding protein	FCGBP	571982.8
Keratin, type II cytoskeletal 6A	KRT6A	195111
Isoform 1 of Serum albumin precursor	ALB	69366.9
Protease I precursor Lysyl endopeptidase Achromobacter lyticus		68125.5
Apolipoprotein A-II	APOA2	14914.4
Bos Taurus 121 kDa Protein		121458.7
Keratin, type II cytoskeletal 2 epidermal	KRT2	201453.3

Table 13 – Full names, gene names and molecular weights of the proteins with a probability count above 95% in both serum and serum-FPLC.

Full names of the proteins identified with a probability count above 95% in both serum and serum-PEG-FPLC	**Gene names of the proteins identified with a probability count above 95% in both serum and serum-PEG-FPLC**	**MW (Da)**
Alpha-1-antitrypsin	SERPINA1	100996.6
Immunoglobulin kappa variable 2-40	IGKV2-40	13310.6
SAA2-SAA4 readthrough	SAA2-SAA4	23354.3
Coagulation factor V	F5	251710.5
Immunoglobulin heavy variable 3-49	IGHV3-49	13056
Complement C1q B chain (Fragment)	C1QB	26722.8
Titin	TTN	3994242.8
Immunoglobulin heavy variable 3-15	IGHV3-15	12926
Immunoglobulin heavy variable 1-18	IGHV1-18	12820.3
Immunoglobulin heavy variable 5-51	IGHV5-51	12674.9
Complement C4-A	C4A	192876.9
Ig-like domain-containing protein (Fragment)	LOC102724971	12964.8
Keratin, type I cytoskeletal 10	KRT10	63347.8
Vitamin K-dependent protein S	PROS1	73758.4
Immunoglobulin heavy variable 3-72	IGHV3-72	11167.5
Immunoglobulin lambda constant 7 (Fragment)	IGLC7	11253.1
Angiotensinogen	AGT	52070.5
Sushi domain-containing protein		169887.5
Complement C5	C5	188623.3
Complement C8 alpha chain	C8A	62616.1
Coagulation factor XII	F12	67790.6
Complement component C8 beta chain	C8B	66947.8
Inter-alpha-trypsin inhibitor heavy chain H3	ITIH3	103776.2

Plasminogen	PLG	92487.6
Apolipoprotein L1	APOL1	47383.3
complement subcomponent C1r	C1R	81890.5
Complement C2	C2	140943.5
Immunoglobulin lambda-like polypeptide 5	IGLL5	23062.9
Apolipoprotein D (Fragment)	APOD	24158.6
HGF activator	HGFAC	71482.3
Protein Z-dependent protease inhibitor	SERPINA10	55115.6
Macrophage stimulating 1	MST1	80317.8
Complement factor I	CFI	65749.8
Cartilage oligomeric matrix protein	COMP	227277.3
Haptoglobin	HP	49105.5
Uncharacterized protein (Fragment)		76884.5
Apolipoprotein C-II	APOC4-APOC2	20049.7
CD5 antigen-like	CD5L	38085.9
Ficolin-3	FCN3	32903.3
Attractin	ATRN	158536.3
Apolipoprotein M	APOM	21253.9
Ceruloplasmin	CP	122221.9
Prothrombin	F2	70036.8
Isoform 2 of Haptoglobin	HP	38451.4
Haptoglobin-related protein	HPR	39029.5
Coagulation factor IX	F9	51777.6
Coagulation factor X	F10	54732.1
Antithrombin-III	SERPINC1	52604.1
Alpha-1-antitrypsin	SERPINA1	46737.9
Alpha-1-antichymotrypsin	SERPINA3	47653
Alpha-2-macroglobulin	A2M	163289.9
Complement C3	C3	187149.1
Isoform LMW of Kininogen-1	KNG1	47883.6
Immunoglobulin J chain	JCHAIN	18098.5
Immunoglobulin kappa variable 3-20	IGKV3-20	12557.7
Immunoglobulin heavy variable 3-7	IGHV3-7	12942.7
Immunoglobulin heavy variable 3-9	IGHV3-9	12945.1
Polymeric immunoglobulin receptor	PIGR	83283.4
Immunoglobulin kappa constant	IGKC	11764.8

Isoform 1 of Immunoglobulin heavy constant gamma 1	IGHG1	36105
Isoform 1 of Immunoglobulin heavy constant gamma 2	IGHG2	35899.2
Isoform 1 of Immunoglobulin heavy constant gamma 3	IGHG3	41285.9
Immunoglobulin heavy constant gamma 4	IGHG4	43830.8
Isoform 1 of Immunoglobulin heavy constant mu	IGHM	49438.8
Isoform 1 of Immunoglobulin heavy constant alpha 1	IGHA1	37653.8
Isoform 1 of Immunoglobulin heavy constant alpha 2	IGHA2	36590.5
Isoform 1 of Immunoglobulin heavy constant delta	IGHD	42352.2
Hemoglobin subunit delta	HBD	16055.2
Apolipoprotein A-I	APOA1	30778.5
Apolipoprotein E	APOE	36153.5
Apolipoprotein C-I	APOC1	9332.4
Fibrinogen alpha chain	FGA	94973.4
Fibrinogen beta chain	FGB	55928.6
Fibrinogen gamma chain	FGG	51513.3
Serum amyloid P-component	APCS	25387.7
Complement C1q subcomponent subunit A	C1QA	26016.6
Complement C1q subcomponent subunit C	C1QC	25774
Complement component C9	C9	63174.9
Beta-2-glycoprotein 1	APOH	38298.5
Leucine-rich alpha-2-glycoprotein	LRG1	38179.7
Isoform 1 of Fibronectin	FN1	256494.2
Protein AMBP	AMBP	38999.6
Alpha-1-acid glycoprotein 1	ORM1	23540.2
Alpha-2-HS-glycoprotein	AHSG	39339.5
Transthyretin	TTR	15886.9
Isoform 3 of Vitamin D-binding protein	GC	55077.9
Serotransferrin	TF	77050.2
Hemopexin	HPX	51676.5
Coagulation factor XI	F11	70109.2
C4b-binding protein alpha chain	C4BPA	67033
Vitronectin	VTN	54306.1
Vitamin K-dependent protein C	PROC	52071.2
Apolipoprotein B-100	APOB	515554.7

Histidine-rich glycoprotein	HRG	59576.6
Alpha-1B-glycoprotein	A1BG	54253.3
Keratin, type II cytoskeletal 1	KRT1	66040.3
von Willebrand factor	VWF	309251.2
Sex hormone-binding globulin	SHBG	43780.6
Immunoglobulin kappa variable 3-11	IGKV3-11	12575.7
Isoform 3 of Plasma protease C1 inhibitor	SERPING1	351432.7
Coagulation factor XIII B chain	F13B	75511.7
Tetranectin	CLEC3B	22537
Thyroxine-binding globulin	SERPINA7	46325.6
Heparin cofactor 2	SERPIND1	57072.9
Cholinesterase	BCHE	68420.1
Immunoglobulin kappa variable 4-1	IGKV4-1	51048.5
Gelsolin	GSN	85697.8
Complement C2	C2	83268.8
Apolipoprotein A-IV	APOA4	45372.3
Complement component C8 gamma chain	C8G	22277.3
Corticosteroid-binding globulin	SERPINA6	45142.1
Apolipoprotein(a)	LPA	282914
Monocyte differentiation antigen CD14	CD14	40076.6
Complement factor H	CFH	139096.2
Alpha-2-antiplasmin	SERPINF2	54566.6
Complement C1s subcomponent	C1S	76684.2
Immunoglobulin lambda constant 3	IGLC3	11265.2
Immunoglobulin heavy variable 4-38-2	IGHV4-38-2	13016.1
Complement component C7	C7	93516.6
Isoform 4 of Clusterin	CLU	48803.6
Complement component C6	C6	104786.2
Carboxypeptidase N catalytic chain	CPN1	52286.4
Lipopolysaccharide-binding protein	LBP	53386
Alpha-1-acid glycoprotein 2	ORM2	23603.3
Inter-alpha-trypsin inhibitor heavy chain H2	ITIH2	106465.5
Inter-alpha-trypsin inhibitor heavy chain H1	ITIH1	101389.8
Pregnancy zone protein	PZP	163862
C4b-binding protein beta chain	C4BPB	28357.2

Glutathione peroxidase 3	GPX3	25553.2
Carboxypeptidase N subunit 2	CPN2	60558.7
Isoform 2 of Vitamin K-dependent protein Z	PROZ	47052.1
Fibulin-1	FBLN1	77211.6
Serum paraoxonase/arylesterase 1	PON1	39732.4
Properdin	CFP	51274.1
Kallistatin	SERPINA4	48544
Keratin, type I cytoskeletal 9	KRT9	62065.9
Isoform 2 of Insulin-like growth factor-binding protein complex acid labile subunit	IGFALS	70239.5
Pigment epithelium-derived factor	SERPINF1	46314.3
Biotinidase	BTD	61133.4
Afamin	AFM	69070.1
Isoform 2 of Mannan-binding lectin serine protease 1	MASP1	81859.6
Lumican	LUM	38431.5
Phospholipid transfer protein	PLTP	54741.2
Hemoglobin subunit beta	HBB	15998
Hemoglobin subunit alpha	HBA1	15257.6
Phosphatidylinositol-glycan-specific phospholipase D	GPLD1	92338.9
Complement factor H-related protein 1	CFHR1	37650.4
Galectin-3-binding protein	LGALS3BP	65332.1
Hyaluronan-binding protein 2	HABP2	62671.4
Inter-alpha-trypsin inhibitor heavy chain H4	ITIH4	103358.4
Serum paraoxonase/lactonase 3	PON3	39608.1
Transforming growth factor-beta-induced protein ig-h3	TGFBI	74682.9
Isoform 4 of Extracellular matrix protein 1	ECM1	63562.7
Isoform C of Proteoglycan 4	PRG4	141093.1
Carboxypeptidase B2	CPB2	48424.7
Beta-Ala-His dipeptidase	CNDP1	56693.1
Isoform 2 of N-acetylmuramoyl-L-alanine amidase	PGLYRP2	68001
Complement factor H-related protein 5	CFHR5	64418.3
Cartilage acidic protein 1	CRTAC1	71421.1
Complement C1r subcomponent-like protein	C1RL	53497.5
Fetuin-B	FETUB	91235.5

IgGFc-binding protein	FCGBP	571982.8
Isoform 1 of Serum albumin precursor	ALB	69366.9
Protease I precursor Lysyl endopeptidase Achromobacter lyticus		68125.5
Apolipoprotein A-II	APOA2	14914.4
Bos Taurus 121 kDa protein		121458.7
Keratin, type II cytoskeletal 2 epidermal	KRT2	201453.3

Table 14 – Full names, gene names and molecular weights of the proteins with a probability count above 95% in both serum and serum-PEG-FPLC.

Full names of the proteins identified with a probability count above 95% in both serum-FPLC and serum-PEG-FPLC	**Gene Names of proteins identified with probability count over 95% in both serum-FPLC and serum-PEG-FPLC**	**MW (Da)**
Alpha-1-antitrypsin	SERPINA1	100996.6
Immunoglobulin lambda variable 4-69	IGLV4-69	12773.7
Immunoglobulin heavy variable 1/OR15-1 (non-functional) (Fragment)	IGHV1OR15-1	13011.6
Immunoglobulin kappa variable 2-40	IGKV2-40	13310.6
Cell adhesion molecule L1 like	CHL1	130796.9
SAA2-SAA4 readthrough	SAA2-SAA4	23354.3
Coagulation factor V	F5	251710.5
Immunoglobulin heavy variable 3-49	IGHV3-49	13056
Complement C1q B chain (Fragment)	C1QB	26722.8
Titin	TTN	3994242.8
Immunoglobulin heavy variable 3-15	IGHV3-15	12926
Immunoglobulin heavy variable 1-18	IGHV1-18	12820.3
Immunoglobulin heavy variable 5-51	IGHV5-51	12674.9
Complement C4-A	C4A	192876.9
Ig-like domain-containing protein (Fragment)	LOC102724971	12964.8
Tenascin-X	TNXB	456176.8
Keratin, type I cytoskeletal 10	KRT10	63347.8
Vitamin K-dependent protein S	PROS1	73758.4
Immunoglobulin heavy variable 3-72	IGHV3-72	11167.5
Immunoglobulin lambda constant 7 (Fragment)	IGLC7	11253.1
Angiotensinogen	AGT	52070.5
Sushi domain-containing protein		169887.5
Complement C5	C5	188623.3
Complement C8 alpha chain	C8A	62616.1
Coagulation factor XII	F12	67790.6

Complement component C8 beta chain	C8B	66947.8
MBL associated serine protease 2	MASP2	74726.5
Inter-alpha-trypsin inhibitor heavy chain H3	ITIH3	103776.2
Proprotein convertase subtilisin/kexin type 9	PCSK9	87202.5
Plasminogen	PLG	92487.6
Apolipoprotein L1	APOL1	47383.3
complement subcomponent C1r	C1R	81890.5
Complement C2	C2	140943.5
Immunoglobulin lambda-like polypeptide 5	IGLL5	23062.9
Apolipoprotein D (Fragment)	APOD	24158.6
HGF activator	HGFAC	71482.3
Neuropilin 1	NRP1	72095.8
Protein Z-dependent protease inhibitor	SERPINA10	55115.6
Macrophage stimulating 1	MST1	80317.8
Complement factor I	CFI	65749.8
Cartilage oligomeric matrix protein	COMP	227277.3
Haptoglobin	HP	49105.5
Uncharacterized protein (Fragment)		76884.5
Actin gamma 1	ACTG1	80113.5
Cathelicidin antimicrobial peptide	CAMP	19591.6
Apolipoprotein C-II	APOC4-APOC2	20049.7
CD5 antigen-like	CD5L	38085.9
Ficolin-3	FCN3	32903.3
Attractin	ATRN	158536.3
Apolipoprotein M	APOM	21253.9
Ceruloplasmin	CP	122221.9
Coagulation factor XIII A chain	F13A1	83268.3
Prothrombin	F2	70036.8
Isoform 2 of Haptoglobin	HP	38451.4
Haptoglobin-related protein	HPR	39029.5
Coagulation factor IX	F9	51777.6
Coagulation factor X	F10	54732.1
Complement factor D	CFD	27032.4
Antithrombin-III	SERPINC1	52604.1
Alpha-1-antitrypsin	SERPINA1	46737.9
Alpha-1-antichymotrypsin	SERPINA3	47653

Alpha-2-macroglobulin	A2M	163289.9
Complement C3	C3	187149.1
Isoform LMW of Kininogen-1	KNG1	47883.6
Immunoglobulin J chain	JCHAIN	18098.5
Immunoglobulin kappa variable 3-20	IGKV3-20	12557.7
Immunoglobulin heavy variable 3-7	IGHV3-7	12942.7
Immunoglobulin heavy variable 3-9	IGHV3-9	12945.1
Polymeric immunoglobulin receptor	PIGR	83283.4
Immunoglobulin kappa constant	IGKC	11764.8
Isoform 1 of Immunoglobulin heavy constant gamma 1	IGHG1	36105
Isoform 1 of Immunoglobulin heavy constant gamma 2	IGHG2	35899.2
Isoform 1 of Immunoglobulin heavy constant gamma 3	IGHG3	41285.9
Immunoglobulin heavy constant gamma 4	IGHG4	43830.8
Isoform 1 of Immunoglobulin heavy constant mu	IGHM	49438.8
Isoform 1 of Immunoglobulin heavy constant alpha 1	IGHA1	37653.8
Isoform 1 of Immunoglobulin heavy constant alpha 2	IGHA2	36590.5
Isoform 1 of Immunoglobulin heavy constant delta	IGHD	42352.2
Hemoglobin subunit delta	HBD	16055.2
Apolipoprotein A-I	APOA1	30778.5
Apolipoprotein E	APOE	36153.5
Apolipoprotein C-I	APOC1	9332.4
Fibrinogen alpha chain	FGA	94973.4
Fibrinogen beta chain	FGB	55928.6
Fibrinogen gamma chain	FGG	51513.3
Serum amyloid P-component	APCS	25387.7
Complement C1q subcomponent subunit A	C1QA	26016.6
Complement C1q subcomponent subunit C	C1QC	25774
Complement component C9	C9	63174.9
Beta-2-glycoprotein 1	APOH	38298.5
Leucine-rich alpha-2-glycoprotein	LRG1	38179.7
Isoform 1 of Fibronectin	FN1	256494.2
Protein AMBP	AMBP	38999.6
Alpha-1-acid glycoprotein 1	ORM1	23540.2
Alpha-2-HS-glycoprotein	AHSG	39339.5
Transthyretin	TTR	15886.9

Isoform 3 of Vitamin D-binding protein	GC	55077.9
Serotransferrin	TF	77050.2
Hemopexin	HPX	51676.5
Coagulation factor XI	F11	70109.2
C4b-binding protein alpha chain	C4BPA	67033
Vitronectin	VTN	54306.1
Vitamin K-dependent protein C	PROC	52071.2
Apolipoprotein B-100	APOB	515554.7
Phosphatidylcholine-sterol acyltransferase	LCAT	140132.7
Histidine-rich glycoprotein	HRG	59576.6
Alpha-1B-glycoprotein	A1BG	54253.3
Keratin, type II cytoskeletal 1	KRT1	66040.3
von Willebrand factor	VWF	309251.2
Sex hormone-binding globulin	SHBG	43780.6
Immunoglobulin kappa variable 3-11	IGKV3-11	12575.7
Isoform 3 of Plasma protease C1 inhibitor	SERPING1	351432.7
Coagulation factor XIII B chain	F13B	75511.7
Tetranectin	CLEC3B	22537
Thyroxine-binding globulin	SERPINA7	46325.6
Heparin cofactor 2	SERPIND1	57072.9
Cholinesterase	BCHE	68420.1
Immunoglobulin kappa variable 4-1	IGKV4-1	51048.5
Gelsolin	GSN	85697.8
Complement C2	C2	83268.8
Apolipoprotein A-IV	APOA4	45372.3
Platelet glycoprotein Ib alpha chain	GP1BA	71542.6
Complement component C8 gamma chain	C8G	22277.3
Profilin-1	PFN1	15054.3
Thrombospondin-1	THBS1	129381.7
Corticosteroid-binding globulin	SERPINA6	45142.1
Apolipoprotein(a)	LPA	282914
Monocyte differentiation antigen CD14	CD14	40076.6
Complement factor H	CFH	139096.2
Alpha-2-antiplasmin	SERPINF2	54566.6
Coagulation factor VII	F7	161349.3
Complement C1s subcomponent	C1S	76684.2

Complement C4-B	C4B	192752.8
Immunoglobulin lambda constant 3	IGLC3	11265.2
Immunoglobulin heavy variable 4-38-2	IGHV4-38-2	13016.1
Complement component C7	C7	93516.6
Isoform 4 of Clusterin	CLU	48803.6
Endoplasmic reticulum chaperone BiP	HSPA5	72334.7
Mannose-binding protein C	MBL2	26144.1
Complement component C6	C6	104786.2
Carboxypeptidase N catalytic chain	CPN1	52286.4
Lipopolysaccharide-binding protein	LBP	53386
Alpha-1-acid glycoprotein 2	ORM2	23603.3
Inter-alpha-trypsin inhibitor heavy chain H2	ITIH2	106465.5
Inter-alpha-trypsin inhibitor heavy chain H1	ITIH1	101389.8
Pregnancy zone protein	PZP	163862
C4b-binding protein beta chain	C4BPB	28357.2
Glutathione peroxidase 3	GPX3	25553.2
Carboxypeptidase N subunit 2	CPN2	60558.7
Isoform 2 of Vitamin K-dependent protein Z	PROZ	47052.1
Fibulin-1	FBLN1	77211.6
Serum paraoxonase/arylesterase 1	PON1	39732.4
Properdin	CFP	51274.1
Kallistatin	SERPINA4	48544
Thrombospondin-4	THBS4	105869.2
Keratin, type I cytoskeletal 9	KRT9	62065.9
Isoform 2 of Insulin-like growth factor-binding protein complex acid labile subunit	IGFALS	70239.5
Pigment epithelium-derived factor	SERPINF1	46314.3
Biotinidase	BTD	61133.4
Afamin	AFM	69070.1
Mannan-binding lectin serine protease 1	MASP1	79247.4
Isoform 2 of Mannan-binding lectin serine protease 1	MASP1	81859.6
Lumican	LUM	38431.5
Phospholipid transfer protein	PLTP	54741.2
Hemoglobin subunit beta	HBB	15998
Hemoglobin subunit alpha	HBA1	15257.6
Phosphatidylinositol-glycan-specific phospholipase D	GPLD1	92338.9
Complement factor H-related protein 1	CFHR1	37650.4

Prolow-density lipoprotein receptor-related protein 1	LRP1	504591.8
Galectin-3-binding protein	LGALS3BP	65332.1
Hyaluronan-binding protein 2	HABP2	62671.4
Inter-alpha-trypsin inhibitor heavy chain H4	ITIH4	103358.4
Procollagen C-endopeptidase enhancer 1	PCOLCE	47972.5
Serum paraoxonase/lactonase 3	PON3	39608.1
Adiponectin	ADIPOQ	26414.2
Isoform 4 of Extracellular matrix protein 1	ECM1	63562.7
Vasorin	VASN	236295.2
Plexin domain-containing protein 2	PLXDC2	59583
Isoform C of Proteoglycan 4	PRG4	141093.1
Carboxypeptidase B2	CPB2	48424.7
Beta-Ala-His dipeptidase	CNDP1	56693.1
Isoform 2 of N-acetylmuramoyl-L-alanine amidase	PGLYRP2	68001
Isoform 9 of Collectin-11	COLEC11	29005.9
Complement factor H-related protein 5	CFHR5	64418.3
Adipocyte plasma membrane-associated protein	APMAP	46481.5
Cartilage acidic protein 1	CRTAC1	71421.1
Complement C1r subcomponent-like protein	C1RL	53497.5
Fetuin-B	FETUB	91235.5
Prenylcysteine oxidase 1	PCYOX1	56642.2
Neurogenic locus notch homolog protein 3	NOTCH3	243622
IgGFc-binding protein	FCGBP	571982.8
Isoform 1 of Serum albumin precursor	ALB	69366.9
Protease I precursor Lysyl endopeptidase Achromobacter lyticus		68125.5
Apolipoprotein A-II	APOA2	14914.4
Bos Taurus 121 kDa protein		121458.7
Keratin, type II cytoskeletal 2 epidermal	KRT2	201453.3

Table 15 – Full names, gene names and molecular weights of the proteins with a probability count above 95% in both serum-FPLC and serum-PEG-FPLC.

Full names of the proteins identified with a probability count above 95% in serum, serum-FPLC and serum-PEG-FPLC	**Gene names of the proteins identified with a probability count above 95% in serum, serum-FPLC and serum-PEG-FPLC**	**MW (Da)**
Alpha-1-antitrypsin	SERPINA1	100996.6
Immunoglobulin kappa variable 2-40	IGKV2-40	13310.6
SAA2-SAA4 readthrough	SAA2-SAA4	23354.3

Coagulation factor V	F5	251710.5
Immunoglobulin heavy variable 3-49	IGHV3-49	13056
Complement C1q B chain (Fragment)	C1QB	26722.8
Titin	TTN	3994242.8
Immunoglobulin heavy variable 3-15	IGHV3-15	12926
Immunoglobulin heavy variable 1-18	IGHV1-18	12820.3
Immunoglobulin heavy variable 5-51	IGHV5-51	12674.9
Complement C4-A	C4A	192876.9
Ig-like domain-containing protein (Fragment)	LOC102724971	12964.8
Keratin, type I cytoskeletal 10	KRT10	63347.8
Vitamin K-dependent protein S	PROS1	73758.4
Immunoglobulin heavy variable 3-72	IGHV3-72	11167.5
Immunoglobulin lambda constant 7 (Fragment)	IGLC7	11253.1
Angiotensinogen	AGT	52070.5
Sushi domain-containing protein		169887.5
Complement C5	C5	188623.3
Complement C8 alpha chain	C8A	62616.1
Coagulation factor XII	F12	67790.6
Complement component C8 beta chain	C8B	66947.8
Inter-alpha-trypsin inhibitor heavy chain H3	ITIH3	103776.2
Plasminogen	PLG	92487.6
Apolipoprotein L1	APOL1	47383.3
complement subcomponent C1r	C1R	81890.5
Complement C2	C2	140943.5
Immunoglobulin lambda-like polypeptide 5	IGLL5	23062.9
Apolipoprotein D (Fragment)	APOD	24158.6
HGF activator	HGFAC	71482.3
Protein Z-dependent protease inhibitor	SERPINA10	55115.6
Macrophage stimulating 1	MST1	80317.8
Complement factor I	CFI	65749.8
Cartilage oligomeric matrix protein	COMP	227277.3
Haptoglobin	HP	49105.5
Uncharacterized protein (Fragment)		76884.5
Apolipoprotein C-II	APOC4-APOC2	20049.7
CD5 antigen-like	CD5L	38085.9
Ficolin-3	FCN3	32903.3

Attractin	ATRN	158536.3
Apolipoprotein M	APOM	21253.9
Ceruloplasmin	CP	122221.9
Prothrombin	F2	70036.8
Isoform 2 of Haptoglobin	HP	38451.4
Haptoglobin-related protein	HPR	39029.5
Coagulation factor IX	F9	51777.6
Coagulation factor X	F10	54732.1
Antithrombin-III	SERPINC1	52604.1
Alpha-1-antitrypsin	SERPINA1	46737.9
Alpha-1-antichymotrypsin	SERPINA3	47653
Alpha-2-macroglobulin	A2M	163289.9
Complement C3	C3	187149.1
Isoform LMW of Kininogen-1	KNG1	47883.6
Immunoglobulin J chain	JCHAIN	18098.5
Immunoglobulin kappa variable 3-20	IGKV3-20	12557.7
Immunoglobulin heavy variable 3-7	IGHV3-7	12942.7
Immunoglobulin heavy variable 3-9	IGHV3-9	12945.1
Polymeric immunoglobulin receptor	PIGR	83283.4
Immunoglobulin kappa constant	IGKC	11764.8
Isoform 1 of Immunoglobulin heavy constant gamma 1	IGHG1	36105
Isoform 1 of Immunoglobulin heavy constant gamma 2	IGHG2	35899.2
Isoform 1 of Immunoglobulin heavy constant gamma 3	IGHG3	41285.9
Immunoglobulin heavy constant gamma 4	IGHG4	43830.8
Isoform 1 of Immunoglobulin heavy constant mu	IGHM	49438.8
Isoform 1 of Immunoglobulin heavy constant alpha 1	IGHA1	37653.8
Isoform 1 of Immunoglobulin heavy constant alpha 2	IGHA2	36590.5
Isoform 1 of Immunoglobulin heavy constant delta	IGHD	42352.2
Hemoglobin subunit delta	HBD	16055.2
Apolipoprotein A-I	APOA1	30778.5
Apolipoprotein E	APOE	36153.5
Apolipoprotein C-I	APOC1	9332.4
Fibrinogen alpha chain	FGA	94973.4
Fibrinogen beta chain	FGB	55928.6
Fibrinogen gamma chain	FGG	51513.3

Serum amyloid P-component	APCS	25387.7
Complement C1q subcomponent subunit A	C1QA	26016.6
Complement C1q subcomponent subunit C	C1QC	25774
Complement component C9	C9	63174.9
Beta-2-glycoprotein 1	APOH	38298.5
Leucine-rich alpha-2-glycoprotein	LRG1	38179.7
Isoform 1 of Fibronectin	FN1	256494.2
Protein AMBP	AMBP	38999.6
Alpha-1-acid glycoprotein 1	ORM1	23540.2
Alpha-2-HS-glycoprotein	AHSG	39339.5
Transthyretin	TTR	15886.9
Isoform 3 of Vitamin D-binding protein	GC	55077.9
Serotransferrin	TF	77050.2
Hemopexin	HPX	51676.5
Coagulation factor XI	F11	70109.2
C4b-binding protein alpha chain	C4BPA	67033
Vitronectin	VTN	54306.1
Vitamin K-dependent protein C	PROC	52071.2
Apolipoprotein B-100	APOB	515554.7
Histidine-rich glycoprotein	HRG	59576.6
Alpha-1B-glycoprotein	A1BG	54253.3
Keratin, type II cytoskeletal 1	KRT1	66040.3
von Willebrand factor	VWF	309251.2
Sex hormone-binding globulin	SHBG	43780.6
Immunoglobulin kappa variable 3-11	IGKV3-11	12575.7
Isoform 3 of Plasma protease C1 inhibitor	SERPING1	351432.7
Coagulation factor XIII B chain	F13B	75511.7
Tetranectin	CLEC3B	22537
Thyroxine-binding globulin	SERPINA7	46325.6
Heparin cofactor 2	SERPIND1	57072.9
Cholinesterase	BCHE	68420.1
Immunoglobulin kappa variable 4-1	IGKV4-1	51048.5
Gelsolin	GSN	85697.8
Complement C2	C2	83268.8
Apolipoprotein A-IV	APOA4	45372.3
Complement component C8 gamma chain	C8G	22277.3

Corticosteroid-binding globulin	SERPINA6	45142.1
Apolipoprotein(a)	LPA	282914
Monocyte differentiation antigen CD14	CD14	40076.6
Complement factor H	CFH	139096.2
Alpha-2-antiplasmin	SERPINF2	54566.6
Complement C1s subcomponent	C1S	76684.2
Immunoglobulin lambda constant 3	IGLC3	11265.2
Immunoglobulin heavy variable 4-38-2	IGHV4-38-2	13016.1
Complement component C7	C7	93516.6
Isoform 4 of Clusterin	CLU	48803.6
Complement component C6	C6	104786.2
Carboxypeptidase N catalytic chain	CPN1	52286.4
Lipopolysaccharide-binding protein	LBP	53386
Alpha-1-acid glycoprotein 2	ORM2	23603.3
Inter-alpha-trypsin inhibitor heavy chain H2	ITIH2	106465.5
Inter-alpha-trypsin inhibitor heavy chain H1	ITIH1	101389.8
Pregnancy zone protein	PZP	163862
C4b-binding protein beta chain	C4BPB	28357.2
Glutathione peroxidase 3	GPX3	25553.2
Carboxypeptidase N subunit 2	CPN2	60558.7
Isoform 2 of Vitamin K-dependent protein Z	PROZ	47052.1
Fibulin-1	FBLN1	77211.6
Serum paraoxonase/arylesterase 1	PON1	39732.4
Properdin	CFP	51274.1
Kallistatin	SERPINA4	48544
Keratin, type I cytoskeletal 9	KRT9	62065.9
Isoform 2 of Insulin-like growth factor-binding protein complex acid labile subunit	IGFALS	70239.5
Pigment epithelium-derived factor	SERPINF1	46314.3
Biotinidase	BTD	61133.4
Afamin	AFM	69070.1
Isoform 2 of Mannan-binding lectin serine protease 1	MASP1	81859.6
Lumican	LUM	38431.5
Phospholipid transfer protein	PLTP	54741.2
Hemoglobin subunit beta	HBB	15998
Hemoglobin subunit alpha	HBA1	15257.6
Phosphatidylinositol-glycan-specific phospholipase D	GPLD1	92338.9

Complement factor H-related protein 1	CFHR1	37650.4
Galectin-3-binding protein	LGALS3BP	65332.1
Hyaluronan-binding protein 2	HABP2	62671.4
Inter-alpha-trypsin inhibitor heavy chain H4	ITIH4	103358.4
Serum paraoxonase/lactonase 3	PON3	39608.1
Isoform 4 of Extracellular matrix protein 1	ECM1	63562.7
Isoform C of Proteoglycan 4	PRG4	141093.1
Carboxypeptidase B2	CPB2	48424.7
Beta-Ala-His dipeptidase	CNDP1	56693.1
Isoform 2 of N-acetylmuramoyl-L-alanine amidase	PGLYRP2	68001
Complement factor H-related protein 5	CFHR5	64418.3
Cartilage acidic protein 1	CRTAC1	71421.1
Complement C1r subcomponent-like protein	C1RL	53497.5
Fetuin-B	FETUB	91235.5
IgGFc-binding protein	FCGBP	571982.8
Isoform 1 of Serum albumin precursor	ALB	69366.9
Protease I precursor Lysyl endopeptidase Achromobacter lyticus		68125.5
Apolipoprotein A-II	APOA2	14914.4
Bos Taurus 121 kDa protein		121458.7
Keratin, type II cytoskeletal 2 epidermal	KRT2	201453.3

Table 16 – Full names, gene names and molecular weights of the proteins with a probability count above 95% in serum, serum-FPLC and serum-PEG-FPLC.

To further explore the overlap of proteins, a Venn diagram has been created to visualize the protein intersections between the samples. This graphical representation helps to illustrate the proteins shared between serum, serum-FPLC, and serum-PEG-FPLC, revealing the degree of protein overlap and identifying proteins unique to each sample.

The Venn diagram analysis (Figure 33) shows that there is still some difference between serum-FPLC and serum-PEG-FPLC. This observation highlights the ability of PEG-based selective precipitation to enrich certain proteins because this method precipitates specific proteins from a mixture by altering their solubility.

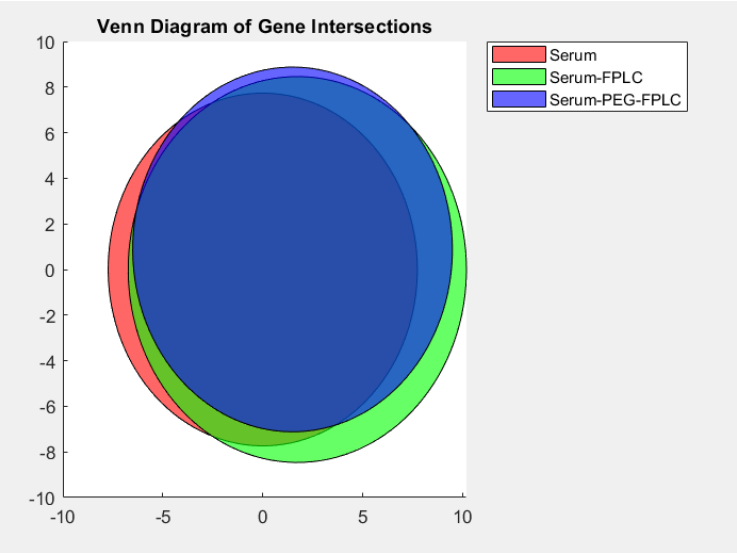

Figure 33 – Venn diagram illustrating the gene intersections between the three analyzed conditions.

Table 17 lists the proteins exclusive to the serum sample, identified only in this fraction and not in the serum-FPLC or serum-PEG-FPLC fractions. These proteins, including apolipoprotein C-III, zinc-alpha-2-glycoprotein, and C-reactive protein, are primarily involved in lipid metabolism, immune responses, and cellular signalling. Indeed, apolipoprotein C-III is found on triglyceride-rich lipoproteins such as chylomicrons, VLDL, and remnant cholesterol, playing a critical role in lipid metabolism [57]. Zinc-alpha-2-glycoprotein is a multifunctional protein involved in regulating lipid and glucose metabolism [58] and C-reactive protein is an acute-phase reactant involved in the immune response, with a well-established role in inflammation and cardiovascular diseases [59]. The molecular weights of these proteins vary significantly, indicating a broad range of protein sizes in the serum fraction, as expected. The identification of these proteins suggests their unique association with the serum matrix, highlighting their functional importance in various physiological processes.

Full names of proteins found exclusively in serum	Gene names of proteins found exclusively in serum	MW (Da)
Apolipoprotein C-III	APOC3	10852.3
Apolipoprotein F	APOF	35400.3
Zinc-alpha-2-glycoprotein	AZGP1	34258.6
Cadherin-5	CDH5	87529.5
C-reactive protein	CRP	25039
Alpha-S1-casein	CSN1S1	22975.2
Insulin-like growth factor-binding protein 3	IGFBP3	31674.1
Immunoglobulin heavy variable 1-24	IGHV1-24	12824.2
Lysozyme C	LYZ	68363.7
Retinol-binding protein	RBP4	22974
L-selectin	SELL	42187.8

Table 17 – Full names, gene names and molecular weights of proteins found exclusively in serum.

The serum-FPLC-exclusive proteins, including fructose-bisphosphate aldolase A, carbonic anhydrase 1, and desmoplakin, play key roles in various metabolic, structural, and cellular processes. The presence of structural proteins such as keratin 13 and other keratins suggests their involvement in maintaining cellular integrity.

These proteins are found exclusively in the serum-FPLC sample and reported in Table 18 suggesting that their presence is influenced by the fractionation process. The collected FPLC fraction corresponds to the first peak, as described in 3.2.1 and shown in Figure 13. This peak likely contains proteins that elute earlier due to their specific physicochemical properties, such as size, charge, or interactions with the chromatography matrix. As a result, the identified proteins may be selectively retained during the separation process, leading to their enrichment in the serum-FPLC sample.

Full names of proteins found exclusively in serum-FPLC	**Gene names of proteins found exclusively in serum-FPLC**	**MW (Da)**
Fructose-bisphosphate aldolase A	ALDOA	39420.6
Fructose-bisphosphate aldolase B	ALDOB	39473.3
Carbonic anhydrase 1	CA1	28870.4
Contactin-1	CNTN1	113322.8
Dermcidin	DCD	11284.1
Desmoplakin	DSP	331781.4
EGF-containing fibulin-like extracellular matrix protein 1	EFEMP1	54639.1
Ficolin-2	FCN2	34001.6
Glyceraldehyde-3-phosphate dehydrogenase	GAPDH	36053.4
Hornerin	HRNR	282372.7
Immunoglobulin lambda variable 3-10	IGLV3-10	12441
Integrin beta	ITGB1	87925.5
Isoform 1 of Keratin, type I cytoskeletal 13	KRT13	104945.1
Keratin 4	KRT4	63912.2
Keratin, type II cytoskeletal 5	KRT5	62379.6
Mannosyl-oligosaccharide 1,2-alpha-mannosidase IA	MAN1A1	72971.7
Pyruvate kinase	PKM	65930.9
Soluble scavenger receptor cysteine-rich domain-containing protein SSC5D	SSC5D	165740.6
Isoform 4 of Tenascin	TNC	230863.6

Table 18 – Full names, gene names and molecular weights of proteins found exclusively in serum-FPLC.

Table 19 lists the full names, gene names, and molecular weights of proteins exclusive to the serum-PEG-FPLC fraction. Proteins such as cytochrome c-Bos Taurus and platelet-activating factor acetylhydrolase are involved in key biochemical processes, including cellular respiration and lipid metabolism, respectively. Additionally, immunoglobulin variable regions are detected, although they appear as fragments, suggesting possible partial degradation or modification during the precipitation process.
The presence of immunoglobulin fragments in this fraction highlights PEG's selective precipitation ability, as PEG is known to preferentially precipitate high-molecular-weight and glycosylated proteins, including immunoglobulins [60]. This process occurs due to PEG's volume exclusion effect, which reduces protein solubility by limiting water availability, leading to protein aggregation and precipitation [60].

Full names of proteins found exclusively in serum-PEG-FPLC	Gene names of proteins found exclusively in serum-PEG-FPLC	MW (Da)
Cytochrome c - Bos taurus (Bovine)	CYCS	11704.1
Immunoglobulin kappa variable 1-17	IGKV1-17	12779
Immunoglobulin lambda variable 5-45 (Fragment)	IGLV5-45	13215.4
Platelet-activating factor acetylhydrolase	PLA2G7	50079.6

Table 19 – Full names, gene names and molecular weights of proteins found exclusively in serum-PEG-FPLC.

4.3.5 Discussion of the Protein Composition of LDL Isolated from Serum with and without DGUC

When comparing the serum samples with and without DGUC, several key differences emerge. The DGUC samples show a consistent abundance of Apo B, with relatively high spectrum counts across all subgroups, indicating that this protein remains abundant regardless of the subsequent DGUC steps. Complement proteins are also present in considerable amounts, suggesting that the density gradient method is effective at isolating these components, though their concentrations vary across the different DGUC samples. Apolipoproteins A-I and A-IV are represented at slightly lower spectrum counts but still appear consistently, demonstrating their stable presence in the DGUC samples. In the DGUC-filtrations-FPLC sample, the presence of Apo B and complement proteins like C3 and C4 remains evident, but at lower concentrations compared to the DGUC samples. This suggests that the filtration steps may have reduced the abundance of some larger or less soluble proteins.
The serum-PEG-FPLC sample shows alpha-2-macroglobulin as a significantly abundant protein, highlighting its dominant presence in this method. Additionally, proteins related to immunoglobulins are more prevalent in both serum-PEG-FPLC and DGUC-PEG-FPLC, indicating that the PEG precipitation method may lead to a higher representation of immune-related proteins compared to the other methods.

5. Conclusions and Future Work

This thesis highlights the significant impact of different isolation and purification strategies on the physical and biochemical properties of LDL particles, particularly in relation to their size distribution, purity, and protein corona formation. By systematically comparing LDL fractions obtained directly from serum with those isolated through DGUC-based methods, key differences in homogeneity, polydispersity, and contaminant removal were identified.

To characterize the protein composition of LDL isolated through different methods, MS-based proteomics was performed. This analysis provided a detailed profile of the proteins associated with LDL, revealing distinct differences between the various isolation strategies. The DGUC-derived samples exhibited a significantly reduced presence of non-LDL-associated proteins, confirming the effectiveness in removing loosely bound serum proteins and minimizing soft corona components. In contrast, LDL extracted directly from serum retained a broader range of associated proteins, suggesting that different isolation techniques influence the final composition of the protein corona. These findings reinforce the idea that the choice of purification strategy directly impacts the protein landscape surrounding LDL, potentially affecting its biological function and interactions.

Interestingly, some differences were observed in protein composition between the serum-FPLC and serum-PEG-FPLC samples, highlighting the selective precipitation ability of PEG. While PEG precipitation can aid in removing certain serum proteins, it does not fully eliminate non-LDL-associated contaminants, as evidenced by the broader particle size distributions and increased polydispersity observed in PEG-treated samples.

These results emphasize the critical role of protein-lipoprotein interactions and the protein corona in defining LDL characteristics. The study confirms that DGUC-based methods are the most effective for isolating a highly purified LDL fraction, minimizing soft corona components, and producing a more uniform nanoparticle population. Understanding and controlling the LDL protein corona through optimized isolation techniques may have significant implications for lipoprotein-based diagnostics and therapeutics, paving the way for more targeted applications in cardiovascular and metabolic research.

6. List of Figures

Figure 1 – Schematic comparison of the main differences between hard and soft coronas [7] ..7
Figure 2 – Schematic illustration depicting the shift from a soft corona to a hard corona [5]....8
Figure 3 – Schematic representation of the equivalent free sites (orange) and occupied ones (green) on the surface of nanomaterial for the Langmuir model [7].....9
Figure 4 – Lipoprotein structural composition [26]. 10
Figure 5 – Schematic overview of the size and density of various lipoproteins, including high-density lipoproteins (HDL), low-density lipoproteins (LDL), intermediate-density lipoproteins (IDL), very low-density lipoproteins (VLDL), and chylomicrons [made with VISME].....12
Figure 6 – Schematic representation of the outlined protocol for LDL extraction. 17
Figure 7 – Photographs of the gradient in the centrifuge tube following lipoproteins separation. (A) In band III, LDL is clearly visible as a distinct orange-yellow band [35]. (B) Consistently with findings from [35], the formation of band III, corresponding to LDL fraction, is also observed in this experiment. 18
Figure 8 – Chromatogram obtained through FPLC according to the outlined protocol. 19
Figure 9 – Schematic representation of the procedure outlined above. 20
Figure 10 – Chromatogram obtained through FPLC according to the outlined method.....20
Figure 11 – Schematic representation of the procedure outlined above. 21
Figure 12 – Chromatogram obtained through FPLC according to the outlined method.....21
Figure 13 – Chromatogram acquired via FPLC from H5667 Human Serum. 22
Figure 14 – Schematic representation of the procedure outlined above. 23
Figure 15 – Chromatogram acquired via FPLC following PEG precipitation of H5667 Human Serum. 23
Figure 16 – ÄKTA go™ protein purification system from Cytiva. 24
Figure 17 – Anton Paar Litesizer 500 Particle Analyzer. 26
Figure 18 – Beckman Coulter XL-I. 27
Figure 19 – In a double-sector centerpiece, the sample moves towards the bottom of the sector-shaped container to minimize convection. The reference sector is typically filled just slightly more than the sample sector to ensure that the solvent meniscus does not overlap with the sample profile [50]. 28
Figure 20 – The light path in an absorbance optical system (Beckman Coulter Optima XL-A/XL-I AUC) [50]. 28
Figure 21 – Mounting the monochromator [51].....29
Figure 22 – Console of Beckman Coulter XL-I. 30
Figure 23 – Number-weighted DLS distribution of LDL particles isolated from different DGUC purification methods. 32
Figure 24 – Number-weighted DLS distribution of LDL particles isolated directly from serum without DGUC. 33
Figure 25 – Negative-stained TEM image of LDL particles extracted via the DGUC-FPLC method.....34
Figure 26 – Negative-stained TEM image of LDL particles extracted via the serum-FPLC method [Ekaterina Poliukhina]. 34
Figure 27 – Normalized sedimentation coefficient distributions of LDL particles obtained through different purification methods using DGUC. 35
Figure 28 – Normalized sedimentation coefficient distributions of LDL particles purified directly from serum using different methods [the serum-PEG-FPLC SV-AUC analysis was

performed by Ekaterina Poliukhina]. 36
Figure 29 – Number-weighted DLS distribution of LDL particles isolated from all different purification methods.....37
Figure 30 – Normalized sedimentation coefficient distributions based on the maximum value of all six analyzed conditions [the serum-PEG-FPLC SV-AUC analysis was performed by Ekaterina Poliukhina]. 38
Figure 31 – (A) SDS-PAGE without reducing agent. (B) SDS-PAGE with reducing agent.....39
Figure 32 – (A) SDS-PAGE without reducing agent. (B) SDS-PAGE with reducing agent.....40
Figure 33 – Venn diagram illustrating the gene intersections between the three analyzed conditions. 87

7. List of Tables

Table 1 – Overview of all the lipoprotein classes [24].....10
Table 2 – Mean and standard deviation values from three measurements for each analyzed sample. 32
Table 3 – Mean and standard deviation values from three measurements for each analyzed sample. 33
Table 4 – Full names, gene names, molecular weights, and spectrum counts of the top 20 proteins with the highest spectrum counts in DGUC-FPLC sample.....42
Table 5 – Full names, gene names, molecular weights, and spectrum counts of the top 20 proteins with the highest spectrum counts in DGUC-PEG-FPLC sample.....43
Table 6 – Full names, gene names, molecular weights, and spectrum counts of the top 20 proteins with the highest spectrum counts in DGUC-filtrations-FPLC sample.....43
Table 7 – Full names, gene names, molecular weights, and spectrum counts of the top 20 proteins with the highest spectrum counts in serum. 44
Table 8 – Full names, gene names, molecular weights, and spectrum counts of the top 20 proteins with the highest spectrum counts in serum-FPLC. 45
Table 9 – Full names, gene names, molecular weights, and spectrum counts of the top 20 proteins with the highest spectrum counts in serum-PEG-FPLC.....46
Table 10 – Full names, gene names, molecular weights, and probability counts of the proteins with a probability count above 95% in serum.....52
Table 11 – Full names, gene names, molecular weights, and probability counts of the proteins with a probability count above 95% in serum-FPLC.....59
Table 12 – Full names, gene names, molecular weights, and probability counts of the proteins with a probability count above 95% in serum-PEG-FPLC.....65
Table 13 – Full names, gene names and molecular weights of the proteins with a probability count above 95% in both serum and serum-FPLC.....71
Table 14 – Full names, gene names and molecular weights of the proteins with a probability count above 95% in both serum and serum-PEG-FPLC.....76
Table 15 – Full names, gene names and molecular weights of the proteins with a probability count above 95% in both serum-FPLC and serum-PEG-FPLC.....81
Table 16 – Full names, gene names and molecular weights of the proteins with a probability count above 95% in serum, serum-FPLC and serum-PEG-FPLC. 86
Table 17 – Full names, gene names and molecular weights of proteins found exclusively in serum. 87
Table 18 – Full names, gene names and molecular weights of proteins found exclusively in serum-FPLC. 88
Table 19 – Full names, gene names and molecular weights of proteins found exclusively in serum-PEG-FPLC. 89

References

[1] Kornmueller, K., Vidakovic, I., Prassl, R., Artificial High Density Lipoprotein Nanoparticles in Cardiovascular Research, 2019, *Molecules*, 24, 2829, [https://doi.org/10.3390/molecules24152829]

[2] Feingold, K.R., Anawalt, B., Blackman, M.R., et al., Introduction to Lipids and Lipoproteins, 2000, *PubMed*, [https://www.ncbi.nlm.nih.gov/books/NBK305896/]

[3] Ohkawa, R., et al., Cholesterol transport between red blood cells and lipoproteins contributes to cholesterol metabolism in blood, 2020, *Journal of Lipid Research*, 61(12):1577 – 1588, [DOI: 10.1194/jlr.RA120000635]

[4] HDL (Good), LDL (Bad) Cholesterol and Triglycerides, American Heart Association, https://www.heart.org/en/health-topics/cholesterol/hdl-good-ldl-bad-cholesterol-and-triglycerides

[5] Fangyuan G., Shuai L., Lianyi W., Mengqi W., Fang W., Yujia W., Yunlong J., Yinzhou D., Qingliang Y., Xiaoyan Y., Gensheng Y., Protein corona, influence on drug delivery system and its improvement strategy: A review, 2024, *International Journal of Biological Macromolecules*, [DOI: 10.1016/j.ijbiomac.2023.128513]

[6] Pareek, V., Bhargava, A., Bhanot, V., Gupta, R., Jain, N., Panwar, J., Formation and Characterization of Protein Corona Around Nanoparticles: A Review, 2018, *J. Nanosci. Nanotechnol.*, 18(10):6653-6670, [DOI: 10.1166/jnn.2018.15766]

[7] García-Álvarez, R., Vallet-Regí, M., Hard and Soft Protein Corona of Nanomaterials: Analysis and Relevance, 2021, *Nanomaterials*, 11(4):888, [DOI: 10.3390/nano11040888]

[8] Zheng, J.J., Agus, J.K., Hong, B.V., et al., Isolation of HDL by sequential flotation ultracentrifugation followed by size exclusion chromatography reveals size-based enrichment of HDL-associated proteins, 2021, *Sci. Rep.*, 11, 16086, [https://doi.org/10.1038/s41598-021-95451-3]

[9] Viikari, J., Precipitation of Plasma Lipoproteins by PEG-6000 and Its Evaluation with Electrophoresis and Ultracentrifugation, 2009, *Scandinavian Journal of Clinical and Laboratory Investigation*, 36(3), [DOI: 10.1080/00365517609055259]

[10] Mourdikoudis, S., Pallares, R.M, Thanh, N.T.K, Characterization techniques for nanoparticles: comparison and complementarity upon studying nanoparticles properties, 2018, *Nanoscale*, 10(27):12871-12934, [DOI: 10.1039/C8NR02278J]

[11] Sun, Y., Zhou, Y., Rehman, M., Wang, Y-F., and Guo, S., Protein Corona of Nanoparticles: Isolation and Analysis, 2024, *Chem. Bio Eng.*, 1(9):757-772, [https://doi.org/10.1021/cbe.4c00105]

[12] Cedervall, T., Lynch, I., Lindman, S., Berggård, T., Thulin, E., Nilsson, H., Dawson, K.A., & Linse, S., Understanding the nanoparticle–protein corona using methods to quantify exchange rates and affinities of proteins for nanoparticles, 2007, *Proc. Natl. Acad. Sci. U.S.A.*, 104(7):2050-2055, [https://doi.org/10.1073/pnas.0608582104]

[13] Li, Z., Wang, Y., Zhu, J., Zhang, Y., Zhang, W., Zhou, M., Luo, C., Li, Z., Cai, B., Gui, S., He, Z., Sun, J., Emerging well-tailored nanoparticulate delivery system based on in situ regulation of the protein corona, 2020, *Journal of Controlled Release*, 320, 1-18, [https://doi.org/10.1016/j.jconrel.2020.01.007]

[14] Böhmert, L., et al. Isolation methods for particle protein corona complexes from protein-rich matrices, 2020, *Nanoscale Advances*, [https://doi.org/10.1039/C9NA00537D]

[15] Gunawan, C., Lim, May., Marquis, C.P., Amal, R., Nanoparticle–protein corona complexes govern the biological fates and functions of nanoparticles, 2014, *J. Mater. Chem. B*, 2, 2060-2083, [https://doi.org/10.1039/C3TB21526A]

[16] Walkey, C., Understanding and Controlling the Interaction of Nanomaterials with Proteins in a Physiological Environment, 2011, *Chemical Society Reviews*, 41(7):2780-99, [DOI: 10.1039/c1cs15233e]

[17] Hirsh, S.L., McKenzie, D.R., Nosworthy, N.J., Denman, J.A., Sezerman, O.U., Bilek, M.M.M., The Vroman effect: Competitive protein exchange with dynamic multilayer protein aggregates, 2013, *Colloids and Surfaces B: Biointerfaces*, 395-404, [https://doi.org/10.1016/j.colsurfb.2012.10.039]

[18] Tomak, A., Cesmeli, S., Hanoglu, B.D., Winkler, D., Oksel Karakus, C., Nanoparticle-protein corona complex: understanding multiple interactions between environmental factors, corona formation, and biological activity, 2021, *Nanotoxicology*,15(10):1331-1357, [DOI: 10.1080/17435390.2022.2025467]

[19] Atkins, P.; de Paula, J.; Keeler, Atkins' Physical Chemistry, 2022, *J. Physical-Chemistry*, [https://global.oup.com/ukhe/product/atkins-physical-chemistry-9780198847816?cc=gb&lang=en&]

[20] Latour, R.A., The Langmuir isotherm: A commonly applied but misleading approach for the analysis of protein adsorption behavior, 2015, *Journal of Biomedical Materials Research Part A*, 103(3), [DOI: 10.1002/jbm.a.35235]

[21] Langmuir, I., The constitution and fundamental properties of solids and liquids, 1916, *J. Am. Chem. Soc.*, 38, 2221–2295, [https://doi.org/10.1021/ja02268a002]

[22] Corbo C., Molinaro R., Taraballi F., Toledano Furman, N., Sherman, M., Parodi, A., Salvatore, F., Tasciotti, E., Effects of the protein corona on liposome-liposome and liposome-cell interactions, 2016, *Int. J. Nanomedicine*, 11:3049-3063, [DOI: 10.2147/IJN.S109059]

[23] Sahneh, F.D., Scoglio, C., Dynamics of Nanoparticle-Protein Corona Complex Formation: Analytical Results from Population Balance Equations, 2013, *PLoS One*, [https://doi.org/10.1371/journal.pone.0064690]

[24] Duan, Y., Gong, K., Xu, S., et al., Regulation of cholesterol homeostasis in health and diseases: from mechanisms to targeted therapeutics, 2022, *Sig. Transduct. Target Ther.*, 7, 265, [https://doi.org/10.1038/s41392-022-01125-5]

[25] Feingold, K.R., Grunfled, C., Lipids: a key player in the battle between the host and microorganisms, [DOI: 10.1194]

[26] Lipoproteins, Cleveland Clinic, https://my.clevelandclinic.org/health/articles/23229-lipoprotein

[27] Smith, L.C., Pownall, H.J., Gotto, A.M. Jr., The plasma lipoproteins: structure and metabolism, 1978, *Annu. Rev. Biochem.*, 47:751-757, [DOI: 10.1146/annurev.bi.47.070178.003535]

[28] Berneis, K.K., Krauss, R.M., Metabolic origins and clinical significance of LDL heterogeneity, 2002, *J. Lipid Res.*, 43(9):1363-1379, [DOI: 10.1194/jlr.r200004-jlr200]

[29] Chroni, A., Leondaritis, G., Karlsson, H., Lipids and Lipoproteins in Atherosclerosis, 2012, *Journal of Lipids*, 2011(1), [https://doi.org/10.1155/2011/160104]

[30] Goldstein, J.L., Brown, M.S., The LDL receptor, 2009, *Arterioscler. Thromb. Vasc. Biol.*, 2009, 29(4):431-438, [DOI: 10.1161/ATVBAHA.108.179564]

[31] Dong, J., Guo, H., Yang, R., Li, H., Wang, S., Zhang, J., Chen, W., Serum LDL- and HDL-cholesterol determined by ultracentrifugation and HPLC, 2011, *J. Lipid Res.*, 52(2):383-388, [DOI: 10.1194/jlr.D008979]

[32] Mahmoudi, M., Landry, M.P., Moore, A., Coreas, R., The protein corona from nanomedicine to environmental science, 2023, *Nat. Rev. Mater.*, 24:1-17, [DOI: 10.1038/s41578-023-00552-2]

[33] Vilanova O., Martinez-Serra, A., Monopoli, M.P., Franzese, G., Characterizing the hard and soft nanoparticle-protein corona with multilayer adsorption, 2025, *Frontiers in Nanotechnology*, 6, [DOI: https://doi.org/10.3389/fnano.2024.1531039]

[34] Norde, W., Anusiem, A.C.I., Adsorption, desorption and re-adsorption of proteins on solid surfaces, 1992, *Colloids and Surfaces*, 66(1):73-80, [https://doi.org/10.1016/0166-6622(92)80122-I]

[35] Redgrave, T.G., Roberts, D.C.K, West, C.E., Separation of plasma lipoproteins by density-gradient ultracentrifugation, 1975, *Analytical Biochemistry*, 65, 42-49, [https://doi.org/10.1016/0003-2697(75)90488-1]

[36] Sharma, K., Fast Protein Liquid Chromatography: Features, Principle, Applications, 2024, https://scienceinfo.com/fast-protein-liquid-chromatography-features-principle-applications/

[37] Superdex 200 Increase small-scale SEC columns, Cytiva Life Sciences, https://www.cytivalifesciences.com/en/us/shop/chromatography/prepacked-columns/size-exclusion/superdex-200-increase-small-scale-size-exclusion-chromatography-columns-p-06190/parts-and-accessories/28990944/accessories?srsltid=AfmBOoqZrvbfLt8rN9mZhxZC001Wjrza1Ir5lVnYgA0_fx5eiN5ta4oQ

[38] The principle and method of polyacrylamide gel electrophoresis (SDS-PAGE), MBL Life Science, https://ruo.mbl.co.jp/bio/e/support/method/sds-page.html

[39] Protein Electrophoresis and SDS-PAGE, Khan Academy, https://www.khanacademy.org/test-prep/mcat/biomolecules/x04f6bc56:protein-analysis-techniques/a/protein-electrophoresis-and-sds-page

[40] The principle of Dynamic Light Scattering, Anton Paar, https://wiki.anton-paar.com/en/the-principles-of-dynamic-light-scattering/

[41] Stetefeld, J., McKenna, S.A., Patel, T.R., Dynamic light scattering: a practical guide and applications in biomedical sciences, 2016, *Biophys Rev*, 8(4):409-427, [doi: 10.1007/s12551-016-0218-6]

[42] Babick, F., Chapter 3.2.1 - Dynamic light scattering (DLS), 2020, *Micro and Nano Technologies*, 137-172, [https://doi.org/10.1016/B978-0-12-814182-3.00010-9]

[43] Transmission Electron Microscopy, NanoScience Instruments, https://www.nanoscience.com/techniques/transmission-electron-microscopy/

[44] MyScope Microscopy Training, Microscopy Australia, https://myscope.training/

[45] Planken, K.L., & Cölfen, H., Analytical ultracentrifugation of colloids, 2010, *Nanoscale*, 2, 1849–1869, [https://doi.org/10.1039/C0NR00215A]

[46] Balbo, A., Brown, P.H., Braswell, E.H., Shuck, P., Measuring protein-protein interactions by equilibrium sedimentation, 2007, *Curr. Protoc. Immunol.*, 18, [doi: 10.1002/0471142735.im1808s79]

[47] Rivas, G., Stafford, W., Minton A.P., Characterization of Heterologous Protein-Protein Interactions Using Analytical Ultracentrifugation, 1999, *Methods*, 19, 194-212, [doi: 10.1006/meth.1999.0851]

[48] Bekdemir, A., Stellacci, F., A centrifugation-based physicochemical characterization method for the interaction between proteins and nanoparticles, 2016, *Nat. Commun.,* 7, 13121, [doi: 10.1038/ncomms13121]

[49] Cole, J.L., Lary, J.W., P. Moody, T., Laue, T.M., Analytical ultracentrifugation: sedimentation velocity and sedimentation equilibrium, 2008, *Methods Cell. Biol.*, 84:143-179, [doi: 10.1016/S0091-679X(07)84006-4]

[50] Ralston, G., Introduction to Analytical Ultracentrifugation

[51] Schirf, V., & Planken, K.L., Analytical Ultracentrifuge User Guide Volume 1: Hardware, 2008

[52] Proteomics Core Facility, EPFL, https://www.epfl.ch/research/facilities/proteomics-core-facility/

[53] Aebersold, R., Mann, M., Mass-spectrometric exploration of proteome structure and function, 2016, *Nature*, 537(7620):347-355, [doi: 10.1038/nature19949]

[54] Domon, B., Aebersold, R., Mass spectrometry and protein analysis, 2006, *Science*, 312(5771):212-217, [doi: 10.1126/science.1124619]

[55] Zhu, W., Smith, J.W., Huang, C.M., Mass spectrometry-based label-free quantitative proteomics, 2009, *J. Biomed. Biotechnol.*, 2010:840518, [doi: 10.1155/2010/840518]

[56] Liu, Z., Fan, S., Liu, H., Yu, J., Qiao, R., Zhou, M., Yang, Y., Zhou, J., Xie, P., Enhanced Detection of Low-Abundance Human Plasma Proteins by Integrating Polyethylene Glycol Fractionation and Immunoaffinity Depletion, 2016, *PLoS One*, 11(11):e0166306, [doi: 10.1371/journal.pone.0166306]

[57] Packard, C.J., Pirillo, A., Tsimikas, S., Ference, B.A., Catapano, A.L., Exploring apolipoprotein C-III: pathophysiological and pharmacological relevance, 2024, *Cardiovasc. Res.*, 119(18):2843-2857, [doi: 10.1093/cvr/cvad177]

[58] Hassan, M.I., Waheed, A., Yadav, S., Singh, T.P., Ahmad, F., Zinc alpha 2-glycoprotein: a multidisciplinary protein, 2008, Mol. Cancer Res., 6(6):892-906, [doi: 10.1158/1541-7786.MCR-07-2195]

[59] C-reactive protein, Wikipedia, https://en.wikipedia.org/wiki/C-reactive_protein

[60] Iverius, P.H., Laurent, T.C., Precipitation of some plasma proteins by the addition of dextran or polyethylene glycol, 1967, Biochim Biophys. Acta., 133(2):371-3, [doi: 10.1016/0005-2795(67)90079-7]

Acknowledgements

I would like to express my sincere gratitude to Professor Francesco Stellacci and Professor Laura Fabris for believing in me from the very first moment, even though we didn't know each other, and for giving me the opportunity to begin finding my path in the world of science.
I will always be grateful for this enriching and formative experience, which I will carry in my heart forever.
I would like to extend my gratitude to Dr. Quy Ong. Your support and expertise have been essential to my project and your deep passion for science have greatly inspired me.
I would like to thank Ding for always being willing to help, providing constant support, and believing in my potential. I truly appreciate your valuable advice and guidance on this project.
I want to sincerely thank the entire SuNMIL group for your kindness and the time shared together. A special thanks to Cécilia for her help with the procedures to access the labs and her support in reassuring me during a challenging moment of this unforgettable experience.
I am also deeply grateful to Katya, my “desk mate”. Your thoughtful advice and the care you showed me made me feel valued and safe, for which I will always be grateful. The genuine laughter we shared is something I will never forget.

A mia madre, la donna che mi ha dato la vita e che ha illuminato il mio cammino, nonostante tu non mi abbia mai insegnato a vivere senza la tua luce accanto a me.
A mio padre e mio fratello, il vostro affetto e bene incommensurato è sempre nel mio cuore, ogni giorno, in ogni passo che faccio.
Grazie è una parola troppo piccola per esprimere la mia gratitudine per tutto il sostegno che mi avete dato, anche quello economico, e per la stima che avete sempre avuto nei miei confronti, spingendomi a non arrendermi mai.
Vi sarò eternamente grata per avermi dato la possibilità di inseguire i miei sogni, anche quando questo significava essere lontani.
Ringrazio tutta la “famiglia speciale” per i momenti indimenticabili che abbiamo condiviso e per i festeggiamenti che non mancano mai ogni volta che torno a casa. Non c’è mai una vera festa finché non siamo tutti insieme e, anche a distanza di mesi, riusciamo a celebrare un compleanno come se fosse il giorno giusto. La vostra capacità di rendere ogni mio ritorno speciale e di riunire la famiglia anche in quei momenti è qualcosa che porto e porterò sempre nel cuore.
Ringrazio Martina, punto fermo e saldo della mia vita. Penso che la nostra amicizia sia qualcosa di davvero unico e raro e che la nostra forza risiede nel sostenerci a vicenda, credendo ardentemente in ciò che facciamo. Solo noi sappiamo quante difficoltà abbiamo affrontato insieme, ma anche quante risate hanno accompagnato questi anni incredibili. Ripensando a quel momento in cui, tre giorni dopo la laurea triennale, eravamo già in viaggio verso Torino, mi rendo conto di quanto coraggio (ed anche un pizzico di follia) ci volesse. Sono convinta che nessuno avrebbe preso quella decisione al nostro posto, ma alla fine, nella vita, senza rischiare e senza coraggio, non si va lontano. Ti ho scelta e ti sceglierò ogni giorno come compagna di vita e chissà… forse un giorno le nostre case saranno così vicine da permetterci di venirci a trovare ogni volta che ne avremo voglia.

Ringrazio di cuore tutti i miei amici, sia quelli che sono al mio fianco da più tempo, che quelli che ho avuto il piacere di conoscere più recentemente. Anche se siamo lontani o ci vediamo dopo mesi, la nostra amicizia rimane sempre forte. Mi sento sempre vicina a voi, come se la distanza non esistesse. Grazie per aver sempre creduto in me, per l'affetto, la compagnia, le risate e il sostegno che mi avete sempre dato.

Desidero dedicare questa tesi a nonno Vito. Sono certa che tu sia stato al mio fianco in ogni momento, specialmente quando mi sono trovata completamente sola in un paese straniero. Spesso vedevo simboli e forme a cuore che immediatamente mi facevano pensare a te, come quella volta in cui, mentre preparavo l'ultimo esame, un evidenziatore si è rotto lasciando una macchia a forma di cuore. So che da lassù vegli su di me e continuerai a farlo, proteggendomi sempre.